for one information bit, giving 50% redundancy. Thus twice the transmission bandwidth is required for the *1B2B* code which restricts its use to systems where pulse dispersion is not a limiting factor. Another example of a *1B2B* code which is illustrated in Figure 11.39(c) is the coded mark inversion (CMI) code. In this code a digit 0 is transmitted as 01 and the digit 1 alternately as 00 or 11.

Timing information is obtained from the frequent positive to negative transitions, but, once again, the code is highly redundant requiring twice as many transmitted bits as input information bits.

More efficient codes of this type requiring less redundancy exist such as the *3B4B*, *5B6B* and the *7B8B* codes. There is a trade-off within this class of code between the complexity of balancing the number of zeros and ones, and the added redundancy. The increase in line symbol rate (bit rate) and the corresponding power penalty over encoded binary transmission is given by the ratio $m:n$. Hence, considering the widely favoured *5B6B* code, the symbol rate is increased by a factor of 1.2 whilst the power penalty is also equal to 1.2 or about 0.8 dB. It is therefore necessary to take into account the increased bandwidth requirement and the power penalty resulting from coding within the optical fiber system design.

Simple error monitoring may be provided with block codes, at the expense of a small amount of additional redundancy, by parity checking. Each block of N bits can be made to have an even (even parity) or odd (odd parity) number of ones so that any single error in a block can be identified. More extensive error detection and error correction may be provided with increased redundancy and equipment complexity. This is generally not considered worth while unless it is essential that the digital transmission system is totally secure (e.g. data transmission applications). Alternatively, error monitoring when using block codes may be performed by measuring the variation in disparity between the numbers of ones and zeros within the received bit pattern. Any variation in the accumulated disparity above an upper limit or below a lower limit allowed by a particular code is indicated as an error. Further discussion of error correction with relation to disparity may be found in Ref. 65. Moreover, variations on the above block codes to provide efficient high speed digital transmission have been devised (e.g. Ref. 66). Such line coding schemes possess a good balance of ones and zeros together with jitter suppression and the capability to provide a simple error monitoring function.

11.7 Analog systems

In Section 11.5 we indicated that the vast majority of optical fiber communication systems are designed to convey digital information (e.g. analog speech encoded as PCM). However, in certain areas of the telecommunication network or for particular applications, information transfer in analog form is still likely to remain for some time to come, or be advantageous. Therefore, analog optical fiber transmission will undoubtedly have a part to play in future communication networks, especially in situations where the optical fiber link is part of a larger

analog network (e.g. microwave relay network). Use of analog transmission in these areas avoids the cost and complexity of digital terminal equipment, as well as degradation due to quantization noise. This is especially the case with the transmission of video signals over short distances where the cost of high speed analog to digital (A–D) and D–A converters is not generally justified. Hence, there are many applications such as direct cable television and common antenna television (CATV) where analog optical fiber systems may be utilized.

There are limitations, however, inherent to analog optical fiber transmission, some of which have been mentioned previously. For instance, the unique requirements of analog transmission over digital are for high signal to noise ratios at the receiver output which necessitates high optical input power (see Section 9.2.5), and high end to end linearity to avoid distortion and prevent crosstalk between different channels of a multiplexed signal (see Section 11.4.2). Furthermore, it is instructive to compare the SNR constraints for typical analog optical fiber and coaxial cable systems.

In a coaxial cable system the fundamental limiting noise is $4KTB$, where K is Boltzmann's constant, T is the absolute temperature, and B is the effective noise bandwidth for the channel. If we assume for simplicity that the coaxial cable loss is constant and independent of frequency, the SNR for a coaxial system is

$$\left(\frac{S}{N}\right)_{\text{coax}} = \frac{V^2 \exp(-\alpha_N)}{Z_0 4KTB} \tag{11.55}$$

where α_N is the attenuation in nepers between the transmitter and receiver, V is the peak output voltage, and Z_0 is the impedance of the coaxial cable.

The SNR for an analog optical fiber system may be obtained by referring to Eq. (9.11) where

$$\left(\frac{S}{N}\right)_{\text{fiber}} = \frac{\eta P_0}{2hfB} \tag{11.56}$$

The expression given in Eq. (11.56) includes the fundamental limiting noise for optical fiber systems which is $2hfB$. Although Eq. (11.56) is sufficiently accurate for the purpose of comparison it applies to an unmodulated optical carrier. A more accurate expression would take into account the depth of modulation for the analog optical fiber system which cannot be unity [Ref. 53].* The average received optical power P_o may be expressed in terms of the average input (transmitted) optical power P_i as

$$P_o = P_i \exp(-\alpha_N) \tag{11.57}$$

Substituting for P_o into Eq. (11.56) gives

$$\left(\frac{S}{N}\right)_{\text{fiber}} = \frac{P_i \exp(-\alpha_N)}{2hfB} \tag{11.58}$$

* Strictly speaking, Eq. (11.56) depicts the optical carrier to noise ratio (CNR).

Equations (11.55) and (11.58) allow a simple comparison to be made of available SNR (or CNR) between analog coaxial and optical fiber systems, as demonstrated in Example 11.10.

Example 11.10

A coaxial cable system operating at a temperature of 17 °C has a transmitter peak output voltage of 5 V with a cable impedance of 100 Ω. An analog optical fiber system uses an injection laser source emitting at 0.85 μm and launches an average of 1 mW of optical power into the fiber cable. The optical receiver comprises a photodiode with a quantum efficiency of 70%. Assuming the effective noise bandwidth and the attenuation between the transmitter and receiver for the two systems is identical, estimate in decibels the ratio of the SNR of the coaxial system to the SNR of the fiber system.

Solution: Using Eqs. (11.55) and (11.58) for the SNRs of the coaxial and fiber systems respectively:

$$Ratio = \frac{\left(\frac{S}{N}\right)_{coax}}{\left(\frac{S}{N}\right)_{fiber}} = \frac{\frac{V^2 \exp(-\alpha_N)}{Z_0 4KTB}}{\frac{\eta P_i \exp(-\alpha_N)}{2hfB}} = \frac{V^2 hf}{2KTZ_0 \eta P_i}$$

$$= \frac{V^2 hc}{2KTZ_0 \eta P_i \lambda}$$

Hence

$$Ratio = \frac{25 \times 6.626 \times 10^{-34} \times 2.998 \times 10^8}{2 \times 1.385 \times 10^{-23} \times 290 \times 100 \times 0.7 \times 1 \times 10^{-3} \times 0.85 \times 10^{-6}}$$

$$= 1.04 \times 10^4 \simeq 40 \text{ dB}$$

The optical fiber channel in Example 11.10 has around 40 dB less SNR available than the alternative coaxial channel exhibiting similar channel losses. This results both from $2hfB$ being larger than $4KTB$ and from the far smaller transmitted power within the optical system. Furthermore, it must be noted that the comparison was made using an injection laser transmitter. If an LED transmitter with 10 to 20 dB less optical output power was compared, the coaxial system would display an advantage in the region 50 to 60 dB. For this reason it is difficult to match with fiber systems the SNR requirements of some analog coaxial links, even though the fiber cable attenuation may be substantially lower than that of the coaxial cable.

The analog signal can be transmitted within an optical fiber communication system using one of several modulation techniques. The simplest form of analog modulation for optical fiber communications is direct intensity modulation (D–IM) of the optical source. In this technique the optical output from the source is

modulated simply by varying the current flowing in the device around a suitable bias or mean level in proportion to the message. Hence the information signal is transmitted directly in the baseband.

Alternatively, the baseband signal can be translated on to an electrical subcarrier by means of amplitude, phase or frequency modulation using standard techniques, prior to intensity modulation of the optical source. Pulse analog techniques where a sequence of pulses are used for the carrier may also be utilized. In this case a suitable parameter such as the pulse amplitude, pulse width, pulse position or pulse frequency is electrically modulated by the baseband signal. Again, the modulated electrical carrier is transmitted optically by intensity modulation of the optical source.

Direct modulation of the optical source in frequency, phase or polarization rather than by intensity requires these parameters to be well defined throughout the optical fiber system. There is much interest in this area and optical component technology has been developed which will allow practical system implementation. These techniques concerned with coherent optical transmission are discussed in Chapter 12.

11.7.1 Direct intensity modulation (D–IM)

A block schematic for an analog optical fiber system which uses direct modulation of the optical source intensity with the baseband signal is shown in Figure 11.40(a). Obviously, no electrical modulation or demodulation is required with this technique, making it both inexpensive and easy to implement.

The transmitted optical power waveform as a function of time $P_{opt}(t)$, an example of which is illustrated in Figure 11.40(b), may be written as:

$$P_{opt}(t) = P_i(1 + m(t)) \tag{11.59}$$

where P_i is the average transmitted optical power (i.e. the unmodulated carrier power) and $m(t)$ is the intensity modulating signal which is proportional to the source message $a(t)$. For a cosinusoidal modulating signal:

$$m(t) = m_a \cos \omega_m t \tag{11.60}$$

where m_a is the modulation index or the ratio of the peak excursion from the average to the average power as shown in Figure 11.40(b), and ω_m is the angular frequency of the modulating signal. Combining Eqs. (11.59) and (11.60) we get:

$$P_{opt}(t) = P_i(1 + m_a \cos \omega_m t) \tag{11.61}$$

Furthermore, assuming transmission medium has zero dispersion, the received optical power will be of the same form as Eq. (11.61), but with an average received optical power P_o. Hence the secondary photocurrent $I(t)$ generated at an APD receiver with a multiplication factor M is given by:

$$I(t) = I_p M(1 + m_a \cos \omega_m t) \tag{11.62}$$

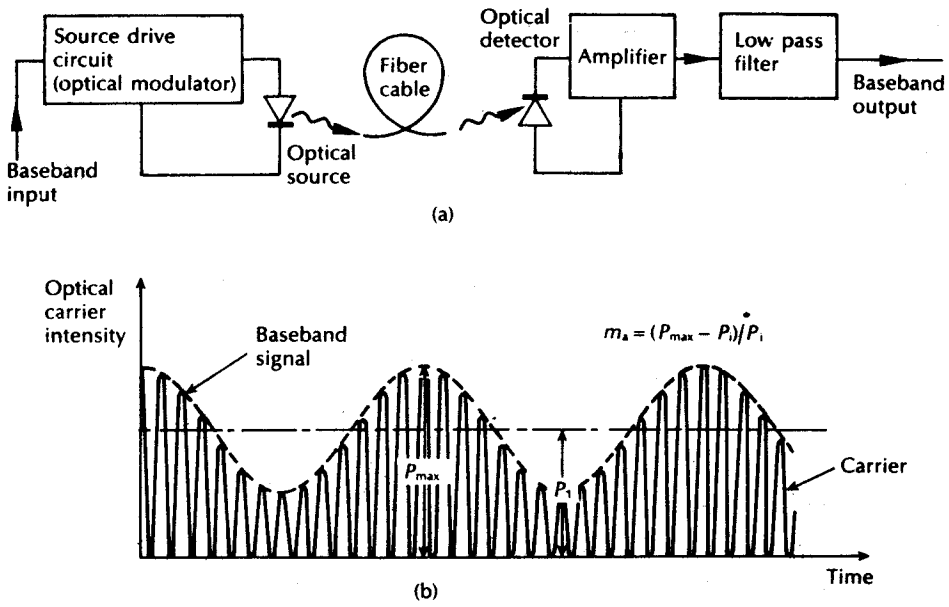

Figure 11.40 (a) Analog optical fiber system employing direct intensity modulation. (b) Time domain representation showing direct intensity modulation of the optical carrier with a baseband analog signal.

where the primary photocurrent obtained with an unmodulated carrier I_p is given by Eq. (8.8) as,

$$I_p = \frac{\eta e}{hf} P_o \tag{11.63}$$

The mean square signal current $\overline{i_{sig}^2}$ which is obtained from Eq. (11.62) is given by:

$$\overline{i_{sig}^2} = \tfrac{1}{2}(m_a M I_p)^2 \tag{11.64}$$

The total average noise in the system is composed of quantum, dark current, and thermal (circuit) noise components. The noise contribution from quantum effects and detector dark current may be expressed as the mean square total shot noise current for the APD receiver $\overline{i_{SA}^2}$ given by Eq. (9.21) where the excess avalanche noise factor is written following Eq. (9.26) as $F(M)$ such that:

$$\overline{i_{SA}^2} = 2eB(I_p + I_d)M^2F(M) \tag{11.65}$$

where B is the effective noise or post detection bandwidth.

Thermal noise generated by the load resistance R_L and the electronic amplifier noise can be expressed in terms of the amplifier noise figure F_n referred to R_L as

given by Eq. (9.17). Thus the total mean square noise current $\overline{i_N^2}$ may be written as:

$$\overline{i_N^2} = 2eB(I_p + I_d)M^2F(M) + \frac{4KTBF_n}{R_L} \tag{11.66}$$

The SNR defined in terms of the ratio of the mean square signal current to the mean square noise current (rms signal power to rms noise power) for the APD receiver is therefore given by:

$$\left(\frac{S}{N}\right)_{rms} = \frac{\overline{i_{sig}^2}}{\overline{i_N^2}} = \frac{\frac{1}{2}(m_a M I_p)^2}{2eB(I_p + I_d)M^2F(M) + (4KTBF_n/R_L)} \text{ (APD)} \tag{11.67}$$

It must be emphasized that the SNR given in Eq. (11.67) is defined in terms of rms signal power rather than peak signal power used previously. When a unity gain photodetector is utilized in the receiver (i.e. *p–i–n* photodiode) Eq. (11.67) reduces to:

$$\left(\frac{S}{N}\right)_{rms} = \frac{\frac{1}{2}(m_a I_p)^2}{2eB(I_p + I_d) + (4KTBF_n/R_L)} \ (p\text{–}i\text{–}n) \tag{11.68}$$

Moreover, the SNR for video transmission is often defined in terms of the peak to peak picture signal power to the rms noise power and may include the ratio of luminance to composite video b. Using this definition in the case of the unity gain detector gives:

$$\left(\frac{S}{N}\right)_{p-p} = \frac{(2m_a I_p b)^2}{2eB(I_p + I_d) + (4KTBF_n/R_L)} \ (p\text{–}i\text{–}n) \tag{11.69}$$

It may be observed that excluding b, the SNR defined in terms of the peak to peak signal power given in Eq. (11.69) is a factor of 8 (or 9 dB) greater than that defined in Eq. (11.68).

Example 11.11

A single TV channel is transmitted over an analog optical fiber link using direct intensity modulation. The video signal which has a bandwidth of 5 MHz and a ratio of luminance to composite video of 0.7 is transmitted with a modulation index of 0.8. The receiver contains a *p–i–n* photodiode with a responsivity of 0.5 $A\,W^{-1}$ and a preamplifier with an effective input impedance of 1 MΩ together with a noise figure of 1.5 dB. Assuming the receiver is operating at a temperature of 20 °C and neglecting the dark current in the photodiode, determine the average incident optical power required at the receiver (i.e. receiver sensitivity) in order to maintain a peak to peak signal power to rms noise power ratio of 55 dB.

Solution: Neglecting the photodiode dark current, the peak to peak signal rms noise power ratio is given following Eq. (11.69) as:

$$\left(\frac{S}{N}\right)_{p-p} = \frac{(2m_a I_p b)^2}{2eBI_p + (4KTBF_n/R_L)}$$

The photocurrent I_p may be expressed in terms of the average incident optical power at the receiver P_o using Eq. (8.4) as:

$$I_p = RP_o$$

where R is the responsivity of the photodiode. Hence

$$\left(\frac{S}{N}\right)_{p-p} = \frac{(2m_aRP_ob)^2}{2eBRP_o + (4KTBF_n/R_L)}$$

and

$$\left(\frac{S}{N}\right)_{p-p}\left(2eBRP_o = \frac{4KTBF_n}{R_L}\right) = (2m_aRP_ob)^2$$

Rearranging

$$(2m_aRb)^2P_o^2 - \left(\frac{S}{N}\right)_{p-p} 2eBRP_o - \left(\frac{S}{N}\right)_{p-p}\frac{4KTBF_n}{R_L} = 0$$

where

$$(2m_aRb)^2 = 4 \times 0.64 \times 0.25 \times 0.49$$
$$= 0.314$$

$$\left(\frac{S}{N}\right)_{p-p} 2eBR = 3.162 \times 10^5 \times 2 \times 1.602 \times 10^{-19} \times 5 \times 10^6 \times 0.5$$
$$= 2.533 \times 10^{-7}$$

$$\left(\frac{S}{N}\right)_{p-p}\frac{4KTBF_n}{R_L} = \frac{3.162 \times 10^5 \times 4 \times 1.381 \times 10^{-23} \times 293 \times 5 \times 10^6 \times 1.413}{10^6}$$
$$= 3.616 \times 10^{-14}$$

Therefore,

$$0.314P_o^2 - 2.533 \times 10^{-7}P_o - 3.616 \times 10^{-14} = 0$$

and

$$P_o = \frac{2.533 \times 10^{-7} \pm \sqrt{[(2.533 \times 10^{-7})^2 - (-4 \times 0.314 \times 3.616 \times 10^{-14})]}}{0.628}$$

$$= 0.93\ \mu W$$

$$= -30.3\ dBm$$

It must be noted that the low noise preamplification depicted in Example 11.11 may not always be obtained, and that higher thermal noise levels will adversely affect the receiver sensitivity for a given SNR. This is especially the case with lower SNRs, as illustrated in the peak to peak signal power to rms noise power ratio

against average received optical power characteristics for a video system shown in Figure 11.41. The performance of the system for various values of mean square thermal noise current $\overline{i_t^2} = 4KTBF_n/R_L$, where $\overline{i_t^2}$ is expressed as a spectral density in $A^2\ Hz^{-1}$, as indicated. The value for the receiver sensitivity obtained in Example 11.11 is approaching the quantum limit, also illustrated in Figure 11.41, which is the best that could possibly be achieved with a noiseless amplifier.

The quantum or shot noise (when ignoring the photodetector dark current) limit occurs with large values of signal current (i.e. primary photocurrent) at the receiver. Considering a p–i–n photodiode receiver, this limiting case which corresponds to large SNR is given by Eq. (11.68) when neglecting the device dark current as:

$$\left(\frac{S}{N}\right)_{rms} \simeq \frac{m_a^2 I_p}{4eB} \text{ (quantum noise limit)} \tag{11.70}$$

Using the relationship between the average received optical power P_o and the primary photocurrent given in Eq. (11.63) allows Eq. (11.70) to be expressed as:

$$P_o \simeq \frac{4hf}{m_a^2 \eta}\left(\frac{S}{N}\right)_{rms} B \tag{11.71}$$

Equation (11.71) indicates that for a quantum noise limited analog receiver, the optical input power is directly proportional to the effective noise or post detection bandwidth B. A similar result was obtained in Eq. (11.37) for the digital receiver.

Alternatively at low SNRs thermal noise is dominant, and the thermal noise limit when I_p is small, which may also be obtained from Eq. (11.68), is given by:

$$\left(\frac{S}{N}\right)_{rms} \simeq \frac{(m_a I_p)^2 R_L}{8KTBF_n} \text{ (thermal noise limit)} \tag{11.72}$$

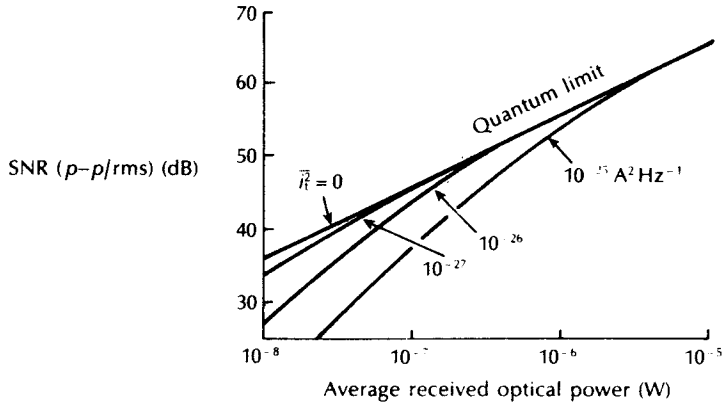

Figure 11.41 Peak to peak signal power to rms noise power ratio against the average received optical power for a direct intensity modulated video system and various levels of thermal noise given by $\overline{i_t^2}$. Reproduced with permission from G. G. Windus, *Marconi Rev*, **XLI**, p. 77. 1981.

Again substituting for I_p from Eq. (11.63) gives:

$$P_o \simeq \frac{hf}{e\eta m_a^2}\left(\frac{8KTF_n}{R_L}\right)^{\frac{1}{2}}\left(\frac{S}{N}\right)^{\frac{1}{2}}_{rms} B^{\frac{1}{2}} \tag{11.73}$$

Therefore it may be observed from Eq. (11.73) that in the thermal noise limit the average incident optical power is directly proportional to $B^{\frac{1}{2}}$ instead of the direct dependence on B shown in Eq. (11.71) for the quantum noise limit. The dependence expressed in Eq. (11.73) is typical of the p–i–n photodiode receiver operating at low optical input power levels. Thus Eq. (11.73) may be used to estimate the required input optical power to achieve a particular SNR for a p–i–n photodiode receiver which is dominated by thermal noise.

Example 11.12

An analog optical fiber link employing D–IM has a p–i–n photodiode receiver in which thermal noise is dominant. The system components have the following characteristics and operating conditions.

p–i–n photodiode quantum efficiency	60%
effective load impedance for the photodiode	50 kΩ
preamplifier noise figure	6 dB
operating wavelength	1 μm
operating temperature	300 K
receiver post detection bandwidth	10 MHz
modulation index	0.5

Estimate the required average incident optical power at the receiver in order to maintain an SNR, defined in terms of the mean square signal current to mean square noise current, of 45 dB.

Solution: The average incident optical power for a thermal noise limited p–i–n photodiode receiver may be estimated using Eq. (11.73) where:

$$P_o \simeq \frac{hf}{e\eta m_a^2}\left(\frac{8KTF_n}{R_L}\right)^{\frac{1}{2}}\left(\frac{S}{N}\right)^{\frac{1}{2}}_{rms} B^{\frac{1}{2}}$$

and

$$\frac{hf}{e\eta m_a^2} = \frac{hc}{e\eta m_a^2 \lambda} = \frac{6.626 \times 10^{-34} \times 2.998 \times 10^8}{1.602 \times 10^{-19} \times 0.6 \times 0.25 \times 1 \times 10^{-6}}$$

$$= 8.267$$

$$\left(\frac{8KTF_n}{R_L}\right)^{\frac{1}{2}} = \left(\frac{8 \times 1.381 \times 10^{-23} \times 300 \times 4}{50 \times 10^3}\right)^{\frac{1}{2}}$$

$$= 1.628 \times 10^{-12}$$

$$\left(\frac{S}{N}\right)^{\frac{1}{2}}_{rms} B^{\frac{1}{2}} = (3.162 \times 10^4 \times 10^7)^{\frac{1}{2}}$$

$$= 5.623 \times 10^5$$

Hence,

$$P_o \simeq 8.267 \times 1.628 \times 10^{-12} \times 5.623 \times 10^5$$
$$= 7.57\ \mu W$$
$$= -21.2\ \text{dBm}$$

Therefore, as anticipated, the receiver sensitivity in the thermal noise limit is low.

11.7.2 System planning

Many of the general planning considerations for optical fiber systems outlined in Section 11.4 may be applied to analog transmission. However, extra care must be taken to ensure that the optical source and, to a lesser extent, the detector have linear input–output characteristics, in order to avoid distortion of the transmitted optical signal. Furthermore, careful optical power budgeting is often necessary with analog systems because of the generally high SNRs required at the optical receiver (40 to 60 dB) in comparison with digital systems (20 to 25 dB), to obtain a similar fidelity. Therefore, although analog system optical power budgeting may be carried out in a similar manner to digital systems (see Section 11.6.6), it is common for the system margin, or the difference between the optical power launched into the fiber and the required optical power at the receiver, for analog systems to be quite small (perhaps only 10 to 20 dB when using an LED source to *p–i–n* photodiode receiver). Consequently, analog systems employing direct intensity modulation of the optical source tend to have a limited transmission distance without repeaters which generally prohibits their use for long-haul applications.

Example 11.13

A D–IM analog optical fiber link of length 2 km employs an LED which launches mean optical power of -10 dBm into a multimode optical fiber. The fiber cable exhibits a loss of 3.5 dB km^{-1} with splice losses calculated at 0.7 dB km^{-1}. In addition there is a connector loss at the receiver of 1.6 dB. The *p–i–n* photodiode receiver has a sensitivity of -25 dBm for an SNR ($\overline{i_{sig}^2}/\overline{i_N^2}$) of 50 dB and with a modulation index of 0.5. It is estimated that a safety margin of 4 dB is required. Assuming there is no dispersion–equalization penalty:

(a) Perform an optical power budget for the system operating under the above conditions and ascertain its viability.
(b) Estimate any possible increase in link length which may be achieved using an injection laser source which launches mean optical power of 0 dBm into the fiber cable. In this case the safety margin must be increased to 7 dB.

Solution: (a) Optical power budget:

Mean power launched into the fiber cable from the LED transmitter	−10 dBm
Mean optical power required at the p–i–n photodiode receiver for SNR of 50 dB and a modulation index of 0.5	−25 dBm
Total system margin	15 dB
Fiber cable loss (2×3.5)	7.0 dB
Splice losses (2×0.7)	1.4 dB
Connector loss at the receiver	1.6 dB
Safety margin	4.0 dB
Total system loss	14.0 dB
Excess power margin	1.0 dB

Hence the system is viable, providing a small excess power margin.

(b) In order to calculate any possible increase in link length when using the injection laser source we refer to Eq. (11.53), where

$$P_i - P_o = (\alpha_{fc} + \alpha_j)L + \alpha_{cr} + M_a \text{ dB}$$

Therefore,

$$0 \text{ dBm} - (-25 \text{ dBm}) = (3.5 + 0.7)L + 1.6 + 7.0$$

and

$$4.2L = 25 - 8.6 = 16.4 \text{ dB}$$

giving

$$L = \frac{16.4}{4.2} = 3.9 \text{ km}$$

Hence the use of the injection laser gives a possible increase in the link length of 1.9 km or almost a factor of 2. It must be noted that in this case the excess power margin has been reduced to zero.

The transmission distance without repeaters for the analog link of Example 11.13 could be extended further by utilizing an APD receiver which has increased sensitivity. This could facilitate an increase in the maximum link length to around 7 km, assuming no additional power penalties or excess power margin. Although this is quite a reasonable transmission distance, it must be noted that a comparable digital system could give in the region of 13 km transmission without repeaters.

The temporal response of analog systems may be determined from system rise time calculations in a similar manner to digital systems (see Section 11.6.5). The maximum permitted 3 dB optical bandwidth for analog systems in order to avoid

dispersion penalties follows from Eq. (11.49) and is given by:

$$B_{opt}(\text{max}) = \frac{0.35}{T_{syst}} \tag{11.74}$$

Hence calculation of the total system 10 to 90% rise time T_{syst} allows the maximum system bandwidth to be estimated. Often this calculation is performed in order to establish that the desired system bandwidth may be achieved using a particular combination of system components.

Example 11.14

The 10 to 90% rise times for possible components to be used in a D–IM analog optical fiber link are specified below:

Source (LED)	10 ns
Fiber cable: intermodal	9 ns km^{-1}
intramodal	2 ns km^{-1}
Detector (APD)	3 ns

The desired link length without repeaters is 5 km and the required optical bandwidth is 6 MHz. Determine whether the above combination of components give an adequate temporal response.

Solution: Equation (11.74) may be used to calculate the maximum permitted system rise time which gives the desired bandwidth where:

$$T_{syst}(\text{max}) = \frac{0.35}{B_{opt}} = \frac{0.35}{6 \times 10^6} = 58.3 \text{ ns}$$

The total system rise time using the specified components can be estimated using Eq. (11.43) as:

$$\begin{aligned} T_{syst} &= 1.1(T_S^2 + T_n^2 + T_c^2 + T_D^2)^{\frac{1}{2}} \\ &= 1.1(10^2 + (9 \times 5)^2 + (2 \times 5)^2 + 3^2)^{\frac{1}{2}} \\ &\simeq 52 \text{ ns} \end{aligned}$$

Therefore the specified components give a system rise time which is adequate for the bandwidth and distance requirements of the optical fiber link. However, there is little leeway for upgrading the system in terms of bandwidth or distance without replacing one or more of the system components.

11.7.3 Subcarrier intensity modulation

Direct intensity modulation of the optical source is suitable for the transmission of a baseband analog signal. However, if the wideband nature of the optical fiber

medium is to be fully utilized it is essential that a number of baseband channels are multiplexed on to a single fiber link. This may be achieved with analog transmission through frequency division multiplexing of the individual baseband channels. Initially, the baseband channels must be translated on to carriers of different frequency by amplitude modulation (AM), frequency modulation (FM) or phase modulation (PM) prior to being simultaneously transmitted as an FDM signal. The frequency translation may be performed in the electrical regime where the baseband analog signals modulate electrical subcarriers and are then frequency division multiplexed to form a composite electrical signal prior to intensity modulation of the optical source.

A block schematic of an analog system employing this technique, which is known as subcarrier intensity modulation, is shown in Figure 11.42. The baseband signals are modulated onto radiofrequency (RF) subcarriers by either AM, FM or PM and multiplexed before being applied to the optical source drive circuit.* Hence an intensity modulated (IM) optical signal is obtained which may be either AM–IM, FM–IM or PM–IM. In practice, however, system output SNR considerations dictate that generally only the latter two modulation formats are used. Nevertheless, systems may incorporate two levels of electrical modulation whereby the baseband channels are initially amplitude modulated prior to frequency or phase modulation [Ref. 68]. The FM or PM signal thus obtained is then used to intensity modulate the optical source. At the receive terminal the transmitted optical signal is detected prior to electrical demodulation and demultiplexing (filtering) to obtain the originally transmitted baseband signals.

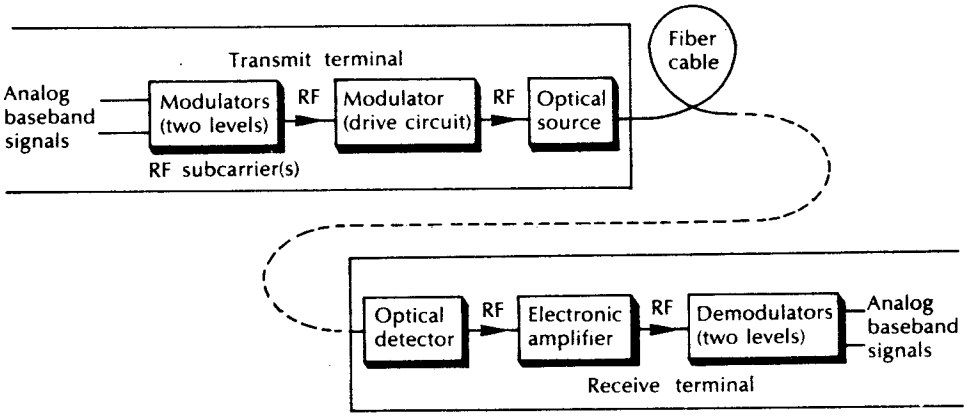

Figure 11.42 Subcarrier intensity modulation system for analog optical fiber transmission.

* When microwave frequency rather than radiofrequency subcarriers are employed the strategy is usually referred to as subcarrier multiplexing or SCM (see Section 11.9.2).

A further major advantage of subcarrier intensity modulation is the possible improvement in SNR that may be obtained during subcarrier demodulation. In order to investigate this process it is necessary to obtain a general expression for the SNR of the intensity modulated optical carrier which may then be applied to the subcarrier intensity modulation formats. Therefore, as with D–IM, considered in the preceding section, an electrical signal $m(t)$ modulates the source intensity. The transmitted optical power waveform is of the same form as Eq. (11.59), where:

$$P_{opt}(t) = P_i(1 + m(t)) \tag{11.75}$$

Also the secondary photon $I(t)$ generated at an APD receiver following Eq. (11.62) is given by:

$$I(t) = I_p M(1 + m(t)) \tag{11.76}$$

The mean square signal current $\overline{i_{sig}^2}$ may be written as [Ref. 65]:

$$\overline{i_{sig}^2} = (I_p M)^2 P_m \tag{11.77}$$

where P_m is the total power of $m(t)$, which can be defined in terms of the spectral density $S_m(\omega)$ of $m(t)$ occupying a one-sided bandwidth B_m Hz as:

$$P_m = \frac{1}{2\pi} \int_{-2\pi B_m}^{2\pi B_m} S_m(\omega)\, d\omega \tag{11.78}$$

Hence the SNR defined in terms of the mean square signal current to mean square noise current (i.e. rms signal power to rms noise power) using Eqs. (11.77) and (11.66) can now be written as:

$$\left(\frac{S}{N}\right)_{rms} = \frac{\overline{i_{sig}^2}}{\overline{i_N^2}} = \frac{(I_p M)^2 P_m}{2eB_m(I_p + I_d)M^2 F(M) + (4KTBF_n/R_L)}$$

$$= \frac{I_p^2 P_m}{2B_m e(I_p + I_d)F(M) + (4KTBF_n/M^2 R_L)}$$

$$= \frac{(RP_o)^2 P_m}{2B_m N_o} \qquad \text{(D–IM)} \tag{11.79}$$

where we substitute for I_p from Eq. (8.4) and for notational simplicity write:

$$N_o = e(I_p + I_d)F(M) + \frac{4KTBF_n}{M^2 R_L} \tag{11.80}$$

The result obtained in Eq. (11.79) gives the SNR for a direct intensity modulated optical source where the total modulating signal power is P_m. In this context Eq. (11.79) is simply a more general form of Eq. (11.67). However, we are now in a position to examine the signal to noise performance of various subcarrier intensity modulation formats.

11.7.4 Subcarrier double sideband modulation (DSB–IM)

A simple way to translate the spectrum of the baseband message signal $a(t)$ is by direct multiplication with the subcarrier waveform $A_c \cos \omega_c t$ giving the modulated waveform $m(t)$ as:

$$m(t) = A_c a(t) \cos \omega_c t \tag{11.81}$$

where A_c is the amplitude, and ω_c the angular frequency of the subcarrier waveform. For a cosinusoidal modulating signal ($\cos \omega_m t$) the subcarrier electric field $E_m(t)$ becomes:

$$E_m(t) = \frac{A_c}{2} \cos (\omega_c + \omega_m)t + \cos (\omega_c - \omega_m)t \tag{11.82}$$

giving the upper and lower sidebands. The time and frequency domain representations of the modulated waveform are shown in Figure 11.43. It may be observed from the frequency domain representation that only the two sideband components are present as indicated in Eq. (11.82). This modulation technique is known as double sideband modulation (DSB) or double sideband suppressed carrier (DSBSC) amplitude modulation. It provides a more efficient method of translating the spectrum of the baseband message signal than conventional full amplitude modulation where a large carrier component is also present in the modulated waveform.

The DSB signal shown in Figure 11.43 intensity modulates the optical source. Therefore the transmitted optical power waveform is obtained by combining Eqs. (11.75) and (11.81) where for simplicity we set the carrier amplitude A_c to unity,

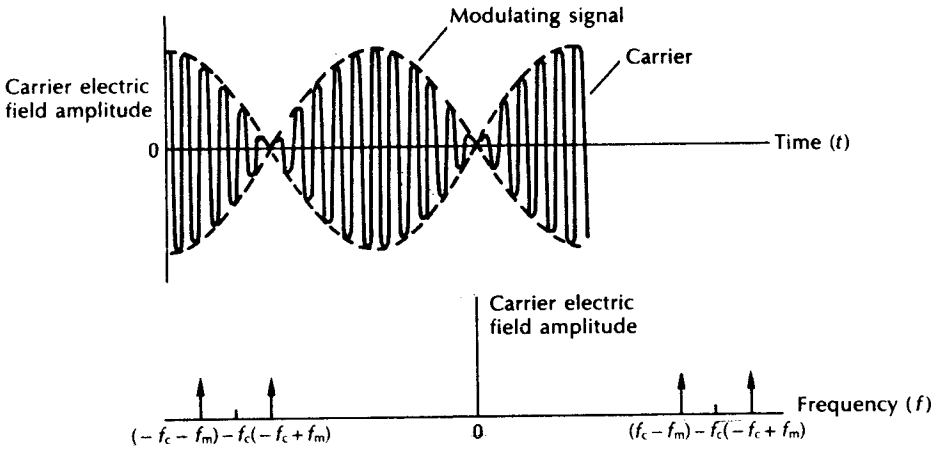

Figure 11.43 Time and frequency domain representations of double sideband modulation.

giving:

$$P_{opt}(t) = \bar{P}(1 + a(t) \cos \omega_c t) \tag{11.83}$$

Furthermore, in order to prevent overmodulation, the value of the message signal is normalized such that $|a(t) \leqslant 1|$ with power $P_a \leqslant 1$. The DSB modulated electrical subcarrier occupies a bandwidth $B_m = 2B_a$, and with a carrier amplitude of unity, $P_m = P_a/2$. Hence, the ratio of rms signal power to rms noise power obtained within the subcarrier bandwidth at the input to the double sideband demodulator is given by Eq. (11.79), where:

$$\left(\frac{S}{N}\right)_{rms} input\ DSB = \frac{(RP_o)^2 P_a/2}{2 \times 2B_a N_o} = \frac{(RP_o)^2 P_a}{8B_a N_o} \tag{11.84}$$

However, an ideal DSB demodulator gives a detection gain of 2 or 3 dB improvement in SNR [Ref. 68]. This yields an output SNR of:

$$\left(\frac{S}{N}\right)_{rms} output\ DSB = 2\left(\frac{S}{N}\right)_{rms} input\ DSB = \frac{(RP_o)^2 P_a}{4B_a N_o} \tag{11.85}$$

Comparison of the result obtained in Eq. (11.85) with that using direct intensity modulation of the baseband signal given by Eq. (11.79) shows a 3 dB degradation in SNR when employing DSB–IM under the same conditions of bandwidth (i.e. $B_m = B_a$), modulating signal power (i.e. $P_m = P_a$), detector photocurrent and noise. For this reason DSB–IM systems (and also AM–IM systems in general) are usually not considered efficient for optical fiber communications. Therefore far more attention is devoted to both FM–IM and PM–IM systems.

11.7.5 Subcarrier frequency modulation (FM–IM)

In this modulation format, the subcarrier is frequency modulated by the message signal. The conventional form for representing the baseband signal which intensity modulates the optical source is [Ref. 68]:

$$m(t) = A_c \cos\left[\omega_c t + k_f \int_0^t a(\tau)\, d\tau\right] \tag{11.86}$$

where k_f is the angular frequency deviation in radians per second per unit of $a(t)$. To prevent intensity over modulation, the carrier amplitude, $A_c \leqslant 1$. The generally accepted expression for the bandwidth which is referred to as Carson's rule is given by:

$$B_m \simeq 2(D_f + 1)B_a \tag{11.87}$$

where D_f is the frequency deviation ratio defined by:

$$D_f = \frac{peak\ frequency\ deviation}{bandwidth\ of\ a(t)} = \frac{f_d}{B_a} \tag{11.88}$$

The peak frequency deviation in the subcarrier FM signal f_d is given by:

$$f_d = k_f \max |a(t)| \tag{11.89}$$

Hence the SNR at the input to the subcarrier FM demodulator is:

$$\left(\frac{S}{N}\right)_{rms} input\ FM = \frac{(RP_o)^2(A_c^2/2)}{2B_m N_o} \tag{11.90}$$

The subcarrier demodulator operating above threshold yields an output SNR [Ref. 65]:

$$\left(\frac{S}{N}\right)_{rms} output\ FM = 6D_f^2(D_f^2 + 1)\frac{P_a(RP_o)^2(A_c^2/2)}{2B_m N_o} \tag{11.91}$$

Substituting for B_m from Eq. (11.87) gives:

$$\left(\frac{S}{N}\right)_{rms} output\ FM = \frac{3D_f^2 P_a(RP_o)^2(A_c^2/2)}{2B_a N_o} \tag{11.92}$$

The result obtained in Eq. (11.92) indicates that a significant improvement in the postdetection SNR may be achieved by using wideband FM–IM as demonstrated in the following example.

Example 11.15

(a) A D–IM and an FM–IM optical fiber communication system are operated under the same conditions of modulating signal power and bandwidth, detector photocurrent and noise. Furthermore, in order to maximize the SNR in the FM–IM system, the amplitude of the subcarrier is set to unity. Derive an expression for the improvement in post detection SNR of the FM–IM system over the D–IM system. It may be assumed that the SNR is defined in terms of the rms signal power to rms noise power.

(b) The FM–IM system described in (a) nas an 80 MHz subcarrier which is modulated by a baseband signal with a bandwidth of 4 kHz such that the peak frequency deviation is 400 kHz. Use the result obtained in (a) to determine the improvement in post detection SNR (in decibels) over the D–IM system operating under the same conditions. Also estimate the bandwidth of the FM signal.

Solution: (a) The output SNR for the D–IM system is given by Eq. (11.79) where we can write $P_m = P_a$ and $B_m = B_a$. Hence:

$$\left(\frac{S}{N}\right)_{rms} output\ D\text{–}IM = \frac{(RP_o)^2 P_a}{2B_a N_o}$$

The corresponding output SNR for the FM–IM system is given by Eq. (11.92)

where setting A_c to unity gives:

$$\left(\frac{S}{N}\right)_{rms} \textit{ output } FM = \frac{3D_f^2 P_a (RP_o)^2}{4B_a N_o}$$

Therefore the improvement in SNR of the FM–IM system over the D–IM system is given by:

$$\textit{SNR improvement} = \frac{[3D_f^2 P_a (RP_o)^2]/(4B_a N_o)}{[(RP_o)^2 P_a]/(2B_a N_o)}$$

$$= \frac{3D_f^2}{2}$$

and,

$$\textit{SNR improvement in decibels} = 10 \log_{10} \frac{3}{2} D_f^2$$

$$= 1.76 + 20 \log_{10} D_f$$

(b) The frequency deviation ratio is given by Eq. (11.88) where:

$$D_f = \frac{f_d}{B_a} = \frac{400 \times 10^3}{4 \times 10^3} = 100$$

Therefore the SNR improvement is:

$$\textit{SNR improvement} = 1.76 + 20 \log_{10} 100$$
$$= 41.76 \text{ dB}$$

The bandwidth of the FM–IM signal may be estimated using Eq. (11.87) where:

$$B_m \simeq 2(D_f + 1)B_a = 2(100 + 1)4 \times 10^3$$
$$= 808 \text{ kHz}$$

This result indicates that the system is operating as a wideband FM–IM system.

Example 11.15 illustrates that a substantial improvement in the post detection SNR over D–IM may be obtained using FM–IM. However, it must be noted that this is at the expense of a tremendous increase in the bandwidth required (808 kHz) for transmission of the 4 kHz baseband channel.

11.7.6 Subcarrier phase modulation (PM–IM)

With this modulation technique the instantaneous phase of the subcarrier is set proportional to the modulating signal. Hence in a PM–IM system the modulating

signal $m(t)$ may be written as [Ref. 68]:

$$m(t) = A_c \cos(\omega_c t + k_p a(t)) \tag{11.93}$$

where k_p is the phase deviation constant in radians per unit of $a(t)$. Again the carrier amplitude $A_c \leqslant 1$ to prevent intensity overmodulation. Moreover, the bandwidth of the PM–IM signal is given by Carson's rule as:

$$B_m \simeq 2(D_p + 1)B_a \tag{11.94}$$

where D_p is the frequency deviation ratio for the PM–IM system. In common with subcarrier frequency modulation the frequency deviation ratio is defined as:

$$D_p = \frac{f_d}{B_a} \tag{11.95}$$

where f_d is the peak frequency deviation of the subcarrier PM signal, which is given by:

$$f_d = k_p \max \left| \frac{da(t)}{dt} \right| \tag{11.96}$$

The SNR at the input to the subcarrier PM modulator is:

$$\left(\frac{S}{N}\right)_{rms} \textit{input PM} = \frac{(RP_o)^2 A_c^2/2}{2B_m N_o} \tag{11.97}$$

The output SNR from an ideal subcarrier PM demodulator operating above threshold is [Ref. 65]:

$$\left(\frac{S}{N}\right)_{rms} \textit{output PM} = \frac{D_p^2 P_a (RP_o)^2 A_c^2/2}{2B_a N_c} \tag{11.98}$$

The result given in Eq. (11.98) suggests that an improvement in SNR over D–IM may be obtained using PM–IM, especially when the SNR is maximized with $A_c = 1$. However, comparison of PM–IM with FM–IM indicates that the latter modulation format gives the greatest improvement.

Example 11.16

A PM–IM and an FM–IM optical fiber communication system are operated under the same conditions of bandwidth, baseband signal power, subcarrier amplitude, frequency deviation, detector photocurrent and noise. Assuming the demodulators for both systems are ideal, determine the ratio (in decibels) of the output SNR from the FM–IM system.

Solution: The output SNR from the FM–IM system is given by Eq. (11.92) where:

$$\left(\frac{S}{N}\right)_{rms} \textit{output FM} = \frac{3D_f^2 P_a (RP_o)^2 A_c^2/2}{2B_a N_o}$$

Substituting for D_f from Eq. (11.88) gives:

$$\left(\frac{S}{N}\right)_{rms} output\ FM = \frac{3f_d^2 P_a (RP_o)^2 A_c^2/2}{2B_a^3 N_o}$$

The output SNR for the PM–IM system is given by Eq. (11.98) where:

$$\left(\frac{S}{N}\right)_{rms} output\ PM = \frac{D_p^2 P_a (RP_o)^2 A_c^2/2}{2B_a N_o}$$

Substituting for D_p from Eq. (11.95) gives:

$$\left(\frac{S}{N}\right)_{rms} output\ PM = \frac{f_d^2 P_a (RP_o)^2 A_c^2/2}{2B_a^3 N_o}$$

The ratio of the output SNRs from the FM–IM and the PM–IM system is:

$$Ratio = \frac{[3f_d^2 P_a (RP_o)^2 A_c^2/2]/(2B_a^3 N_o)}{[f_d^2 P_a (RP_o)^2 A_c^2/2]/(2B_a^3 N_o)}$$

$$= 3$$

$$= 4.77\,\text{dB}$$

Example 11.16 shows that the FM–IM system has a superior output SNR by some 4.77 dB over the corresponding PM–IM system. Nevertheless, this does not prohibit the use of PM–IM systems for analog optical fiber communications as they still exhibit a substantial improvement in output SNR over D–IM systems, as well as allowing frequency division multiplexing. It should be noted, however, that a similar bandwidth penalty to FM–IM is incurred using this modulation format.

11.7.7 Pulse analog techniques

Pulse modulation techniques for analog transmission, rather than encoding the analog waveform into PCM, were mentioned within the system design considerations of Section 11.4. The most common techniques are pulse amplitude modulation (PAM), pulse width modulation (PWM), pulse position modulation (PPM) and pulse frequency modulation (PFM). All the pulse analog techniques employ pulse modulation in the electrical regime prior to intensity modulation of the optical source. However, PAM–IM is affected by source nonlinearities and is less efficient than D–IM, and therefore is usually discounted. PWM–IM is also inefficient since a large part of the transmitted energy conveys no information as only variations of the pulse width about a nominal value are of interest [Ref. 69]. Alternatively, PPM–IM and PFM–IM offer distinct advantages since the modulation affects the timing of the pulses, thus allowing the transmission of very narrow pulses. Hence, PPM–IM and PFM–IM provide similar signal to noise

performance to subcarrier phase and frequency modulation whilst avoiding problems involved with source linearity. These techniques therefore prove advantageous for longer-haul analog fiber links. Although PPM–IM is slightly more efficient it provides less SNR improvement over D–IM, than that gained with PFM–IM, where wideband FM gain may be obtained. Furthermore, the terminal equipment required for PFM–IM is less complex and therefore it is generally the preferred pulse analog technique [Refs. 70 and 74 to 79]. For these reasons the system aspects of pulse analog transmission will be considered in relation to PFM–IM.

A block schematic of a PFM–IM optical fiber system is shown in Figure 11.44. Pulse frequency modulation in which the pulse repetition rate is varied in sympathy with the modulating signal is performed in the PFM modulator which consists of a voltage controlled oscillator (VCO). This in turn operates the optical source by means of either a fixed pulse width or a fixed duty cycle (e.g. 50%). Demodulation in the system shown in Figure 11.44 is by regenerative baseband recovery, whereby the individual pulses are detected in a wideband receiver before they are regenerated with a limiter and monostable. This provides the desired modulating signal as a baseband component which is recovered through a low pass filter.

Regenerative baseband recovery gives the best SNR at the system output. A simpler PFM demodulation technique for fixed width pulse transmission is direct baseband recovery. In this case, because a baseband component is generated at the transmit terminal, detection may be performed with a low bandwidth receiver and the modulating signal obtained directly from a low pass filter. However, this technique gives a reduced SNR for a given optical power and therefore does not find wide application.

The SNR in terms of the peak to peak signal power to rms noise power of a PFM–IM system using regenerative baseband recovery is given by [Ref. 70]:

$$\left(\frac{S}{N}\right)_{p-p} = \frac{3(T_0 f_D M R P_{po})^2}{(2\pi T_R B)^2 \overline{i_N^2}} \tag{11.99}$$

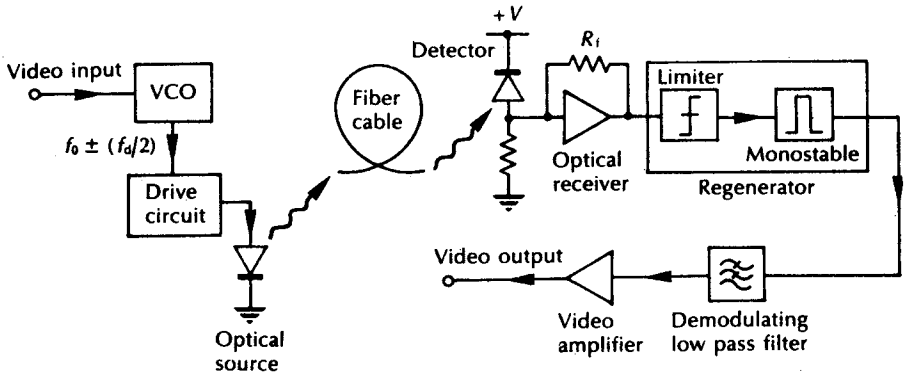

Figure 11.44 A PFM–IM optical fiber system employing regenerative baseband recovery.

where T_0 is the nominal pulse period which is equivalent to the reciprocal of the pulse rate f_o, f_D is the peak to peak frequency deviation, R is the photodiode responsivity, M is the photodiode multiplication factor, P_{po} is the peak received optical power, T_R is the pulse rise time at the regenerator circuit input, B is the post detection or effective baseband noise bandwidth and $\overline{i_N^2}$ is the receiver mean square noise current. It may be noted that improved SNRs are obtained with short rise time detected pulses. Moreover, the pulse rise time at the regenerator circuit input is dictated by the overall 10 to 90% system rise time T_{syst}, so there is no advantage in using a wideband receiver with a better pulse rise time than this. In fact, such a receiver would degrade the system performance by passing increased front end noise. Therefore, in an optimized PFM regenerative receiver design, $T_R = T_{syst}$ and following Eq. (11.43):

$$T_R \simeq 1.1\ (T_S^2 + T_n^2 + T_c^2 + T_D^2)^{\frac{1}{2}} \tag{11.100}$$

where T_S, T_n, T_c and T_D are the rise times of the source (or transmitter), the fiber (intermodal and intramodal) and the detector (or receiver) respectively.

Example 11.17

An optical fiber PFM–IM system for video transmission employs regenerative baseband recovery. The system uses multimode graded index fiber and an APD detector and has the following operational parameters:

Nominal pulse rate	20 MHz
Peak to peak frequency deviation	5 MHz
APD responsivity	0.7
APD multiplication factor	60
Total system 10 to 90% rise time	12 ns
Baseband noise bandwidth	6 MHz
Receiver mean square noise current	1×10^{-17} A^2

Calculate: (a) the optimum receiver bandwidth; (b) the peak to peak signal power to rms noise power ratio obtained when the peak input optical power to the receiver is -40 dBm.

Solution: (a) For an optimized design the pulse rise time at the regenerator circuit is equal to the total system rise time, hence $T_R = 12$ ns. The optimum receiver bandwidth is simply obtained by taking the reciprocal of T_R giving 83.3 MHz.

(b) The nominal pulse period $T_0 (= 1/f_0)$ is 5×10^{-8} s and the peak optical power at the receiver is 1×10^{-7} W. Therefore, the peak to peak signal to rms noise ratio

may be obtained using Eq. (11.99), where:

$$\left(\frac{S}{N}\right)_{p-p} = \frac{3(T_0 f_D M R P_{po})^2}{(2\pi T_R B)^2 \bar{i}_N^2}$$

$$= \frac{3(5\times10^{-8}\times5\times10^{6}\times60\times0.7\times10^{-7})^2}{(2\pi\times12\times10^{-9}\times6\times10^{6})^2\times10^{-17}}$$

$$= 1.62\times10^{6}$$

$$= 62.1 \text{ dB}$$

The result of Example 11.17(b) illustrates the possibility of acquiring high SNRs at the output to a PFM–IM system using a regenerative receiver with achievable receiver noise levels and with moderate input optical signal power to the receiver.

11.8 Distribution systems

Thus far, the considerations in this chapter have effectively concerned only point-to-point and primarily unidirectional optical fiber communication systems. A strategy for obtaining bidirectional optical transmission on the same fiber link is described in Section 11.9.3, whilst in this section we discuss the implementation aspects of a growing area of activity within optical fiber communications, namely that of multiterminal distribution systems. For example, two major areas of application for such multiterminal distribution systems or networks which are dealt with in Chapter 14 are the telecommunication local access network (Section 14.2.3) and local area networks (Section 14.7).

Although many variants or hybrid topologies have been explored, the three basic multiterminal system architectures comprise the ring, bus and star configurations. The former topology, which has largely found implementation as a closed path or loop where consecutive nodes or terminals are connected by a series of point-to-point fiber links, is discussed in relation to the fiber distributed data interface covered in Section 14.7.1. With the latter topologies, however, substantial progress has been made into the realization of multiterminal distribution systems and networks which do not simply comprise a series of point-to-point fiber links. In particular, they make use of the basic passive coupling devices described in Section 5.6

It is instructive to form a comparison between the topological implementations of the bus and star distribution systems when each employ passive optical couplers to direct the signals to particular nodes. Block schematics for these two configurations are shown in Figure 11.45 where, for the purposes of the comparison, the linear nature of the bus is replicated in the star network through

the positioning of the nodes in a linear manner. It is clear, however, that the star network configurations shown in Figures 14.4(c) and 14.28(d) are more representative of the use of the star topology to provide a widely distributed multiterminal network. Moreover the star–bus network implementation displayed in Figure 11.45(b) is not very economic in its use of fiber cable in comparison with the bus topology (Figure 11.45(a)) for a linear ordering of the network nodes.

The bus configuration illustrated in Figure 11.45(a) utilizes three port fiber couplers (see Section 5.6.1) to act as both beam splitter/combiner devices for the transmit and receive paths at each node, as well as passive fiber access couplers or taps along the bus link. However, whereas in the former case the split ratio is around 50%, in the latter tapping application the split ratio is often reduced to between 5 and 10% for the tap fiber so that the throughput optical power is a factor of 9 to 18 times greater than the optical power tapped off. Such an arrangement enables a larger optical power level to be transmitted down the bus and thus ensures adequate power at nodes distant from the transmit terminal.

Let us consider the total loss between node 1 and node $N-1$. It should be noted in the configuration shown in Figure 11.45(a) that the path between nodes 1 and $N-1$ exhibits the maximum loss because the final fiber tap couples only 10% of the incident optical power into the beam splitter of node $N-1$. By contrast, the path to node N obtains a factor of nine times this power level. Clearly, this situation could be modified by using a fiber beam splitter in place of the fiber tap in order to connect these two final nodes on to the bus.

Notwithstanding the above point we now consider the optical power budget for the worst case node interconnection (nodes 1 to $N-1$) for the multiterminal bus system of Figure 11.45(a). It is apparent that to obtain the total channel loss $C_L(1, N-1)$ between these two nodes the losses through each of the components must be summed. Let us commence at the transmit terminal, node 1. Then designating the connector losses in decibels as α_{cr} and assuming no excess loss in combining the transmitted signal on to the bus, a loss of $2\alpha_{cr}$ is obtained after the first beam splitter. The loss per kilometre exhibited by the fiber cable α_{fc} enables the total fiber cable loss between the two terminals to be written as $(N-1)\alpha_{fc}L_{bu}$ where L_{bu} is equal to the fiber length between each of the access couplers. Furthermore, the total loss incurred by the signal in passing through the access couplers or taps between nodes 1 and $N-1$ (excepting the final access coupler at which the signal to node $N-1$ is tapped off) is given by $(2\alpha_{cr} + L_{ac})(N-3)$ where L_{ac} is the insertion loss of the access coupler. At the final access coupler before node $N-1$ the loss obtained is $(2\alpha_{cr} + L_{tr})$ where L_{tr} is the loss due to the tap ratio of the device. Finally, a splitting loss L_{sp} occurs at the beam splitter together with a further connector loss α_{cr} at the optical receiver of node $N-1$. The total channel

Figure 11.45 (overleaf) Distribution system implementations: (a) linear bus system/network; (b) star system/network configured as a bus for comparative purposes.

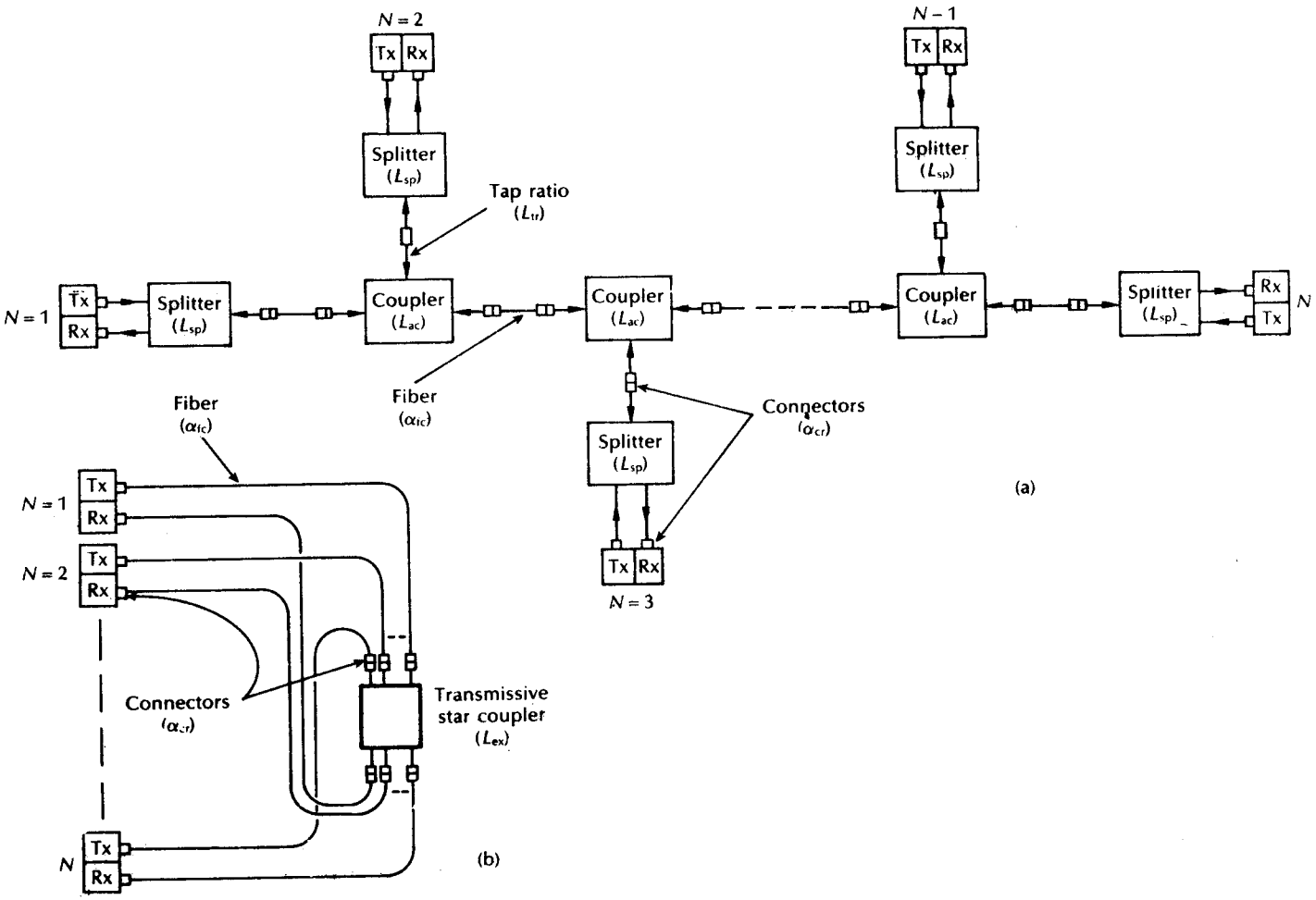
N = 2
Tx
Rx
Splitter
(L_{sp})
Tap ratio
(L_{tr})
N – 1
N = 1
Coupler
(L_{ac})
Fiber
(α_{fc})
Connectors
(α_{cr})
N = 3
(a)
Transmissive
star coupler
(L_{ex})
N
(b)

loss between nodes 1 and $N-1$ can therefore be written as:

$$C_L(1, N-1) = 2\alpha_{cr} + (N-1)\alpha_{fc}L_{bu} + (2\alpha_{cr} + L_{ac})(N-3) + (2\alpha_{cr} + L_{tr}) + L_{sp} + \alpha_{cr} \quad (11.101)$$

To incorporate the overall channel losses into an optical power budget for the multiterminal bus distribution system, the mean power obtained at the optical transmitter P_t at node 1, together with the mean incident optical power at the receiver, P_o of node $N-1$ must be included. Hence the optical power budget may be written as:

$$P_t = P_o + 2\alpha_{cr} + (N-1)\alpha_{fc}L_{bu} + (2\alpha_{cr} + L_{ac})(N-3) + (2\alpha_{cr} + L_{cr}) + L_{sp} + \alpha_{cr} + M_a \text{ dB} \quad (11.102)$$

where M_a is the system safety margin (see Section 11.6.6).

The star distribution system configuration displayed in Figure 11.45(b) employs a passive transmissive star coupler which provides two fibers to each node terminal (see Section 5.6.2). Hence an $N \times N$ star coupler allows the interconnection of N terminals. Assuming that the fiber cable lengths to each node are equal, then the same system loss is incurred for transmission between any two nodes. In this case the total system loss comprises the four connector losses at the transmitter, the receiver and the input and output ports of the star coupler $4\alpha_{cr}$; the total fiber cable loss $\alpha_{fc}L_{st}$ where L_{st} is the total fiber length in both arms of the star; the star splitting loss given by Eq. (5.18) as $10 \log_{10} N$ and the star excess loss L_{ex} provided by Eq. (5.19). In the case of equal fiber lengths the total channel loss between any two nodes is given by:

$$C_L(\text{star}) = 4\alpha_{cr} + \alpha_{fc}L_{st} + 10 \log_{10} N + L_{ex} \quad (11.103)$$

Again to incorporate the overall channel losses into an optical power budget for the multiterminal star distribution system, we designate the mean power obtained at the output of the optical transmitter P_t and the mean optical power incident at the receiver P_o so that:

$$P_t = P_o + 4\alpha_{cr} + \alpha_{fc}L_{st} + 10 \log_{10} N + L_{ex} + M_a \text{ dB} \quad (11.104)$$

where M_a is the system safety margin. A comparison of the optical power efficiencies of the two distribution systems is illustrated in the following example.

Example 11.18

Form a graphical comparison showing total channel loss against number of nodes for the bus and star distribution systems which incorporate components with the following performance parameters.

Connector loss:	1 dB
Access coupler insertion loss:	1 dB

Fiber cable loss:	5 dB km^{-1}
Access coupler tap ratio:	10 dB
Splitter loss:	3 dB
Star coupler excess loss:	0 dB

The distance between nodes on the bus system should be taken as 100 m and the worst case channel loss should be considered. It can be assumed that the total fiber cable length between all nodes on the star system is equal to 100 m.

Solution: Bus distribution system: using Eq. (11.101) the total channel loss is

$$\begin{aligned} C_L(1, N-1) &= 2 \times 1 + (N-1)5 \times 0.1 + (2 \times 1 + 1)(N-3) \\ &\quad + (2 \times 1 + 10) + 3 + 1 \text{ dB} \\ &= 0.5(N-1) + 3(N-3) + 18 \text{ dB} \\ &= 3.5N + 8.5 \text{ dB} \end{aligned}$$

Star distribution system: the total loss is given by Eq. (11.103) as

$$\begin{aligned} C_L(\text{star}) &= 4 \times 1 + 5 \times 0.1 + 10 \log_{10} N + 0 \text{ dB} \\ &= 4.5 + 10 \log_{10} N \text{ dB} \end{aligned}$$

The two expressions above for the bus and star distribution systems are plotted in Figure 11.46. It may be observed that the star configuration provides substantially greater efficiency in the utilization of optical power than the bus topology,

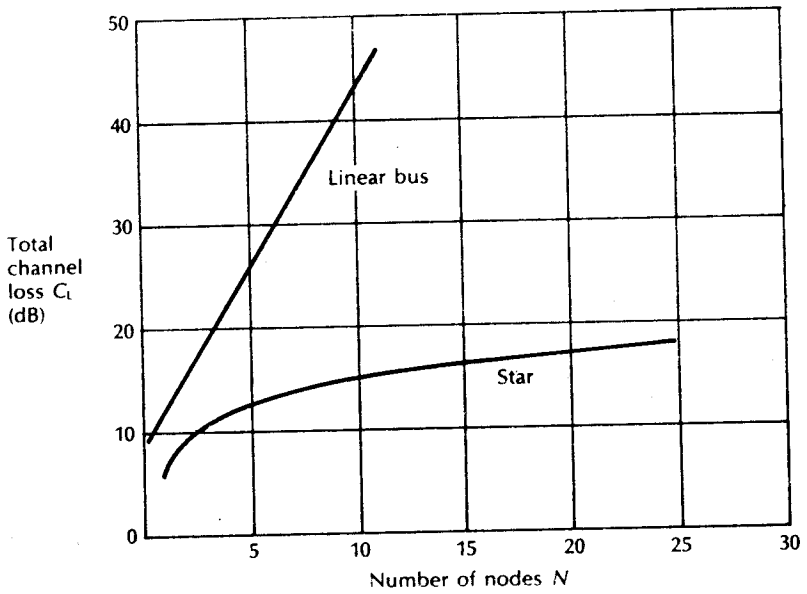

Figure 11.46 Characteristics showing the total channel loss against the number of nodes for the two distribution systems specified in Example 11.18.

particularly when the number of nodes becomes larger. It must be noted, however, that no excess loss for the star coupler has been included in the calculation and therefore it is anticipated that the total losses for the two distribution systems would be a little closer. Nevertheless, this factor would only make the optical power budgetary performance of the two configurations become similar when less than five terminals are interconnected.

11.9 Advanced multiplexing strategies

The basic multiplexing techniques which can be employed with IM/DD optical fiber systems were outlined in Section 11.4.2. Furthermore, the major baseband digital strategy, namely time division multiplexing was discussed in some detail in Section 11.5. In this section, however, the most significant of these multiplexing techniques are discussed in greater detail with particular emphasis on those strategies which allow greater exploitation of the available fiber bandwidth. We commence by further consideration of the multiplexing of digital signals prior to the more detailed description of techniques that may be employed for multiplexing either digital or analog intensity modulated signals, or a combination of both signal types.

11.9.1 Optical time division multiplexing

It was indicated in Section 10.5 that electronic circuits meet practical limitations on their speed of operation at frequencies around 10 GHz. Therefore, although more recently the feasibility of 10 Gbit s^{-1} direct intensity modulation and transmission over substantial distances (100 km) has been demonstrated (e.g. Ref. 80), electronic multiplexing at such speeds remains difficult and presents a restriction on the bandwidth utilization of a single-mode fiber link. An alternative strategy for increasing the bit rate of digital optical fiber systems beyond the bandwidth capabilities of the drive electronics is known as optical time division multiplexing (OTDM) [Ref. 81]. A block schematic of an OTDM system which has demonstrated 16 Gbit s^{-1} transmission over 8 km is shown in Figure 11.45 [Ref. 82]. The principle of this technique is to extend time division multiplexing by optically combining a number of lower speed electronic baseband digital channels. In the case illustrated in Figure 11.47, the optical multiplexing and demultiplexing ratio is 1 : 4, with a baseband channel rate of 4 Gbit s^{-1}. Hence the system can be referred to as a four channel OTDM system.

The four optical transmitters in Figure 11.47 were driven by a common 4 GHz clock using quarter bit period time delays. Mode-locked semiconductor laser sources which produced short optical pulses (around 15 ps long) were utilized at the transmitters to provide low duty cycle pulse streams for subsequent time multiplexing. Data was encoded onto these pulse streams using integrated optical

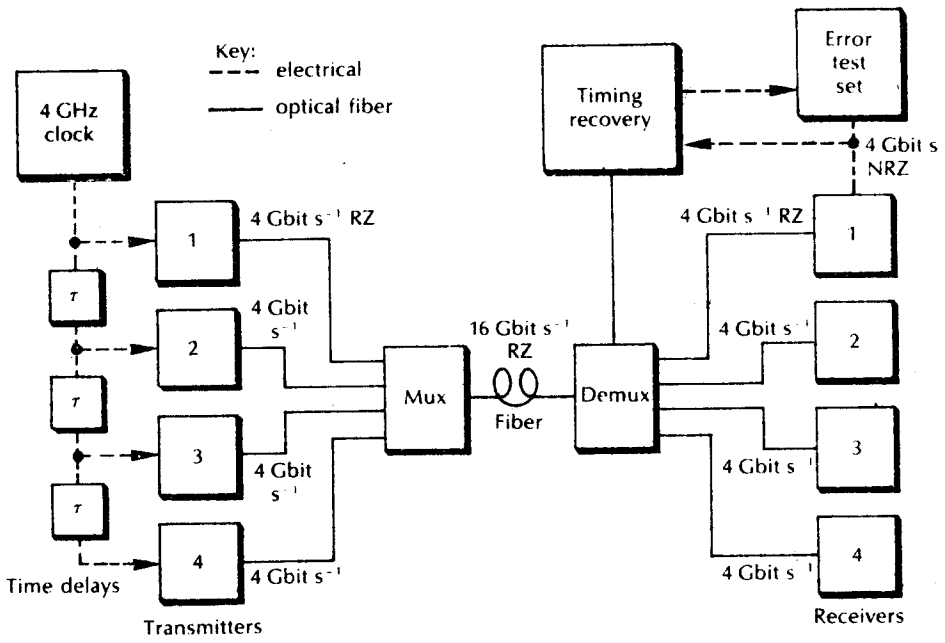

Figure 11.47 Four channel OTDM fiber system.

intensity modulators (see Section 10.6.2) which gave return to zero transmitter outputs at 4 Gbit s^{-1}. These IO devices were employed to eliminate the laser chirp (see Section 6.7.3) which would result in dispersion of the transmitted pulses as they propagated within the single-mode fiber, thus limiting the achievable transmission distance.

The four 4 Gbit s^{-1} data signals were combined in a passive optical power combiner but, in principle, an active switching element could be utilized. Although four optical sources were employed, they all emitted at the same optical wavelength within a tolerance of ± 0.1 nm and hence the 4 Gbit s^{-1} data streams were bit interleaved to produce the 16 Gbit s^{-1} signal. At the receive terminal the incoming signal was decomposed into the 4 Gbit s^{-1} baseband components in a demultiplexer which comprised two levels. Again, IO waveguide devices were used to provide a switching function at each level (see Section 10.6.1). At the first level the IO switch was driven by a sinusoid at 8 GHz to demultiplex the incoming 16 Gbit s^{-1} stream into two 8 Gbit s^{-1} signals. At the second level two similar switches, each operating at 4 GHz, demultiplexed each of the 8 Gbit s^{-1} data streams into two 4 Gbit s^{-1} signals. Hence single wavelength 16 Gbit s^{-1} optical transmission was obtained with electronics which only required a maximum bandwidth of about 2.5 GHz, as return to zero pulses were employed.

11.9.2 Subcarrier multiplexing

The use of radiofrequency subcarriers modulated by analog signals prior to intensity modulation of an optical source was discussed in Section 11.7.3. More recently, however, the utilization of substantially higher frequency microwave subcarriers multiplexed in the frequency domain before being applied to intensity modulate a high speed injection laser source has generated significant interest [Refs. 83 to 87]. Such microwave subcarrier multiplexing (SCM) enables multiple broadband signals to be transmitted over single-mode fiber and appears particularly attractive for video distribution systems [Refs. 86 to 88]. In addition, with SCM, conventional microwave techniques can be employed to subdivide the available intensity modulation bandwidth in a convenient way. The result is a useful multiplexing technique which does not require sophisticated optics or source wavelength specification (see Section 11.9.3). Either digital or analog modulation of the subcarriers can be utilized by upconverting to a narrowband channel at high frequency employing either amplitude, frequency or phase shift keying (i.e. ASK, FSK or PSK), and either amplitude, frequency or phase modulation (i.e. AM, FM or PM) respectively. For digital signals, FSK has the advantage of being simple to implement, both at the modulator and demodulator, whereas for analog video signals the modulation of the high frequency carrier (upconversion) is often carried out using either AM–VSB (vestigial sideband) or FM techniques. In both cases, the multicarrier signal is formed by frequency division multiplexing (FDM) of the modulated microwave subcarriers in the electrical domain prior to conversion to an intensity modulated optical signal.

A block schematic of a basic subcarrier multiplexed system is shown in Figure 11.48 [Ref. 86]. The modulated microwave subcarrier signals are obtained by frequency upconversion from the baseband using voltage controlled oscillator (VCOs). These subcarrier signals f_i are then summed in a microwave power combiner prior to the application of the composite signal to an injection laser which is d.c. biased at around 5 mW in order to produce the desired intensity modulation. The IM optical signal is then transmitted over single-mode fiber and directly detected using a wideband photodiode before demultiplexing and demodulation using a conventional microwave receiver.

Although relatively straightforward to implement using available components, SCM does exhibit some disadvantages, the most important of which is the problem associated with source nonlinearity [Ref. 87]. Distortion caused by this phenomenon can be particularly noticeable when several subcarriers are transmitted from a single optical source. Moreover, despite the fact that the receivers require narrow bandwidth, SCM systems, with the exception of those employing AM–VSB modulation, must operate at high frequency, often in the gigahertz range. In addition, for digital systems SCM requires more bandwidth per channel than a time division multiplexed system. The upconversion results in the bandwidth expansion so that a 50 Mbit s^{-1} channel may require some 80 MHz of bandwidth [Ref. 83]. Any reduction of this bandwidth overhead necessitates the adoption of more

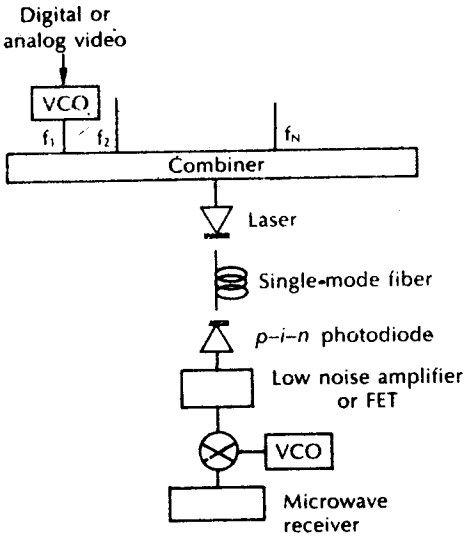

Figure 11.48 Basic subcarrier multiplexed (SCM) fiber system.

complex and less robust modulation techniques. For example, AM–VSB systems transmitting a standard cable television (CATV) multichannel spectrum tend to minimize the required bandwidth, but the signal must be received with a carrier to noise ratio of between 45 and 55 dB to avoid degradation of picture quality [Ref. 87].

The transmission of multiple CATV channels over substantial unrepeatered distances with good quality reception has, however, been demonstrated with SCM using frequency modulation (i.e. FM–FDM). For example, thirty-four multiple sub-nyquist-sampling encoding (MUSE) high definition television (HDTV) channels, each requiring an FM bandwidth of 27 MHz, have been transmitted over an unrepeatered distance of 42 km [Ref. 88]. This transmission system, which operated at a wavelength of 1.3 μm, provided a carrier to noise ratio of 17.5 dB at the receive terminal. Furthermore, an unrepeatered transmission distance in excess of 100 km has also been demonstrated with SCM when operating at a wavelength of 1.54 μm [Ref. 89]. In this case some eight baseband video channels, each of which was frequency modulated to occupy around 30 MHz of bandwidth, were then frequency multiplexed over a range 840 to 1160 MHz before directly modulating a distributed feedback laser.

Apart from the possibility of combining digital and analog subcarrier multiplexed signals into a composite signal, an alternative attractive strategy is the so-called hybrid SCM system which combines a baseband digital signal with a high frequency composite microwave signal [Ref. 86]. In this case the receiver shown in Figure 11.48 cannot be narrowband but must have a bandwidth from d.c. to beyond the

highest microwave signal frequency employed. As mentioned previously, SCM is under investigation for application in video distribution systems and networks. In such systems only a single channel needs to be selected for demodulation. Hence a tunable local oscillator, mixer and narrow band filter can be utilized at the receive terminals (Figure 11.48) to simultaneously select the desired SCM channel and downconvert it to a more convenient intermediate frequency (IF) signal. Finally, the IF signal can be input to an appropriate demodulator to recover the baseband video signal.

11.9.3 Wavelength division multiplexing

Wavelength division multiplexing (WDM) involves the transmission of a number of different peak wavelength optical signals in parallel on a single optical fiber. Although in spectral terms optical WDM is analogous to electrical frequency division multiplexing, it has the distinction that each WDM channel effectively has access to the entire intensity modulation fiber bandwidth which with current technology is of the order of several gigahertz. The technique is illustrated in Figure 11.49, where a conventional (i.e. single nominal wavelength) optical fiber

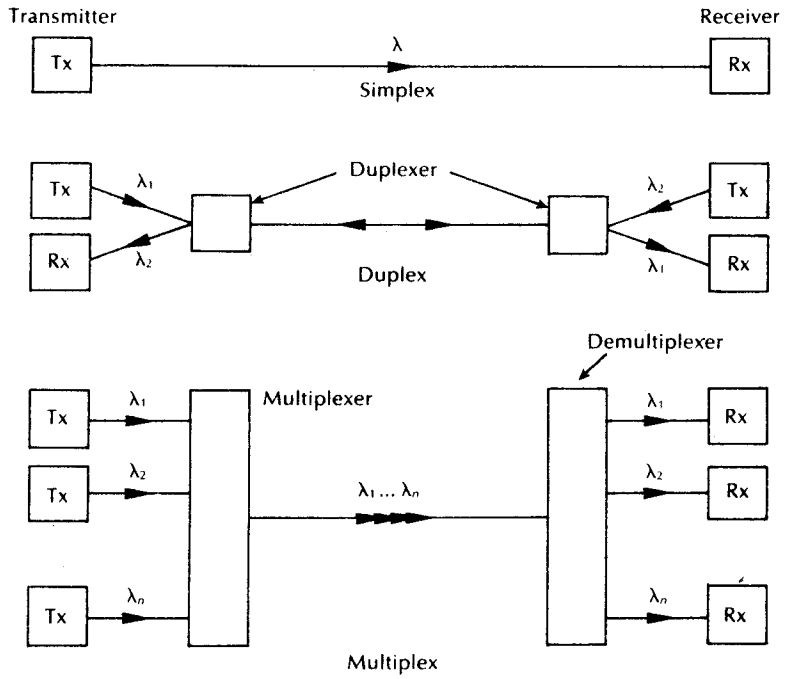

Figure 11.49 Optical fiber system operating modes illustrating wavelength division multiplexing (WDM).

communication system is shown together with a duplex (i.e. two different nominal wavelength optical signals travelling in opposite directions providing bidirectional transmission), and also a multiplex (i.e. two or more different nominal wavelength optical signals transmitted in the same direction) fiber communication system. It is the latter wavelength division multiplex operation which has generated particular interest within telecommunications. For example, two channel WDM is very attractive for a simple system enhancement such as piggybacking a 565 Mbit s^{-1} system onto an installed 140 Mbit s^{-1} link, or for doubling the capacity of a 565 Mbit s^{-1} link [Ref. 90]. Moreover, this multiplexing strategy overcomes certain power budgetary restrictions associated with electrical time division multiplexing. When the transmission rate over a particular optical link is doubled using TDM, a further 3 to 6 dB of optical power is generally required at the receiver (see Section 11.6.3). In the case of WDM, however, additional losses are also incurred from the incorporation of wavelength multiplexers and demultiplexers (see Section 5.6.3).

Wavelength division multiplexing in IM/DD optical fiber systems can be implemented using either LED or injection laser sources with either multimode or single-mode fiber. More recently, however, the wide scale deployment of single-mode fiber has encouraged the investigation of WDM on this transmission medium. In particular, the potential utilization of the separate wavelength channels to provide dedicated communication services to individual subscriber terminals is an attractive concept within telecommunications. For example, a multiwavelength, single-mode optical star network called LAMBDANET has been developed using commercial components [Ref. 91]. This network, which is internally nonblocking, has been configured to allow the integration of point-to-point and point-to-multipoint wideband services, including video distribution applications.

A block schematic of the LAMBDANET star network is shown in Figure 11.50. The network incorporated a sixteen port passive transmission star coupler (see Section 5.6.2). Each node was equipped with a single distributed feedback laser selected with centre wavelengths spaced at 2 nm intervals over the range 1527 to 1561 nm. Hence, each node transmitted at a unique wavelength, providing a contention-free broadcast capability to all other nodes. At the receive terminals every node could detect transmissions from all other nodes using a wavelength demultiplexer and sixteen optical receivers. Moreover, the wavelength channels on the network were demonstrated to operate at a transmission rate of 2 Gbit s^{-1} over a distance of 40 km [Ref. 92].

Another WDM strategy which has been investigated for both telecommunication and nontelecommunication applications is illustrated in Figure 11.51. [Ref. 93]. In this case, in place of narrow linewidth injection laser sources, wide spectral width (63 nm) edge-emitting LEDs were utilized to provide the multiwavelength optical carrier signals which were transmitted on single-mode optical fiber. The full spectral output from each ELED was not, however, transmitted for each wavelength channel. Instead, a relatively narrow spectral slice (3.65 nm) for each separate channel was obtained using the diffraction grating WDM multiplexer device, as shown in Figure 11.51, prior to transmission down the optical link. This technique,

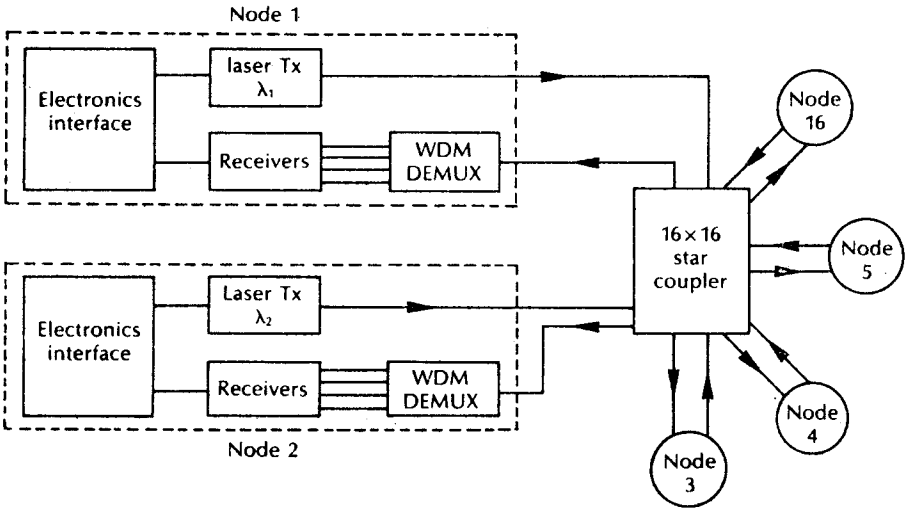

Figure 11.50 The LAMBDANET star network [Ref. 91].

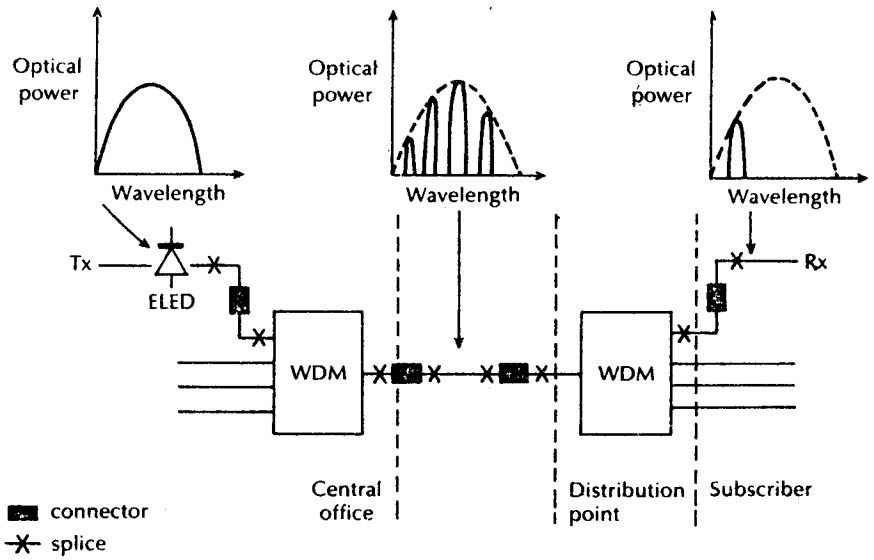

Figure 11.51 Spectral slicing of LED outputs to form several WDM channels.

which is known as spectral slicing, could enable LEDs with the same overall spectral output to be employed whilst still providing the distinctive wavelength channels for transmission between each subscriber terminal. In this case a WDM demultiplexer device is located at a distribution point in order to separate and distribute the different wavelength optical channels to the appropriate subscriber receive terminals. A similar strategy has been demonstrated for sixteen channels using superluminescent LEDs, again transmitting on single-mode fiber [Ref. 94]. Moreover, the technique has also been employed in nontelecommunication areas to provide multiple wavelength channels from single LED sources, usually on multimode fiber, in order to, for example, service a multiple optical sensor system (see Section 14.5) in which each wavelength channel supplies a signal to a different optical sensor device [Ref. 95].

11.10 Application of optical amplifiers

The use of electronics-based regenerative repeaters in long-haul optical fiber communications was discussed in Sections 11.4 and 11.6.1. It is clear, however, that such devices not only increase the cost and complexity of the optical communication system, but they may also act as a bottle-neck by restricting the system operational bandwidth. Hence the recent developments in optical amplifier technology described in Sections 10.2 to 10.4 have started to provide an additional, welcome flexibility in the design and implementation of IM/DD optical fiber systems.

The above flexibility stems from the ability for the transmitted optical signal to remain in the optical domain over the entire length of a long-haul link. Optical amplifiers (both semiconductor and fiber devices) therefore exhibit interesting features which assist in the system design, as illustrated in Figure 11.52. It may be observed from Figure 11.52(a) that, in a similar manner to electronic repeaters (see Figure 11.27), optical amplifiers may be employed in a simplex mode where each transmitted optical signal is carried on a separate fiber link. However, optical amplifiers have the ability to operate simultaneously in both directions at the same carrier wavelength,* as shown in Figure 11.52(b). Moreover, in this bidirectional mode they offer an added degree of reliability in that a single fiber break would only disable one half of communication capacity per fiber pair rather than causing a complete system failure, as is the case with the present unidirectional systems (i.e. one transmission path between all user pairs is disabled).

A further range of flexibility associated with optical amplifiers concerns the ability of particular devices to simultaneously amplify multiple wavelength division multiplexed (WDM) optical signals (see Section 11.9.3). Both SLAs and fiber amplifiers with spectral bandwidths in the range 20 to 50 nm can be realized (see

* It is obviously necessary to intensity modulate the optical carriers at different speeds to avoid signal interference.

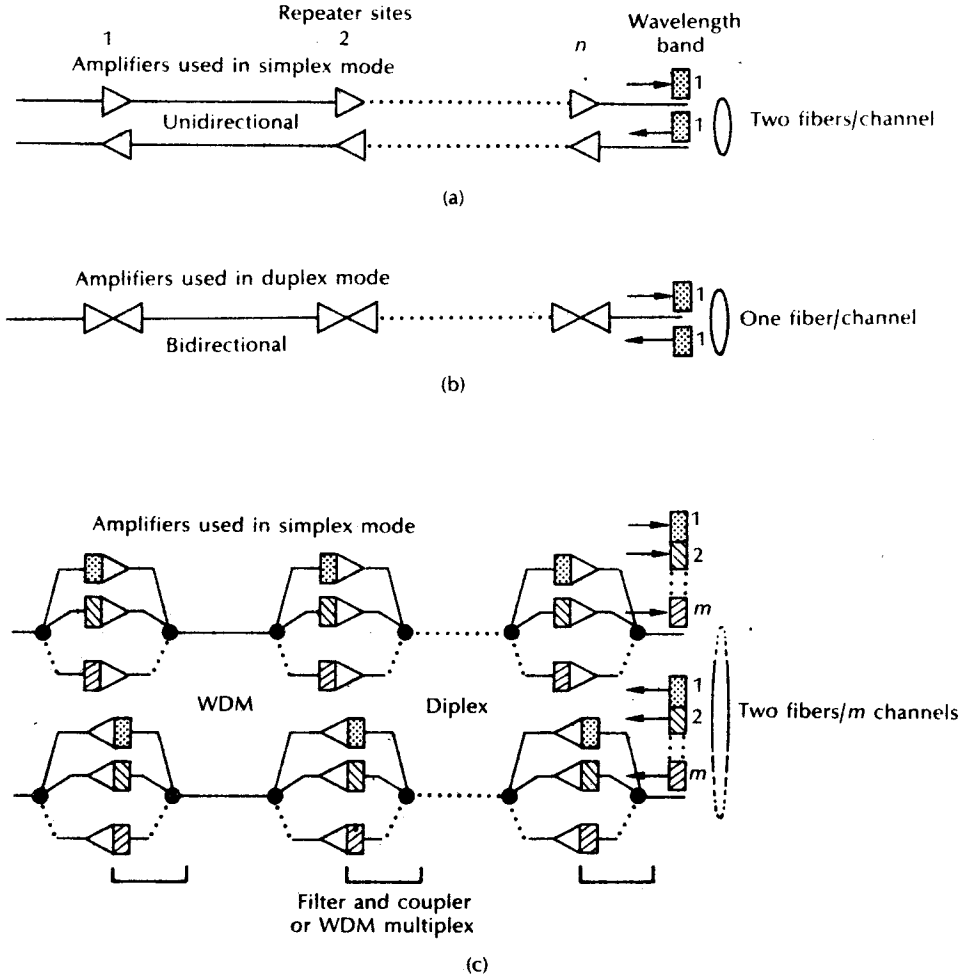

Figure 11.52 Potential point-to-point system applications for optical amplifiers: (a) simplex mode; (b) duplex mode; (c) multiamplifier configuration for wavelength division multiplex (WDM) operation.

Sections 10.3 and 10.4) which will allow single amplifiers to support in excess of ten intensity modulated WDM channels. Moreover, the parallel multiamplifier configuration illustrated in Figure 11.52(c) could be envisaged which would enable contiguously spectrally aligned amplifiers to span a complete wavelength window (say around 1.55 μm). Such configurations could increase system reliability in the event of an individual amplifier failure, whilst also relaxing the linearity and overload characteristics for amplifiers operating with densely packed WDM hierarchies [Ref. 96].

It was mentioned in Section 10.4 that optical amplifiers could be used in a broad range of system applications: namely, as power amplifiers at the optical transmitter; as in-line repeater amplifiers; and as preamplifiers at optical receivers. Moreover, the latter system application was dealt with in Section 9.6. Therefore, in this section we concentrate on the utilization of optical amplifiers as in-line repeaters within IM/DD optical fiber systems. It must be remembered, however, that in contrast to regenerative repeaters, optical amplifiers simply act as gain blocks on an optical fiber link and hence they do not reconstitute a transmitted digital optical signal. A drawback with this operation is that both noise and signal distortions are continuously amplified as the optical signal passes down a link which uses cascaded amplifiers. A benefit, however, is that optical amplifiers are transparent to any type of signal modulation (i.e. digital or analog) and to any modulation bandwidth.

It was mentioned in Section 10.3.2 that noise in travelling wave SLAs may determine the number of devices that can be cascaded as linear repeaters. Since the mean noise power resulting from spontaneous emission in optical amplifiers accumulates in proportion to the number of repeaters, gain saturation occurs when the total noise power becomes equal to the signal power. A simple model for the noise behaviour of such devices which is valid under conditions of high signal to noise ratio and high gain is shown in Figure 11.53. It comprises an ideal noiseless amplifier with gain G preceded by an additive noise source of spectral density $S(f)$ given by [Ref. 97]:

$$S(f) = Khf \tag{11.105}$$

where K, which is dependent on the population inversion and the cavity loss, provides a measure of the amplifier quality and hf constitutes photon energy. A minimum theoretical value for K is unity, which would only occur for the ideal case of complete inversion and no cavity loss. However, in this case $S = hf$ which indicates that it is theoretically impossible for the TWA to be noiseless. Nevertheless, in practice $K < 2$ has been obtained, demonstrating that amplifiers with less than 3 dB more noise than the theoretical limit can be achieved [Ref. 98].

The cascading of optical amplifiers in a long-haul communication system is illustrated in Figure 11.54(a). Following each section of fiber cable length L there is an optical amplifier with gain G which just compensates for the fiber cable loss

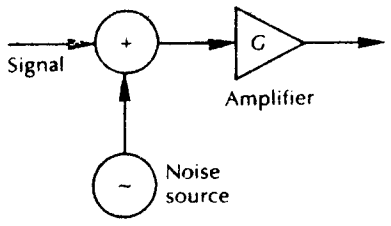

Figure 11.53 Noise model for travelling wave optical amplifier.

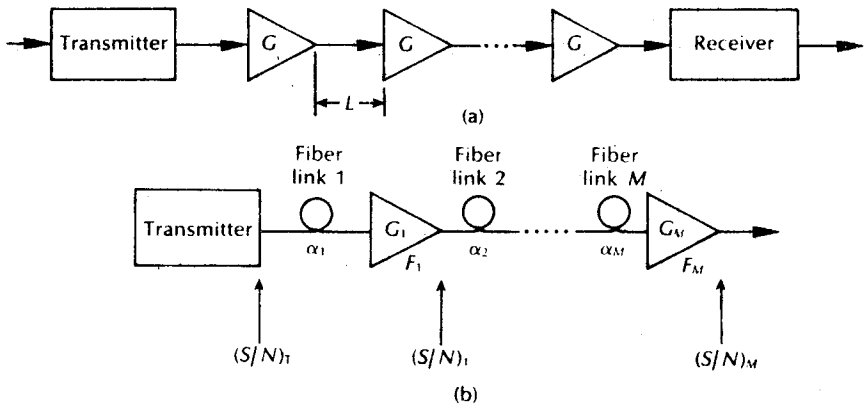

Figure 11.54 Cascaded optical amplifiers: (a) fiber system with cascaded optical amplifiers; (b) signal to noise ratios in a cascaded amplifier chain.

such that:

$$G = 10^{-(\alpha_{fc} + \alpha_j)L/10} \tag{11.106}$$

where α_{fc} and α_j are the fiber cable losses and joint losses respectively, both in dB km^{-1}. Furthermore, as the optical signal travels through the amplifier cascade the noise levels increase because the additive noise from each device is cumulative. Hence, using Eqs. (11.105) and (11.106) the signal to noise ratio at the end of a cascaded link may be written as:

$$\frac{S}{N} \simeq \frac{P_i 10^{-(\alpha_{fc} + \alpha_j)L/10}}{(L_{to}/L)KhfB} \tag{11.107}$$

where P_i is the power launched into the link at the transmitter, L_{to} the total system length and hence (L_{to}/L) is approximately equal to the total number of amplifier repeaters,* and the noise bandwidth equals the system bandwidth B. Equation (11.107) therefore enables the maximum transmission distance for a system using cascaded travelling wave SLAs to be deduced.

Example 11.19

A long-haul digital single-mode fiber system operating at a wavelength of 1.55 μm is envisaged employing travelling wave SLAs spaced at intervals of 100 km. The power launched into the link at the transmitter is 0 dBm and the fiber cable attenuation is 0.22 dB km^{-1}. In addition, there are splice losses which average out

* The total number of amplifier repeaters is actually $(L_{to}/L - 1)$; however for a long link and a large number of repeaters this approximates to (L_{to}/L).

at 0.03 dB km^{-1}. A signal to noise ratio of 17 dB is required at the system receive terminal to provide an acceptable BER at the operating transmission rate of 1.2 Gbit s^{-1}. Assuming that the system bandwidth is equal to the transmission bit rate and that K for the amplifiers is equal to 4, estimate the maximum system length such that satisfactory performance is maintained.

Solution: Using Eq. (11.107), then

$$(L_{to}/L) \simeq \frac{P_i \lambda 10^{-(\alpha_{ic} + \alpha_j)L/10}}{KhcB} \left(\frac{S}{N}\right)^{-1}$$

Hence for a link with a large number of cascaded amplifiers:

$$L_{to} \simeq \left(\frac{P_i \lambda 10^{-(\alpha_{ic} + \alpha_j)L/10}}{KhcB}\right)\left(\frac{S}{N}\right)^{-1} L$$

$$= \frac{(10^{-3} \times 1.55 \times 10^{-6} \times 10^{-2.5}) 100 \times 10^3}{4 \times 6.626 \times 10^{-34} \times 2.998 \times 10^8 \times 1.2 \times 10^9 \times 50}$$

$$\simeq 1 \times 10^4 \text{ km}$$

Thus the maximum system length obtained in Example 11.19 is very large and would allow the interconnection of most points on the earth using a chain of optical amplifiers. However, the calculation does not take account of the nonregenerative nature of the amplifier repeaters in which pulse spreading as well as noise down the link is accumulated. Fiber dispersion therefore imposes serious limitations on the system performance, as discussed in Section 11.6.5, and it will restrict both the maximum system span as well as the maximum transmission rate.

Another parameter which is often specified in relation to the noise performance of optical amplifiers is the noise figure of the devices. The noise figure F for an optical amplifier is defined in a similar manner to an electrical amplifier as the signal to noise degradation between the device input and the device output:

$$F = \frac{(S/N)_{in}}{(S/N)_{out}} \tag{11.108}$$

Again, it is governed by factors including the population inversion, the number of transverse modes in the amplifier cavity, the number of incident photons on the amplifier and the optical bandwidth of the amplified spontaneous emissions. Typical noise figures range from 4 to 8 dB, with SLAs generally towards the bottom end of the range and fiber amplifiers towards the top end.

We now consider a system with M cascaded optical amplifiers, as illustrated in Figure 11.54(b). In this case the link attenuation (both fiber cable and joint losses) in front of the kth amplifier is denoted by α_k, whilst the amplifier has a signal gain of G_k and a noise figure F_k. The input and output SNRs for such a cascaded link can be defined at the transmitter output T and the Mth amplifier output,

respectively, so that in a similar manner to electrical amplifiers the total noise figure for the system F_{to} is:

$$F_{to} = \frac{(S/N)_T}{(S/N)_M}$$

$$= \frac{F_1}{\alpha_1} + \frac{F_2}{\alpha_1 G_1 \alpha_2} + \frac{F_3}{\alpha_1 G_1 \alpha_2 G_2 \alpha_3} + \cdots + \frac{F_M}{\alpha_M \sum_{k=1}^{M-1} (\alpha_k G_k)} \tag{11.109}$$

The above expression can therefore enable determination of the total noise figure for the amplifier cascade.

Example 11.20

An optical fiber system is configured with a series of M optical amplifiers in cascade. The fiber cable and joint losses on each span between amplifiers on the link are compensated by the following amplifier gain. Obtain an expression for the total noise figure for the system and determine its value when all the amplifiers are identical.

Solution: As the amplifier gain compensates for the losses, then $\alpha_k G_k = 1$. Hence using Eq. (11.109) the total noise figure is given by:

$$F_{to} = \frac{F_1 G_1}{\alpha_1 G_1} + \frac{F_2 G_2}{\alpha_1 G_1 \alpha_2 G_2} + \cdots + \frac{F_M G_M}{\alpha_m \sum_{k=1}^{M-1} (\alpha_k G_k)}$$

$$= F_1 G_1 + F_2 G_2 + \cdots + F_M G_M$$

$$= \sum_{k=1}^{M} F_k G_k$$

When all the repeaters are identical then $F_1 G_1$, $F_2 G_2$, ..., $F_M G_M$ are equal to FG. Therefore, the total noise figure becomes:

$$F_{to} = MFG$$

At the output from the first amplifier repeater a degradation in signal to noise ratio of FG occurs followed by a decrease $1/M$.

A typical experimental system configuration employing five travelling wave SLAs and operating over a distance of some 500 km at a transmission rate of 565 Mbit s^{-1} is shown in Figure 11.55 [Refs. 99, 100]. The system was designed to give a bit error rate better than 10^{-9}. In addition, as discussed above, the noise in TWSLAs can largely determine the number of devices that may be cascaded as linear repeaters. However, the spontaneous emission noise profile is relatively broadband, typically

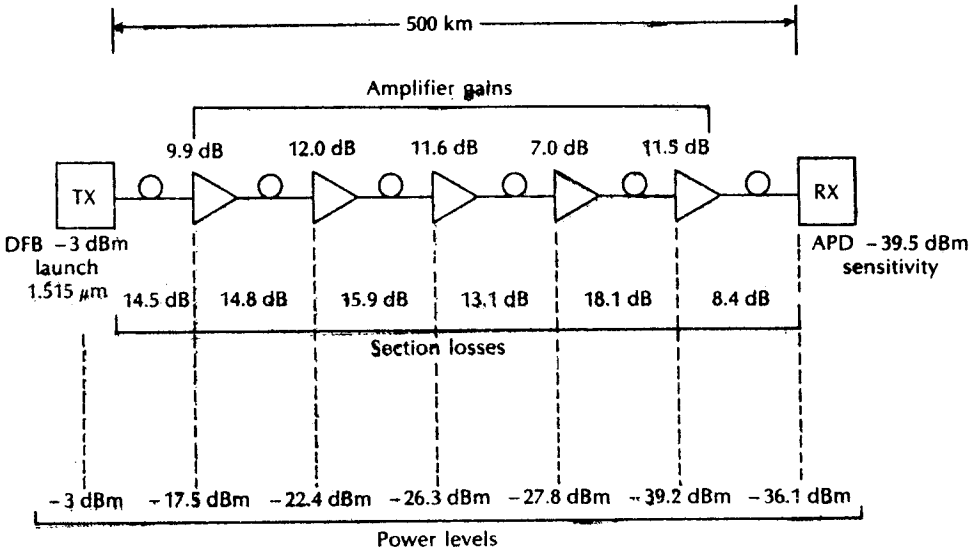

Figure 11.55 Experimental system incorporating five cascaded travelling wave semiconductor laser amplifiers [Refs. 99, 100].

occupying around 30 nm, and therefore optical filtering can be used as a method of reducing overall noise levels. It is suggested that filters with bandwidths in the range 5 to 10 nm would be required for systems spanning greater than 500 km [Ref. 100]. Nevertheless, a higher speed IM/DD optical fiber system operating at 2.4 Gbit s^{-1} over a distance of 516 km has been demonstrated by cascading ten TWSLAs [Ref. 101].

Although the technology associated with SLAs is at present more established than that of fiber amplifiers, there appear to be significant drawbacks with these former devices in relation to their active nature, mechanical structure, reliability and yield performance which may inhibit their application in future systems. By contrast, in fiber amplifiers these parameters are largely defined by the atomic structure and hence they exhibit greater stability. Furthermore, although the signal gain–bandwidth of TWSLAs is generally more appropriate to WDM applications, they are also prone to crosstalk problems which tends to limit their suitability in this area [Ref. 102].

When considering fiber amplifiers for use in WDM systems the Raman device (see Section 10.4.2) offers a gain bandwidth similar to the TWSLA (i.e. 20 to 50 nm). However, in practice there are a number of difficulties associated with the use of these fiber amplifiers. In particular, very high pump source powers of the order of 300 mW into the fiber are required to provide gains of around 15 dB [Ref. 103]. Also, the fiber length needed for the Raman fiber amplifier is generally greater than 1 km. For example, recent predictions obtained using a 10 km length device

indicated a Raman gain of 13.5 dB (net gain of 8.5 dB) when the pump power was 200 mW [Ref. 104]. Raman amplification has, however, been demonstrated in a 310 km span remotely pumped 1.8 Gbit s^{-1} IM/DD system experiment [Ref. 105]. In this case Raman amplification in the dispersion shifted fiber after the transmitter as well as before the receiver (an in-line erbium fiber amplifier was also employed) provided gains of 4.3 dB and 5.5 dB respectively. By contrast the gain provided by the remotely pumped erbium doped fiber device was 13.2 dB.

There is increasing interest in the investigation of erbium doped fiber amplifiers to provide optical gain within IM/DD optical fiber systems. Both long span and high gain operation of these devices around 1.53μm has been demonstrated [Refs. 106–108]. Moreover, typical good performance characteristics display a signal gain of 25 dB with a spectral bandwidth of 35 nm for a pump power of 50 mW at 1.49 μm [Ref. 107]. In particular, the realization of a relatively broad 3 dB spectral bandwidth for these devices has provided an impetus for their application within WDM optical fiber systems.

Recent system demonstrations have underlined the use of single erbium doped fiber amplifiers within WDM systems for small numbers of wavelength channels [Refs. 110, 111]. Furthermore, four wavelength channels, each modulated at 2.4 Gbit s^{-1} have been transmitted over 459 km using six cascaded erbium fiber amplifiers [Ref. 112]. A block schematic of this experimental system is shown in Figure 11.56. Distributed feedback (DFB) laser transmitters emitting over a range 1548.8 to 1554.7 nm were externally modulated using Mach–Zehnder IO devices (see Section 10.6.2). It may be observed from Figure 11.56 that a booster power amplifier was employed immediately after the four port coupler followed by five in-line repeater amplifiers. Moreover, the 3 dB spectral bandwidths for the amplifiers utilized were only around 10 nm.

Increased numbers of WDM channels have been demonstrated for broadcast

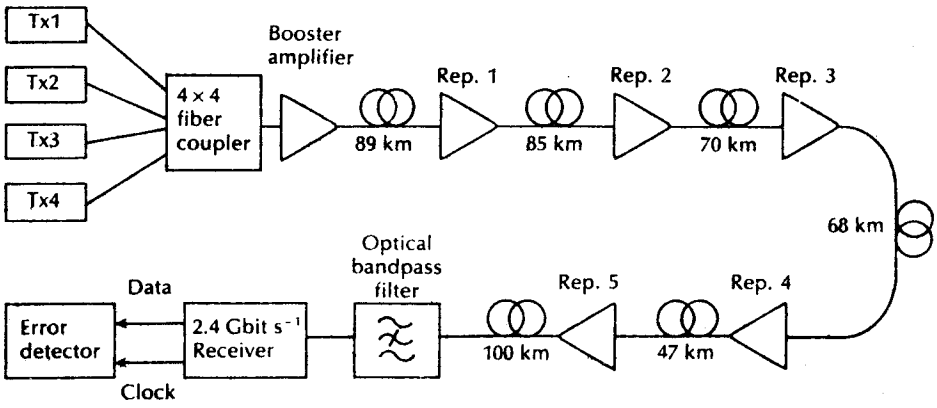

Figure 11.56 Experimental system demonstrating the transmission of four WDM channels through six cascaded erbium doped fiber amplifiers covering a distance of 459 km [Ref. 112].

network applications targeted at the future local access network and cable TV applications (see Sections 14.2.3 and 14.4.1). In particular, twelve closely spaced wavelength channels in the range 1530 to 1534 nm obtained from twelve separate DFB lasers were successfully transmitted through two erbium doped fiber amplifier stages [Ref. 113]. The spectrum provided by the twelve DFB lasers after two stages of amplification is shown in Figure 11.57. Furthermore, the use of twelve wavelength channels and two stages of erbium doped fiber amplification demonstrated the feasibility of broadcasting up to 384 digital video channels over a passive optical network with a range of 27.7 km to some 39.5 million customer terminals [Ref. 113].

The amplification of sixteen wavelength channels separated at 2 nm intervals over a range from 1527 to 1561 nm has also been demonstrated through a single erbium doped fiber amplifier stage [Ref. 114]. Again, DFB laser transmitters were employed for the transmission of either ten analog FM video signals subcarrier multiplexed (see Section 11.8.2) between 300 and 700 MHz or data at 622 Mbit s^{-1}. In this case the amplifier provided between 17 and 24 dB of gain per channel.

An advantage provided by erbium doped fiber amplifiers when used in WDM optical fiber systems is that the lifetimes associated with the lasing process in these devices are such that crosstalk in the presence of a number of wavelengths is significantly reduced. Moreover, recent a.c. crosstalk measurements suggest that the crosstalk is heavily dependent upon the modulating frequency and is negligible above a transmission rate of 140 Mbit s^{-1} [Ref. 115]. In addition, spectral broadening resulting from amplifier phase noise does not appear to be a significant

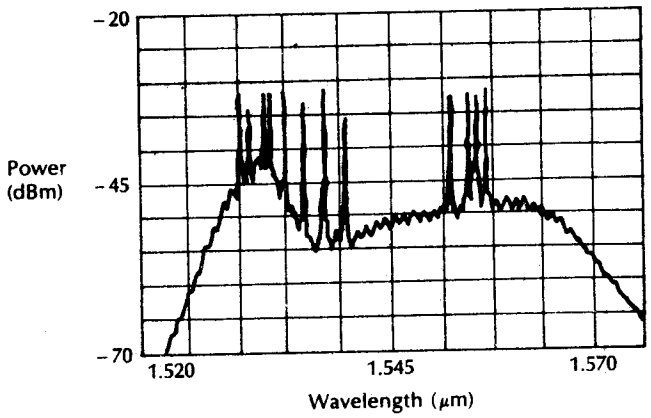

Figure 11.57 Spectrum showing twelve WDM channels after two stages of amplification using erbium doped fiber amplifiers. Reproduced with permission from A. M. Hill, R. Wyatt, J. F. Massicott, K. J. Blyth, D. S. Forrester, R. A. Lobbett, P. J. Smith and D. B. Payne, '39.5 million-way WDM broadcast network employing two stages of erbium-doped fibre amplifiers', *Electron. Lett.*, **26**, p. 1882, 1990.

problem for the operation of intensity modulated WDM long-haul or distribution systems which utilize erbium doped fiber devices [Ref. 116].

Problems

11.1 Discuss the major considerations in the design of digital drive circuits for:

(a) an LED source;
(b) an injection laser source.

Illustrate your answer with an example of a drive circuit for each source.

11.2 Outline, with the aid of suitable diagrams, possible techniques for:

(a) the linearization of LED transmitters;
(b) the maintenance of constant optical output power from an injection laser transmitter.

11.3 Discuss, with the aid of a block diagram, the function of the major elements of an optical fiber receiver. In addition, describe possible techniques for automatic gain control in APD receivers.

11.4 Equalization within an optical receiver may be provided using the simple frequency 'rollup' circuit shown in Figure 11.58(a). The normalized frequency response for this circuit is illustrated in Figure 11.58(b).

The amplifier indicated in Figure 11.58(a) presents a load of 5 kΩ to the photodetector and together with the photodetector gives a total capacitance of 5 pF. However, the desired response from the amplifier–equalizer configuration has an upper 3 dB point or corner frequency at 30 MHz. Assuming R_2 is fixed at 100 Ω determine the required values for C_1 and R_1 in order to obtain such a response.

11.5 Describe the conversion of an analog signal into a pulse code modulated waveform for transmission on a digital optical fiber link. Furthermore, indicate how several signals may be multiplexed on to a single fiber link.

A speech signal is sampled at 8 kHz and encoded using a 256 level binary code. What is the minimum transmission rate for this single pulse code modulated speech signal? Comment on the result.

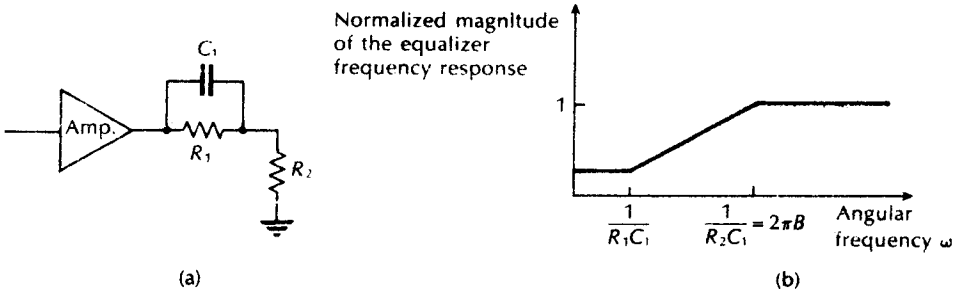

Figure 11.58 The equalizer of problem 11.4: (a) the frequency 'rollup' circuit; (b) the spectral transfer characteristic for the circuit.

11.6 A 1.5 MHz information signal with a dynamic range of 64 mV is sampled, quantized and encoded using a direct binary code. The quantization is linear with 512 levels. Determine:

(a) the maximum possible bit duration;
(b) the amplitude of one quantization level.

11.7 Describe, with the aid of a suitable block diagram, the operation of an optical fiber regenerative repeater. Indicate reasons for the occurrence of bit errors in the regeneration process and outline a technique for establishing the quality of the channel.

11.8 Twenty-four 4 kHz speech channels are sampled, quantized, encoded and then time division multiplexed for transmission as binary PCM on a digital optical fiber link. The quantizer is linear with 0.5 mV steps over a dynamic range of 2.048 V.

Calculate:

(a) the frame length of the PCM transmission, assuming an additional channel time slot is used for signalling and synchronization;
(b) the required channel bandwidth assuming NRZ pulses.

11.9 Develop a relationship between the error probability and the received SNR (peak signal power to rms noise power ratio) for a baseband binary optical fiber system. It may be assumed that the number of ones and zeros are equiprobable and that the decision threshold is set midway between the one and zero level.

The electrical SNR (defined as above) at the digital optical receiver is 20.4 dB. Determine:

(a) the optical SNR;
(b) the BER.

It may be assumed that $\text{erfc}\ (3.71) \simeq 1.7 \times 10^{-7}$.

11.10 The error function (erf) is defined in the text by Eq. (11.16). However, an error function also used in communications is defined as:

$$\text{Erf}(u) = \frac{1}{\sqrt{(2\pi)}} \int_{-\infty}^{u} \exp\ (-x^2/2)\ \mathrm{d}x$$

where a capital E is used to denote this form of the error function. The corresponding complementary error function is:

$$\text{Erfc}(u) = 1 - \text{Erf}(u) = \frac{1}{\sqrt{(2\pi)}} \int_{u}^{\infty} \exp\ (-x^2/2)\ \mathrm{d}x$$

This complementary error function is also designated as $Q(u)$ in certain texts. Use of $\text{Erfc}(u)$ or $Q(u)$ is sometimes considered more convenient within communication systems.

Develop a relationship for $\text{erfc}(u)$ in terms of $\text{Erfc}(u)$. Hence, obtain an expression for the error probability $P(e)$ as a function of the Erfc for a binary digital optical fiber system where the decision threshold is set midway between the one and zero levels and the number of transmitted ones and zeros are equiprobable. In addition, given that $\text{Erfc}\ (4.75) \simeq 1 \times 10^{-6}$ estimate the required peak signal power to rms noise power ratios (both optical and electrical) at the receiver of such a system in order to maintain a BER of 10^{-6}.

11.11 Show that Eq. (9.27) reduces to Eq. (11.28). Hence determine $F(M)$ when $k = 0.3$ and $M = 20$.

11.12 A silicon APD detector is utilized in a baseband binary PCM receiver where the decision threshold is set midway between the one and zero signal level. The device has a quantum efficiency of 70% and a ratio of carrier ionization rates of 0.05. In operation the APD has a multiplication factor of 65. Assuming a raised cosine signal spectrum and a zero disparity code, and given that erfc $(4.47) \simeq 2 \times 10^{-10}$:

(a) estimate the number of photons required at the receiver to register a binary one with a BER of 10^{-10};

(b) calculate the required incident optical power at the receiver when the system is operating at a wavelength of 0.9 μm and a transmission rate of 34 Mbit s^{-1};

(c) indicate how the value obtained in (b) should be modified to compensate for a 3*B*4*B* line code.

11.13 A p–i–n photodiode receiver requires 2×10^4 incident photons in order to register a binary one with a BER of 10^{-9}. The device has a quantum efficiency of 65%. Estimate in decibels the additional signal level required in excess of the quantum limit for this photodiode to maintain a BER of 10^{-9}.

11.14 An optical fiber system employs an LED transmitter which launches an average of 300 μW of optical power at a wavelength of 0.8 μm into the optical fiber cable. The cable has an overall attenuation (including joints) of 4 dB km^{-1}. The APD receiver requires 1200 incident photons in order to register a binary one with a BER of 10^{-10}. Determine the maximum transmission distance (without repeaters) provided by the system when the transmission rate is 1 Mbit s^{-1} and 1 Gbit s^{-1} such that a BER of 10^{-10} is maintained.

Hence sketch a graph showing the attenuation limit on transmission distance against the transmission rate for the system.

11.15 An optical fiber system uses fiber cable which exhibits a loss of 7 dB km^{-1}. Average splice losses for the system are 1.5 dB km^{-1}, and connector losses at the source and detector are 4 dB each. After safety margins have been allowed, the total permitted channel loss is 37 dB. Assuming the link to be attenuation limited, determine the maximum possible transmission distance without a repeater.

11.16 Assuming a linear increase in pulse broadening with fiber length, show that the transmission rate $B_T(DL)$ at which a digital optical fiber system becomes dispersion limited is given by:

$$B_T(DL) \simeq \frac{(\alpha_{dB} + \alpha_j)}{5\sigma_T(\text{km})} \frac{1}{10 \log_{10}(P_i/P_o)}$$

where σ_T(km) is the total rms pulse broadening per kilometre on the link (hint: refer to Eqs. (3.3) and (3.11)).

(a) A digital optical fiber system using an injection laser source displays rms pulse broadening of 1 ns km^{-1}. The fiber cable has an attenuation of 3.5 dB km^{-1} and joint losses average out to 1 dB km^{-1}. Estimate the transmission rate at the dispersion limit when the difference in optical power levels between the input and output is 40 dB.

(b) Calculate the dispersion limited transmission distance for the system described in (a) when the transmission rates are 1 Mbit s^{-1} and 1 Gbit s^{-1}. Hence sketch a graph showing the dispersion limit on transmission distance against the transmission rate for the system.

11.17 The digital optical fiber system described in problem 11.16(a) has a transmission rate of 50 Mbit s^{-1} and operates over a distance of 12 km without repeaters. Assuming Gaussian shaped pulses, calculate the dispersion–equalization penalty exhibited by the system for the cases when:

(a) there is no mode coupling; and

(b) there is mode coupling.

11.18 A digital optical fiber system uses an RZ pulse format. Show that the maximum bit rate for the system $B_T(\text{max})$ may be estimated using the expression:

$$B_T(\text{max}) = \frac{0.35}{T_{syst}}$$

where T_{syst} is the total system rise time. Comment on the possible use of the factor 0.44 in place of 0.35 in the above relationship.

An optical fiber link is required to operate over a distance of 10 km without repeaters. The fiber available exhibits a rise time due to intermodal dispersion of 0.7 ns km^{-1}, and a rise time due to intramodal dispersion of 0.2 ns km^{-1}. In addition the APD detector has a rise time of 1 ns. Estimate the maximum rise time allowable for the source in order for the link to be successfully operated at a transmission rate of 40 Mbit s^{-1} using an RZ pulse format.

11.19 An edge-emitting LED operating at a wavelength of 1.3 μm launches −22 dBm of optical power into a single-mode fiber pigtail. The pigtail is connected to a single-mode fiber link which exhibits an attenuation of 0.4 dB km^{-1} at this wavelength. In addition, the splice losses on the link provide an average loss of 0.05 dB km^{-1}. The transmission rate of the system is 280 Mbit s^{-1} so that the sensitivity of the *p–i–n* photodiode receiver is −35 dBm. Penalties on the link require an allowance of 1.5 dB and a safety margin of 6 dB is also specified. If the connector losses at the LED transmitter and *p–i–n* photodiode receiver are each 1 dB, calculate the unrepeatered distance over which the link will operate.

11.20 A digital single-mode optical fiber system is designed for operation at a wavelength of 1.5 μm and a transmission rate of 560 Mbit s^{-1} over a distance of 50 km without repeaters. The single-mode injection laser is capable of launching a mean optical power of −13 dBm into the fiber cable which exhibits a loss of 0.25 dB km^{-1}. In addition, average splice losses are 0.1 dB at 1 km intervals. The connector loss at the receiver is 0.5 dB and the receiver sensitivity is −39 dBm. Finally, an extinction ratio penalty of 1 dB is predicted for the system. Perform an optical power budget for the system and determine the safety margin.

11.21 Briefly discuss the reasons for the use of block codes in digital optical fiber transmission. Indicate the advantages and drawbacks when a *5B6B* code is employed.

11.22 A D–IM analog optical fiber system utilizes a *p–i–n* photodiode receiver. Derive an expression for the rms signal power to rms noise power ratio in the quantum limit for this system.

The *p–i–n* photodiode in the above system has a responsivity of 0.5 at the operating wavelength of 0.85 μm. Furthermore the system has a modulation index of 0.4 and transmits over a bandwidth of 5 MHz. Sketch a graph of the quantum limited receiver sensitivity against the received SNR (rms signal power to rms noise power) for the system over the range 30 to 60 dB. It may be assumed that the photodiode dark current is negligible.

11.23 In practice, the analog optical fiber receiver of Problem 11.22 is found to be thermal noise limited. The mean square thermal noise current for the receiver is

2×10^{-23} A^2 Hz^{-1}. Determine the peak to peak signal power to rms noise power ratio at the receiver when the average incident optical power is -17.5 dBm.

11.24 An analog optical fiber system has a modulation bandwidth of 40 MHz and a modulation index of 0.6. The system utilizes an APD receiver with a responsivity of 0.7 and is quantum noise limited. An SNR (rms signal power to rms noise power) of 35 dB is obtained when the incident optical power at the receiver is -30 dBm. Assuming the detector dark current may be neglected, determine the excess avalanche noise factor at the receiver.

11.25 A simple analog optical fiber link operates over a distance of 15 m. The transmitter comprises an LED source which emits an average of 1 mW of optical power into air when the drive current is 40 mA. Plastic fiber cable with an attenuation of 500 dB km^{-1} at the transmission wavelength is utilized. The minimum optical power level required at the receiver for satisfactory operation of the system is 5 μW. The coupling losses at the transmitter and receiver are 8 and 2 dB respectively. In addition, a safety margin of 4 dB is necessary. Calculate the minimum LED drive current required to maintain satisfactory system operation.

11.26 An analog optical fiber system employs an LED which emits 3 dBm mean optical power into air. However, a coupling loss of 17.5 dB is encountered when launching into a fiber cable. The fiber cable which extends for 6 km without repeaters exhibits a loss of 5 dB km^{-1}. It is spliced every 1.5 km with an average loss of 1.1 dB per splice. In addition, there is a connector loss at the receiver of 0.8 dB. The PIN–FET receiver has a sensitivity of -54 dBm at the operating bandwidth of the system. Assuming there is no dispersion–equalization penalty, perform an optical power budget for the system and establish a safety margin.

11.27 Indicate the techniques which may be used for analog optical fiber transmission where an electrical subcarrier is employed. Illustrate your answer with a system block diagram showing the multiplexing of several signals onto a single analog optical fiber link.

11.28 Subcarrier amplitude modulation (AM–IM) is employed on the RF carriers of an analog optical fiber system. When a large number of the RF subcarriers, each with random phases, are frequency division multiplexed, then they add on a power basis so that the optical modulation index m is related to the per-channel modulation index m_k by:

$$m = \left(\sum_{k=1}^{N} m_k^2 \right)^{\frac{1}{2}}$$

where N equals the number of channels. An FDM signal incorporates eighty AM subcarriers. When forty of these signals have a per-channel modulation index of 2%, twenty signals have a 3% and the other twenty signals a 4% per channel modulation index, calculate the optical modulation index of the transmitter.

11.29 A narrowband FM–IM optical signal has a maximum frequency deviation of 120 kHz when the frequency deviation ratio is 0.2. Compare the post detection SNR of this signal with that of a DSB–IM optical signal having the same modulating signal power, bandwidth, detector photocurrent and noise. Also estimate the bandwidth of the FM–IM signal. Comment on both results.

11.30 A frequency division multiplexed optical fiber system uses FM–IM. It has fifty equal amplitude voice channels each bandlimited to 3.5 kHz. A 1 kHz guard band is

provided between the channels and below the first channel. The peak frequency deviation for the system is 1.35 MHz. Determine the transmission bandwidth for this FDM system.

11.31 An FM–IM system utilizes pre-emphasis and de-emphasis to enhance its performance in noise [Ref. 65]. The de-emphasis filter is a first order RC low pass filter placed at the demodulator to reduce the total noise power. This filter may be assumed to have an amplitude response $H_{de}(\omega)$ given by:

$$|H_{de}(\omega)| = \frac{1}{1 + (\omega/\omega_c)^2}$$

where $\omega_c = 2\pi f_c = 1/RC$.

The SNR improvement over FM–IM without pre-emphasis and de-emphasis is given by:

$$SNR_{de}\ improvement = \frac{1}{3}\left(\frac{B_a}{f_c}\right)^2$$

where B_a is the bandwidth of the baseband signal and $f_c \ll B_a$.

(a) Write down an expression for the amplitude response of the pre-emphasis filter so that there is no overall signal distortion.

(b) Deduce an expression for the post detection SNR improvement in decibels for the FM–IM system with pre-emphasis and de-emphasis over a D–IM system operating under the same conditions of modulating signal power and bandwidth, photocurrent and noise. It may be assumed that $f_c \ll B_a$.

(c) A baseband signal with a bandwidth of 300 kHz is transmitted using the FM–IM system with pre-emphasis and de-emphasis. The maximum frequency deviation for the system is 4 MHz. In addition the de-emphasis filter comprises a 500 Ω resistor and a 0.1 μF capacitor. Determine the post detection SNR improvement for this system over a D–IM system operating under the same conditions of modulating signal power and bandwidth, photocurrent and noise.

11.32 A PM–IM optical fiber system operating above threshold has a frequency deviation ratio of 15 and a transmission bandwidth of 640 kHz.

(a) Estimate the bandwidth of the baseband message signal.

(b) Compute the post detection SNR improvement for the system over a D–IM system operating with the same modulating signal power and bandwidth, detector photocurrent and noise.

11.33 Discuss the advantages and drawbacks of the various pulse analog techniques for optical fiber transmission. Describe the operation of a PFM–IM optical fiber system employing regenerative baseband recovery.

11.34 An optical fiber PFM–IM system uses regenerative baseband recovery. The optical receiver which incorporates a *p–i–n* photodiode has an optimized bandwidth of 125 MHz. The other system parameters are:

Nominal pulse rate	35 MHz
Peak to peak frequency deviation	8 MHz
p–i–n photodiode responsivity	0.6 $A\,W^{-1}$
Baseband noise bandwidth	10 MHz
Receiver mean square noise current	$3 \times 10^{-25}\ A^2\,Hz^{-1}$

(a) Calculate the peak level of incident optical power necessary at the receiver to maintain a peak to peak signal power to rms noise power ratio of 60 dB.
(b) The source and detector have rise times of 3.5 and 5.0 ns respectively. Estimate the maximum permissible total rise time for the fiber cable utilized in the system such that satisfactory operation is maintained. Comment on the value obtained.

11.35 Considering the bus and star distribution systems of Example 11.18, compare the losses associated with the addition of an extra node when the original number of nodes is twelve. How does this alter if the connector losses increase to 1.5 dB and the distance between the nodes on the bus/combined length of two arms from the star hub increases to 400 m? Comment on the results.

11.36 An optical fiber data bus is to be implemented to interconnect nine stations, each separated by 50 m. Multimode fiber cable with an attenuation of 3 dB km^{-1} is to be used along with LED transmitters which launch 200 μW of optical power into their fiber pigtails. The PIN–FET hybrid receivers have a sensitivity of -50 dBm at the desired BER, whilst the connector losses are 1.1 dB each. The access couplers to be used have a tap ratio or power tap-off factor of 8% together with an insertion loss of 0.9 dB. Finally, the beam splitter can be assumed to have a loss of 3 dB. Determine the safety margin for the system when considering the highest loss terminal interconnection path.

11.37 Repeat Problem 11.36 when considering a thirty terminal star distribution network where the combined distance in the two fiber cable arms is 200 m and the excess loss of the star coupler hub is 3.4 dB. Comment on the result.

11.38 Compare and contrast the merits and drawbacks associated with the advanced multiplexing techniques discussed in Section 11.9. Comment on the possibilities for combining two of the techniques in order to provide increased information transfer.

11.39 Describe, with the aid of simple sketches, the ways in which optical amplifiers may be configured on long-haul telecommunication links in order to provide both bidirectional and multichannel optical transmission.

Suggest how optical amplifiers might be incorporated into optical fiber distribution systems to facilitate the interconnection of a larger number of nodes.

11.40 It is desired to obtain the maximum signal to noise ratio on a single-mode fiber communication link incorporating cascaded travelling wave SLAs. If only noise considerations are taken into account, determine the optimum length between the amplifier repeaters when the system is operating at:

(a) a wavelength of 1.3 μm where the fiber cable and joint losses are 0.41 dB km^{-1} and 0.04 dB km^{-1} respectively; and
(b) a wavelength of 1.55 μm where the fiber cable and joint losses are 0.20 dB km^{-1} and 0.02 dB km^{-1} respectively.

Comment on the values obtained.

11.41 The following specifications are envisaged for a single-mode fiber communication system employing cascaded travelling wave SLAs:

operating wavelength:	1.30 μm
power launched at transmitter:	2 dBm
fiber cable loss:	0.40 dB km^{-1}
fiber splice losses:	0.02 dB km^{-1}
K (amplifiers):	6
amplifier separation:	50 km
received SNR:	20 dB

Assuming amplifier noise to be the limiting factor estimate the maximum transmission rate allowed for the system when the total system length is 8000 km.

11.42 The SNR at the transmitter output for a single-mode fiber system employing cascaded travelling wave SLAs is 48.6 dB. The final SLA is positioned as a preamplifier to the optical receiver on the link and the output SNR from this device is 15 dB. In addition the amplifiers each have a noise figure of 4.5 dB and a fiber to fiber gain of 9.7 dB, and the attenuation of the link prior to each amplifier is 5.2 dB. Assuming the SNR position to remain constant, how many amplifiers can be cascaded on the link?

Answers to numerical problems

11.4 53.0 pF, 472 Ω
11.5 64 kbit s^{-1}
11.6 (a) 37 ns; (b) 125 μV
11.8 (a) 300 bits; (b) 1.2 MHz
11.9 (a) 10.2 dB; (b) 3.4×10^{-7}
11.10 $P(e) = \text{Erfc}\,|(S/N)^{1/2}|$, 9.8 dB, 19.6 dB
11.11 7.4
11.12 (a) 1400; (b) −52.8 dBm; (c) −51.8 dBm
11.13 27.9 dB
11.14 15.76 km, 8.26 km
11.15 3.41 km
11.16 (a) 22.5 Mbit s^{-1}; (b) 200 km, 0.2 km
11.17 (a) 16.6 dB; (b) 0.1 dB.
11.18 3.04 ns
11.19 7.8 km
11.20 2.1 dB
11.22 40 nW, 40 μW
11.23 52.1 dB
11.24 3.1
11.25 35.5 mA
11.26 5.4 dB
11.28 25.7%
11.29 Ratio of output SNRs (rms signal power to rms noise power) for FM–IM to DSB–IM is −9.21 dB, 1200 kHz
11.30 3.15 MHz
11.31 (a) $1 + (\omega/\omega_c)^2$; (b) $-3 + 20 \log_{10}(D_f B_a / f_c)$; (c) 59.0 dB
11.32 (a) 20 kHz; (b) 20.5 dB
11.34 (a) −24.4 dBm; (b) 4.6 ns
11.35 3.5 dB, 0.35 dB, 6.0 dB, 0.35 dB
11.36 3.7 dB
11.37 19.8 dB
11.40 (a) 9.6 km; (b) 19.7 km
11.41 858 Mbit s^{-1} (RZ)
11.42 87

References

[1] C. C. Timmermann, 'Highly efficient light coupling from GaAlAs lasers into optical fibers', *Appl. Opt.*, **15**(10), pp. 2432–2433, 1976.

[2] M. Maeda, I. Ikushima, K. Nagano, M. Tanaka, H. Naskshima, R. Itoh, 'Hybrid laser to fiber coupler with a cylindrical lens', *Appl. Opt.*, **16**(7), pp. 1966–1970, 1977.

[3] R. W. Dawson, 'Frequency and bias dependence of video distortion in Burrus-type homostructure and heterostructure LED's', *IEEE Trans Electron. Devices*, **ED-25**(5), pp. 550–553, 1978.

[4] J. Strauss, 'The nonlinearity of high-radiance light-emitting diodes', *IEEE J. Quantum Electron.*, **QE-14**(11), pp. 813–819, 1978.

[5] K. Asatani and T. Kimura, 'Non-linear phase distortion and its compensation in LED direct modulation', *Electron. Lett.*, **13**(6), pp. 162–163, 1977.

[6] G. White and C. A. Burrus, 'Efficient 100 Mb/s driver for electroluminescent diodes', *Int. J. Electron.*, **35**(6), pp. 751–754, 1973.

[7] P. W. Shumate Jr and M. DiDomenico Jr, 'Lightwave transmitters', in H. Kressel (Ed.), *Semiconductor Devices for Optical Communications, Topics in Applied Physics*, Volume 39, pp. 161–200, Springer-Verlag, 1982

[8] L. Foltzer, 'Low-cost transmitters, receivers serve well in fibre-optic links', *EDN*, pp. 141–146, 20 October 1980.

[9] A. Albanese and H. F. Lenzing, 'Video transmission tests, performed on intermediate-frequency light wave entrance links', *J. SMPTE (USA)*, **87**(12), pp. 821–324, 1978.

[10] J. Strauss, 'Linearized transmitters for analog fiber links', *Laser Focus (USA)*, **14**(10), pp. 54–61, 1978.

[11] A. Prochazka, P. Lancaster and R. Neumann, 'Amplifier linearization by complementary pre or post distortion', *IEEE Trans. Cable Telev.*, **CATV-1**(1), pp. 31–39, 1976.

[12] K. Asatani and T. Kimura, 'Nonlinear distortions and their compensations in light emitting diodes', *Proceeding of International Conference on Integrated Optics and Optical Fiber Communications*, p. 105, 1977.

[13] K. Asatani and T. Kimura, 'Linearization of LED nonlinearity by predistortions', *IEEE J. Solid State Circuits*, **SC-13**(1), pp. 133–138, 1978.

[14] J. Strauss, A. J. Springthorpe and O. I. Szentesi, 'Phase shift modulation technique for the linearisation of analogue optical transmitters', *Electron. Lett.*, **13**(5), pp. 149–151, 1977.

[15] J. Strauss and D. Frank, 'Linearisation of a cascaded system of analogue optical links', *Electron. Lett.*, **14**(14), 436–437, 1978.

[16] H. S. Black, US Patent 1686792, issued Oct 9, 1929.

[17] B. S. Kawasaki and K. O. Hill, 'Low-loss access coupler for multimode optical fiber distribution network', *Appl. Opt.*, **16**(7), p. 1794, 1977.

[18] J. Strauss and O. I. Szentesi, 'Linearisation of optical transmitters by a quasifeedforward compensation technique', *Electron. Lett.*, **13**(6), pp. 158–159, 1977.

[19] S. M. Abbott, W. M. Muska, T. P. Lee, A. G. Dentai and C. A. Burrus, '1.1 Gb/s pseudorandom pulse-code modulation of 1.27μm wavelength CW InGaAsP/InP DH lasers', *Electron. Lett.*, **14**(11), pp. 349–350, 1978.

[20] J. Gruber, P. Marten, R. Petschacher and P. Russer, 'Electronic circuits for high bit rate digital fiber optic communication systems', *IEEE Trans. Commun.*, **COM-26**(7), pp. 1088–1098, 1978.

[21] P. K. Runge, 'An experimental 50 Mb/s fiber optic PCM repeater', *IEEE Trans. Commun.*, **COM-24**(4), pp. 413–418, 1976.

[22] U. Wellens, 'High-bit-rate pulse regeneration and injection laser modulation using a diode circuit', *Electron. Lett.*, **13**(18), pp. 529–530, 1977.

[23] A. Chappell (Ed.), *Optoelectronics: Theory and Practice*, McGraw-Hill, 1978.

[24] S. R. Salter, D. R. Smith, B. R. White and R. P. Webb, 'Laser automatic level control for optical communications systems', *Third European Conf. on Optical Communications*, Munich, September 1977, VDE-Verlag GmbH, Berlin, 1977.

[25] A. Fausone, 'Circuit considerations', *Optical Fibre Communication*, by Tech. Staff of CSELT, pp. 777–800, McGraw-Hill, 1981.

[26] A. Moncalvo and R. Pietroiusti, 'Transmission systems using optical fibres', *Telecommunication J. (Switzerland)*, **49**, pp. 84–92, 1982.

[27] S. D. Personick, 'Design of receivers and transmitters for fibre systems', in M. K. Barnoski (Ed.), *Fundamentals of Optical Fiber Communications* (2nd edn), pp 295–328, Academic Press, 1981.

[28] T. L. Maione and D. D. Sell, 'Experimental fiber-optic trransmission system for interoffice trunks', *IEEE Trans. Commun.*, **COM-25**(5), pp. 517–522, 1977.

[29] R. G. Smith and S. D. Personick, 'Receiver design for optical fibre communication systems', in H. Kressel (Ed.), *Semiconductor Devices for Optical Communications*, Topics in Advanced Physics, Vol. 39, pp. 88–160, Springer-Verlag, 1982.

[30] R. G. Smith, C. A. Brackett and H. W. Reinbold, 'Atlanta fiber system experiment, optical detector package', *Bell Syst. Tech. J.*, **57**(6), pp. 1809–1822, 1978.

[31] J. L. Hullett and T. V. Muoi, 'A feedback amplifier for optical transmission systems', *IEEE Trans. Commun.*, **COM-24**, pp. 1180–1185, 1976.

[32] J. L. Hullett, 'Optical communication receivers', *Proc. IREE Australia*, pp. 127–134, September 1979.

[33] N. J. Bradley, 'Fibre optic systems design', *Electronic. Eng.*, pp. 98–101, mid April 1980.

[34] T. L. Maione, D. D. Sell and D. H. Wolaver, 'Practical 45 Mb/s regenerator for lightwave transmission', *Bell Syst. Tech. J.*, **57**(6), pp. 1837–1856, 1978.

[35] S. D. Personick, 'Receiver design for optical systems', *Proc. IEEE*, **65**(12), pp. 1670–1678, 1977.

[36] J. E. Goell, 'Input amplifiers for optical PCM receivers', *Bell Syst. Tech. J.*, **53**(9), pp. 1771–1793, 1974.

[37] S. D. Personick, 'Time dispersion in dielectric waveguides', *Bell Syst. Tech. J.*, **50**(3), pp. 843–859, 1971.

[38] I. Garrett 'Receivers for optical fibre communications', *Radio Electron. Eng. J. IERE*, **51**(7/8). pp. 349–361, 1981.

[39] S. D. Personick, 'Receiver design', in S. E. Miller and A. G. Chynoweth (Eds.), *Optical Fiber Telecommunications*, pp. 627–651, Academic Press Inc., 1979.

[40] A. Moncalvo and L. Sacchi, 'System considerations', *Optical Fibre Communication*, by Tech. Staff of CSELT, pp. 723–776, McGraw-Hill, 1981.

[41] M. Rocks and R. Kerstein, 'Increase in fiber bandwidth for digital systems by means of multiplexing', *ICC 80 1980 International Conf. on Commun.*, Seattle, WA, USA, Part 28, 5/1–5, June 1980.

[42] W. Koester and F. Mohr, 'Bidirectional optical link', *Electrical Commun.*, **55**(4), pp. 342–349, 1980.

[43] H. Taub and D. L. Schilling, *Principles of Communication System* (2nd edn), McGraw-Hill, 1986.

[44] P. Hensel and R. C. Hooper, 'The development of high performance optical fibre data links', *IERE Conference Proceedings Fibre Optics*, 1–2 March 1982 (London) pp. 91–98, 1982.

[45] D. C. Gloge and T. Li, 'Multimode-fiber technology for digital transmission', *Proc. IEEE*, **68**(10), pp. 1269–1275, 1980.

[46] G. E. Stillman,: 'Design consideration, for fibre optic detectors', *Proc. SPIE Int. Soc. Opt. Eng. (USA)*, **239**, pp. 42–52, 1980.

[47] P. P. Webb, R. J. McIntyre and J. Conradi, 'Properties of avalanche photodiodes', *RCA Rev.*, **35**, pp. 234–278, 1974.

[48] J. E. Midwinter, *Optical Fibers for Transmission*, John Wiley, 1979.
[49] I. Garrett and J. E. Midwinter, 'Optical communication systems', in M. J. Howes and D. V. Morgan (Eds.), *Optical Fibre Communications: Devices, Circuits, and Systems*, pp. 251–300, John Wiley, 1980.
[50] R. J. McIntyre and J. Conradi, 'The distribution of gains in uniformly multiplying avalanche photodiodes', *IEEE Trans. Electron. Devices*, **ED-19**, pp. 713–718, 1972.
[51] K. Mouthaan, 'Teleconmunications via glass–fibre cables', *Philips Telecommun. Rev.*, **37**(4), pp. 201–214, 1979.
[52] H. F. Wolf, 'System aspects', in H. F. Wolf (Ed.), *Handbook of Fiber Optics: Theory and applications*, pp. 377–427, Granada, 1979.
[53] S. D. Personick, N. L. Rhodes, D. C. Hanson and K. H. Chan, 'Contrasting fiber-optic-component-design requirements in telecommunications, analog, and local data communications applications', *Proc. IEEE*, **68**(10), pp. 1254–1262, 1980.
[54] S. E. Miller, 'Transmission system design', in S. E. Miller and A. G. Chynoweth (Eds.), *Optical Fiber Telecommunications*, pp. 653–683, Academic Press, 1979.
[55] C. K. Koa, *Optical Fiber Systems: Technology, design and applications*, McGraw-Hill, 1982.
[56] C. Kleekamp and B. Metcalf, *Designer's Guide to Fiber Optics*, Cahners Publishing Company, 1978.
[57] G. R. Elion and H. A. Elion, *Fiber Optics in Communications Systems*, Marcel Dekker, 1978.
[58] S. Shimada, 'Systems engineering for long-haul optical-fiber transmission', *Proc. IEEE*, **68**(10), pp. 1304–1309, 1980.
[59] J. H. C. van Heuven, 'Techniques for optical transmission', in *Proceedings of 11th European Microwave Conference*, Amsterdam, Netherlands, pp. 3–10, 1981.
[60] R. Tell and S. T. Eng, 'Optical fiber communication at 5 Gbit/sec', *Appl. Opt.*, **20**(22), pp. 3853–3858, 1981.
[61] P. Wells, 'Optical-fibre systems for telecommunications', *GEC J. Sci. Tech.*, **46**(2), pp. 51–60, 1980.
[62] M. Chown and K. C. Koa, 'Some broadband fiber system design considerations', in *Proceedings of IEEE International Conference on Communications*, Philadelphia PA, 1972, pp. 12/1–5, IEEE, 1972.
[63] I. Garrett and C J. Todd, 'Optical fiber transmission systems at 1.3 and 1.5 μm wavelength', in *Proceedings of IEEE 1981 International Conference on Communications*, New York, Vol. 1, Pt. 16,2/1–5, IEEE, 1981.
[64] J. L. Hullett and T. V. Muoi, 'Optical fiber systems analysis', *Proc. IREE Australia*, **38**(1–2), pp. 390–397, 1977.
[65] A. Luvison, Topics in optical fibre communication theory', *Optical Fibre Communications*, by Technical Staff of CSELT, pp. 647–721, McGraw-Hill; 1981.
[66] S. Kawanishi, N. Yoshikai, J.-I. Yamada and K. Nakagawa, 'DmBIM code and its performance, in a very high-speed optical transmission system', *IEEE Trans. on Commun.*, **36**(8), pp. 951–956, 1988.
[67] M. Chown, A. W. Davis, R. E. Epworth and J. G. Farrington, 'System design', in C. P. Sandbank (Ed.), *Optical Fibre Communication Systems*, pp. 206–283, John Wiley, 1980.
[68] K. Sam Shanmugan, *Digital and Analog Communication Systems*, John Wiley, 1979
[69] S. Y. Suh, 'Pulse width modulation for analog fiber-optic communications', *J. of Lightwave Technol.*, **LT-5**(1), pp. 102–112, 1987.

[70] G. G. Windus, 'Fibre optic systems for analogue transmission', *Marconi Rev.*, **XLIV**(221), pp. 78–100, 1981.

[71] W. Horak, 'Analog TV signal transmission over multimode optical waveguides', *Siemens Research and Development Reports*, **5**(4), pp. 192–202, 1976.

[72] K. Sato and K. Asatani, 'Analogue baseband TV transmission experiments using semiconductor laser diodes', *Electron. Lett.*, **15**(24), pp. 794–795, 1979.

[73] R. M. Gagliadi and S. Karp, *Optical Communications*, John Wiley, 1976.

[74] C. C. Timmerman, 'Signal to noise ratio of a video signal transmitted by a fiber-optic system using pulse-frequency modulation', *IEEE Trans. Broadcasting*, **BC-23**(1), pp. 12–16, 1976.

[75] C. C. Timmerman, 'A fiber optical system using pulse frequency modulation', *NTZ*, **30**(6), pp. 507–508, 1977.

[76] D. J. Brace and D. J. Heatley, 'The application of pulse modulation schemes for wideband distribution to customers (integrated optical fibre systems)', in *Sixth European Conference on Optical Communication*, York, UK, 16–19 Sept. 1980, pp. 446–449, 1980.

[77] E. Yoneda, T. Kanada and K. Hakoda, 'Design and performance of optical fibre transmission systems for color television signals', *Rev. Elect. Commun. Lab.*, **29**(11–12), pp. 1107–1117, 1981.

[78] T. Kanada, K. Hakoda and E. Yoneda, 'SNR fluctuation and nonlinear distortion in PFM optical NTSC video transmission systems', *IEEE Trans. Commun.*, **COM-30**(8), pp. 1868–1875, 1982.

[79] S. F. Heker, G. J. Herskowitz, H. Grebel and H. Wichansky, 'Video transmission in optical fiber communication systems using pulse frequency modulation', *IEEE Trans. on Commun.*, **36**(2), pp. 191–194, 1988.

[80] S. Fujita, M. Kitamura, T. Torikai, N. Henmi, H. Yamada, T. Suzaki, I. Takano and M. Shikada, '10 Gbit/s, 100 km optical fibre transmission experiment using high-speed MQW DFB-LD and back illuminated GaInAs APD', *Electron. Lett.*, **25**(11), pp. 702–703, 1989.

[81] R. S. Tucker, G. Eisenstein, S. K. Korotky, U. Koren, G. Raybon, J. J. Veselka, L. L. Buhl, B. L. Kasper and R. C. Alferness, 'Optical time-division multiplexing in a multigigabit/second fibre transmission system', *Electron. Lett.*, **23**(5), pp. 208–209, 1987.

[82] R. C. Alferness, 'Multigigabit fibre optics', *Communications International*, **15**(4), pp. 42–51, 1988.

[83] T. E. Darcie, M. E. Dixon, B. L. Kasper and C. A. Burrus, 'Lightwave system using microwave subcarrier multiplexing', *Electron. Lett.*, **22**(15), pp. 774–775, 1986.

[84] R. Olshansky and V. A. Lanziera, '60 channel FM video subcarrier multiplexed optical communications system', *Electron. Lett.*, **23**, pp. 1196–1197, 1987.

[85] T. E. Darcie, P. P. Iannone, B. L. Kasper, J. R. Talman, C. A. Burrus and T. A. Baker, 'Wide-band lightwave distribution system using subcarrier multiplexing', *J. of Lightwave Technol.*, **7**(6), pp. 997–1005, 1989.

[86] R. Olshansky and V. A. Lanziera, 'Subcarrier multiplexed lightwave systems for broad-band distribution', *J. of Lightwave Technol.*, **7**(9), pp. 1329–1342, 1989.

[87] T. E. Darcie, 'Subcarrier multiplexing for lightwave networks and video distribution systems', *IEEE J. on Selected Areas in Commun.*, **8**(7), pp. 1240–1248, 1990.

[88] M. Maeda and M. Yamamoto, 'FM–FDM optical CATV transmission experiment

and system design for MUSE HDTV signals', *IEEE J. on Selected Areas in Commun.*, **8**(7), pp. 1257–1267, 1990.

[89] P. A. Rosher and S. C. Fenning, 'Multichannel video transmission over 100 km of step index single mode fibre using a directly modulated distributed feedback laser', *Electron. Lett.*, **26**(8), pp. 534–536, 1990.

[90] A. C. Carter, 'Wavelength multiplexing for enhanced fibre-optic performance', *Telecommunications*, pp. 30–36, October 1986.

[91] H. Kobrinski, R. M. Bulley, M. S. Goodman, M. P. Vecchi and C. A. Brackett, 'Demonstration of high capacity in the LAMBDANET architecture: a multiwavelength optical network', *Electron. Lett.*, **23**(16), pp. 824–826, 1987.

[92] M. P. Vecchi, R. M. Bulley, M. S. Goodman, H. Kobrinski and C. A. Brackett, 'High-bit-rate measurements in the LAMBDANET multiwavelength optical star network', *Opt. Fiber Commun. Conf. OFC'88* (USA), paper WO2 January 1988.

[93] A. Hunwicks, L. Bickers, M. H. Reeve and S. Hornung, 'An optical transmission system for single-mode local-loop applications using a sliced spectrum technique', *Twelfth Internat. Fiber Optic Commun. and Local Area Networks Exposition FOC/LAN'88* (USA), pp. 237–240, September 1988.

[94] S. S. Wagner and T. E. Chapuran, 'Broadband high-density WDM transmission using superluminescent diodes', *Electron. Lett.*, **26**(11), pp. 696–697, 1990.

[95] J. M. Senior and S. D. Cusworth, 'Wavelength division multiplexing in optical sensor systems and networks: a review', *Opt. and Laser Technol.*, **22**(2), pp. 113–126, 1990.

[96] P. Cockrane, 'Future directions in undersea fibre optic system technology', *Proc. IOOC'89*, Kobe, Japan, paper 21B1–2, July 1989.

[97] P. S. Henry, R. A. Linke and A. H. Gnauck, 'Introduction to Lightwave Systems', in S. E. Miller and I. P. Kaminow (Eds.), *Optical Fiber Telecommunications II*, Academic Press, pp. 781–831, 1988.

[98] C. H. Henry, 'Theory of spontaneous emission noise in optical resonators and its application to lasers and optical amplifiers', *J. Lightwave Technol.*, **LT-4** pp. 288–297, 1986.

[99] W. A. Stallard, J. D. Cox, D. J. Malyon, A. E. Ellis and K. H. Cameron, 'Long span high capacity optical transmission system employing laser amplifier repeaters', *Proc. Internat. Conf. on Integrated Optics and Fibre Commun., IOOC'89*, Kobe (Japan), paper 21B2–2, July 1989.

[100] P. Cockrane, 'Future directions in long haul fibre optic systems, *Br. Telecom Technol. J.*, **8**(2), pp. 5–17, 1990.

[101] S. Yamamoto, H. Taga, N. Edagawa, K. Mochizuki anbd H. Wakabayashi, '516 km, 2.4 Gbit/s optical fiber transmission experiment using 10 semiconductor laser amplifiers and measurement of jitter accumulation', *Proc. Internat. Conf. on Integrated Optics and Fibre Commun., IOOC'89*, Kobe (Japan), paper 20PDA-9. July 1989.

[102] N. H. Taylor and A. Hadjitotiou, 'Optical amplification and its applications', *Proc. SPIE, Int. Soc. Opt. Eng*, **1314**, pp. 64–67, 1990.

[103] M. J. O'Mahony, 'Progress in optical amplifiers', *Internat. Workshop on Digital Commun.*, Session 6, paper 3, Tirrenia, Italy, September 1989.

[104] D. M. Spirit, L. C. Blank, S. T. Davey and D. L. Williams, 'Systems aspects of Raman fibre amplifiers, *IEE Proc., Pt. J.*, **137**(4), pp. 221–224, 1990.

[105] K. Aida, S. Nishi, Y. Sato, K. Hagimoto and K. Nakagawa, 'Design and performance of a long-span IM/DD optical transmission system using remotely pumped optical amplifiers', *IEE Proc., Pt. J.*, **137**(4), pp. 225–229, 1990.

[106] N. Edagawa, K. Mochizuki and H. Wakabayashi, '1.2 Gbit/s, 218 km transmission using inline Er-doped optical fibre amplifier', *Electron. Lett.*, **25**(5), pp. 363–365, 1989.

[107] K. Hagimoto, K. Iwatsuki, A. Takada, M. Nakazawa, M. Saruwatari, K. Aida and K. Nakagawa, '250 km nonrepeated transmission experiment at 1.8 Gb/s using LD pumped E^{3+}-doped fibre amplifiers in IM/direct detection system', *Electron. Lett.*, **25**(10), pp. 662–664, 1989.

[109] J. F. Massicott, R. Wyatt, B. J. Ainslie and S. P. Craig-Ryan, 'Efficient, high power, high gain doped silica fibre amplifier', *Electron. Lett.*, **26**(14), pp. 1038–1039, 1990.

[109] C. G. Atkins, J. F. Massicott, J. R. Armitage, R. Wyatt, B. J. Ainslie and S. P. Craig-Ryan, 'A high gain, broad spectral bandwidth erbium doped fibre amplifier pumped near 1.5 μm', *Electron. Lett.*, **25**(14), pp. 910–911, 1989.

[110] P. D. D. Kilkelly, P. J. Chidgey and G. Hill, 'Experimental demonstration of a three channel WDM system over 110 km using superluminescent diodes', *Electron. Lett.*, **26**(20), pp. 1671–1673, 1990.

[111] P. J. Chidgey and G. R. Hill, 'Diverse routing in wavelength selective networks', *Electron. Lett.*, **26**(20), pp. 1709–1711, 1990.

[112] H. Taga, Y. Yoshida, N. Edagawa, S. Yamamoto and H. Wakabayashi, '459 km, 2.4 Gbit/s four wavelength multiplexing optical fibre transmission experiment using six Er-doped fibre amplifiers', *Electron. Lett.*, **26**(8), pp. 500–501, 1990.

[113] A. M. Hill, R. Wyatt, J. F. Massicott, K. J. Blyth, D. S. Forrester, R. A. Lobbett, P. J. Smith and D. B. Payne, '39.5 million-way WDM broadcast network employing two stages of erbium-doped fibre amplifiers', *Electron. Lett.*, **26**(22), pp. 1882–1884, 1990.

[114] W. I. Way, S. S. Wagner, M. M. Choy, C. Lin, R. C. Menendez, H. Tohme, A. Yi-Yan, A. C. von Lehman, R. E. Spicer, M. Andrejco, M. A. Saifi and H. Lemberg, 'Distribution of 100 FM-TV channels and six 622 Mb/s channels to 4096 terminals using high-density WDM and a broadband in-line erbium-doped fiber amplifier', *Optical Fiber Communications Conf., OFC'90* (USA), Post Deadline Paper PD21, January 1990.

[115] M. J. Pettitt, A. Hadjifotiou and R. A. Baker, 'Crosstalk in erbium doped fibre amplifiers', *Electron. Lett.*, **25**(6), pp. 416–417, 1989.

[116] G. J. Cowle, P. R. Morkel, R. I. Laming and D. N. Payne, 'Spectral broadening due to fibre amplifier phase noise', *Electron. Lett.*, **26**(7), pp. 424–425, 1990.

12

Optical fiber systems 2: coherent

12.1 Introduction

The direct detection of an intensity modulated optical carrier is basically a photon counting process where each detected photon is converted into an electron–hole pair (or, in the case of the APD, a number of pairs due to avalanche gain). It was indicated in Section 7.5 that this process which ignores the phase and polarization of the electromagnetic carrier may be readily implemented with currently available optical components. Thus all the preceding discussion in Chapter 11 involving both digital and analog systems concerned only an intensity modulated optical carrier being transmitted to a direct detection optical receiver or IM/DD optical fiber systems.

Conventional direct detection receivers, however, are generally limited by noise generated in the detector and preamplifier (see Chapter 9) except at very high signal to noise ratios (SNRs). The sensitivity of such square law detection systems is therefore reduced below the fundamental quantum noise limit by at least 10 to 20 dB [Ref. 1]. This is particularly the case at longer wavelengths (i.e. 1.3 to 1.6 μm) and at higher transmission rates since the electronic preamplifier usually has a rising input optical power with frequency requirement* (see Eq. (11.37)). For a good APD receiver operating in the wavelength range 1.3 to 1.6 μm this corresponds to between 700 and 1000 photons per bit required to maintain a bit error rate (BER) of 10^{-9} [Ref. 2].

Improvements in receiver sensitivity, together with wavelength selectivity, may be obtained using the well-known coherent detection techniques (i.e. heterodyne and homodyne detection) for the optical signal [Ref. 3]. Unlike direct detection in which the optical signal is converted directly into a demodulated electrical output, such coherent optical receivers first add to the incoming optical signal from a locally generated optical wave prior to detecting the sum.† The resulting photocurrent is a replica of the original signal which is translated down in frequency from the optical domain (around 10^5 GHz) to the radio domain (up to several GHz) and where conventional electronic techniques can be used for further signal processing and demodulation. Hence an ideal coherent receiver operating in the 1.3 to 1.6 μm wavelength region requires a signal energy of only 10 to 20 photons per bit to achieve a BER of 10^{-9}. It should therefore be noted that coherent detection provides the greatest benefit for high speed systems operating at longer wavelengths.

A potential improvement in receiver sensitivity using coherent detection of up to 20 dB can be obtained over direct detection [Ref. 4]. Furthermore, such enhanced receiver sensitivity could translate into increases in repeater spacings of the order of 100 km when using low loss fiber at a wavelength of 1.55 μm. Hence, the improved sensitivity of 5 to 20 dB which results from the photomixing gain in the coherent receiver could provide:

(a) increased repeater spacings for both inland and undersea transmission systems;
(b) higher transmission rates over existing routes without reducing repeater spacings;
(c) increased power budgets to compensate for losses associated with couplers and optical multiplexer/demultiplexer devices (see Section 5.6.3) in distribution networks;
(d) improved sensitivity to optical test equipment such as optical time domain reflectometers (see Section 13.10.1).

* This requirement corresponds to a rising noise versus frequency characteristic.

† Current usage in optical fiber communications is that the term 'coherent' refers to any system or technique which employs nonlinear mixing between two optical waves. Typically, one of these is the information carrying signal and the other a locally generated signal (by a local oscillator) at the receiver. The result of this process is a new signal (for heterodyne detection, the intermediate frequency) which appears at a microwave frequency given by the difference between the frequencies of the incoming signal and the local oscillator.

Although possible increases in transmission distance between repeaters initially created the impetus for the pursuit of coherent transmission within optical fiber communications, such techniques also allow a further massive step to be taken in the exploitation of the transmission capacity of optical fiber systems. The inherent wavelength selectivity afforded by the coherent receiver could be used to access efficiently the vast optical bandwidth available in single-mode fiber. For example, the optical bandwidth provided by the low loss window between 1.3 and 1.6 μm is over 50 000 GHz [Ref. 5]. Therefore, as a result of its improved selectivity over direct detection, a coherent receiver could permit wavelength division multiplexing* with channel spacings of only a few hundred MHz [Ref. 6] instead of the minimum of around 100 GHz (i.e. 0.5 nm) provided by conventional optical multiplexing technology. It is this factor in particular which has more recently focused interest on coherent optical fiber transmission because wavelength/frequency selectivity may well be more important than improved receiver sensitivity in the provision of future wideband distribution networks within telecommunications [Refs. 7, 8]. Finally, a further potentially important attribute of coherent reception is that it allows the use of electronic equalization compensate for the effects of optical pulse dispersion in the fiber.

The modulation formats that may be employed within coherent optical fiber communications are essentially the same as those used in coherent electrical line and radio communications. Modulation formats of this type were discussed in Sections 11.7.3 to 11.7.6 in a slightly different context, namely the generation of subcarriers for electrical frequency division multiplexing prior to intensity modulation of the optical source. In these cases direct detection of the optical signal is carried out at the receiver with subsequent electrical demodulation for the subcarriers. Such systems only provide improvements in the SNR over baseband IM/DD systems at the expense of a substantial bandwidth penalty. When a narrow linewidth injection laser (less than 1 MHz) is used in an optical fiber communication system, however, it is possible to directly modulate the coherent optical carrier in amplitude (direct AM), frequency (direct FM) and phase (direct PM) prior to demodulation using a coherent optical receiver. In the case of digital transmission this implies amplitude, frequency or phase shift keying (i.e. ASK, FSK or PSK) modulation techniques [Ref. 3].

The discussion is continued in Section 12.2 through a brief historical review of the development of coherent optical transmission prior to the description of the basic coherent optical fiber communication system, together with its important features. This leads into the consideration of the fundamental detection principles associated with the coherent optical receiver (i.e. heterodyne and homodyne detection) in Section 12.3. There are, however, a number of practical constraints which have in the past inhibited the development of coherent optical fiber systems, and even now they create certain limitations on the choice of system components. These issues are therefore dealt with in Section 12.4. This is followed in Section 12.5

* In this case it is often referred to as frequency division multiplexing.

by discussion of the various modulation formats that may be employed for coherent optical transmission prior to the description of the numerous demodulation schemes which have been applied within the coherent detection process in Section 12.6. A comparison of the various major modulation and demodulation techniques in relation to receiver sensitivity is then provided in Section 12.7. Finally, in Section 12.8 we describe the major features and performance characteristics of some advanced coherent optical fiber transmission systems. In particular, the field trial of a single carrier system is discussed prior to the consideration of recent demonstrations of multicarrier coherent systems using optical frequency division multiplexing techniques.

12.2 Basic system

Since the invention of the laser in 1960, research efforts have focused on techniques by which the coherent properties of laser light could be utilized for coherent optical communications. Improved SNRs over direct detection were demonstrated in free space optical communication systems using gas lasers in the late 1960s [Refs. 9, 10]. In addition, the concept of optical frequency division multiplexing using coherent detection schemes was proposed in 1970 [Ref. 11]. However, it was only in the latter half of the 1970s, when single-mode transmission from a narrow linewidth AlGaAs semiconductor laser was demonstrated [Ref. 12], that the proposals for coherent optical fiber transmission began taking shape. Nevertheless, it was appreciated that the polarization stability of the transmission medium was crucial for successful coherent detection. Ideally, for coherent transmission the fiber would be required to maintain a single linear polarization state throughout its length. This factor, in part, led to the investigations on polarization maintaining (PM) fibers in the early 1980s (see Section 3.13.2). Moreover, for a brief period the use of PM fibers was a favoured potential approach to the problem [Ref. 13]. For example, the use of optical adaptors (e.g. birefringent plates) at the transmit and receive terminals was suggested in order to allow only a single polarization state of the fundamental mode to be launched into, and received from, the PM fiber [Ref. 14].

It was clear, however, that if conventional circularly symmetric single-mode fiber, which did not maintain a single polarization state over its length (see Section 13.3.1), were to be employed then some form of polarization matching of the incoming optical signal with the locally generated optical signal would be necessary. Although the first successful demonstration of optical frequency shift keyed heterodyne detection using a semiconductor laser source and local oscillator was reported in 1989 [Ref. 15], a period elapsed before the polarization stability measurements on installed conventional single-mode fiber indicated the real possibility of its use within coherent optical transmission systems [Ref. 16]. It is therefore only comparatively recently that coherent transmission techniques have proved feasible within optical fiber communications [Ref. 5].

A block schematic of a generalized coherent optical fiber communication system is illustrated in Figure 12.1. The broken lines enclose the main elements which distinguish the coherent system from its direct detection equivalent. At the transmitter a CW narrow linewidth semiconductor laser is shown which acts as an optical frequency oscillator. An external optical modulator usually provides amplitude, frequency or phase shift keying of the optical carrier by the information signal. At present external modulators are generally waveguide devices fabricated from lithium niobate or the group III–V compound semiconductors (see Section 10.6.2). Internal modulation of the injection laser drive current may, however, also be utilized to produce either ASK or FSK [Refs. 17, 18].

Modulated carrier waveforms for the three standard modulation techniques with binary data are illustrated in Figure 12.2. It may be observed from Figure 12.2(a) where binary ASK is often referred to as on-off keying (OOK). Figure 12.2(b) shows FSK in which the binary 1 is transmitted at a higher optical frequency than the binary 0 bit. The 180° phase shift between the binary 1 and 0 bits displayed in Figure 12.2(c) depicts PSK. Furthermore, it should be noted that whereas with ASK the amplitude of the carrier waveform is effectively switched on and off, the amplitude of the optical carrier remains constant in the other two modulation schemes shown in Figure 12.2. Variants on these standard modulation techniques exist, such as continuous phase FSK and differential PSK, which has also been applied in experimental coherent optical fiber transmission systems. Moreover, an alternative digital scheme based on the modulation of the polarization properties of the optical signal has more recently come under investigation. This strategy, known

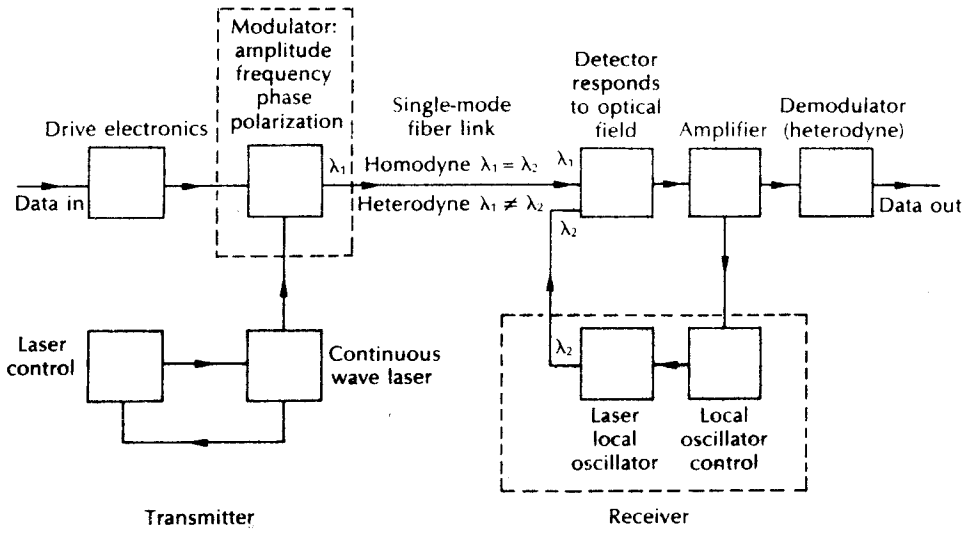

Figure 12.1 The generalized coherent optical fiber system.

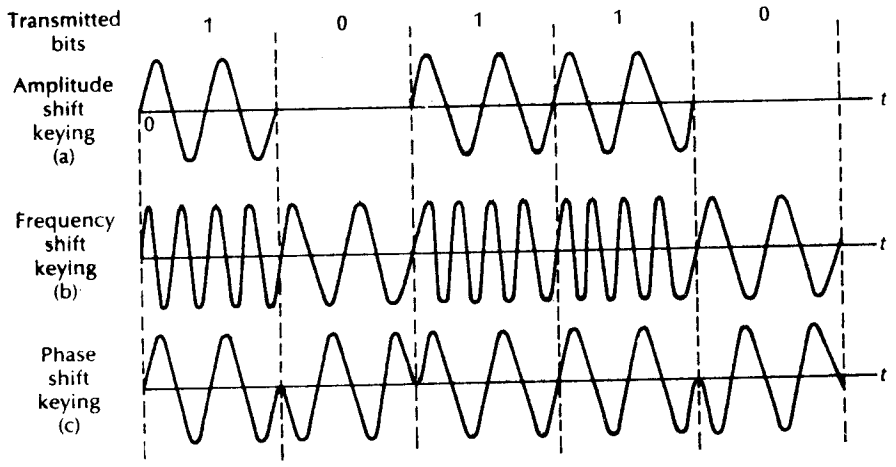

Figure 12.2 Modulated carrier waveforms used for binary data transmission: (a) amplitude shift keying (ASK); (b) frequency shift keying (FSK); (c) phase shift keying (PSK).

as polarization shift keying (PolSK), is discussed further along with the other modulation formats in Section 12.5.

Referring now to the receiver shown in Figure 12.1, then the incoming signal is combined (or mixed) with the optical output from a semiconductor laser local oscillator. This function can be provided by a single-mode fiber fused biconical coupler (see Section 5.6.1), a device which gives excellent wavefront matching of the two optical signals. However, integrated optical waveguide couplers (see Section 10.6.1) may also be utilized. The combined signal is then fed to a photodetector for direct detection in the conventional square law device. Nevertheless, to permit satisfactory optical coherent detection the optical coupler device must combine the polarized optical information-bearing signal field with the similarly polarized local oscillator signal field in the most efficient manner.

When the optical frequencies (or wavelengths) of the incoming signal and the local oscillator laser output are identical, then the receiver operates in a homodyne mode and the electrical signal is recovered directly in the baseband. For heterodyne detection, however, the local oscillator frequency is offset from the incoming signal frequency and therefore the electrical spectrum from the output of the detector is centred on an intermediate frequency (IF) which is dependent on the offset and is chosen according to the information transmission rate and the modulation characteristics. This IF, which is a difference signal (or difference frequency), contains the information signal and can be demodulated using standard electrical techniques [Ref. 3].

The electrical demodulator block shown in Figure 12.1 is required in particular for an optical heterodyne detection system which can utilize either synchronous

or nonsynchronous/asynchronous electrical detection. Synchronous or coherent* demodulation implies an estimation of phase of the IF signal in transferring it to the baseband. Such an approach requires the use of phase-locking techniques in order to follow phase fluctuations in the incoming and local oscillator signals. Alternatively, nonsynchronous or noncoherent (envelope) IF demodulation schemes may be employed which are less demanding but generally produce a lower performance than synchronous detection techniques [Ref. 5]. Optical homodyne detection is by definition, however, a synchronous demodulation scheme and as the detected signal is brought directly into the baseband, then optical phase estimation is required. These issues are discussed further in Section 12.6.

12.3 Detection principles

A simple coherent receiver model for ASK is displayed in Figure 12.3. The low level incoming signal field e_S is combined with a second much larger signal field e_L derived from the local oscillator laser. It is assumed that the electromagnetic fields obtained from the two lasers (i.e. the incoming signal and local oscillator devices) can be represented by cosine functions and that the angle $\phi = \phi_S - \phi_L$ represents the phase relationship between the incoming signal phase ϕ_S and the local oscillator signal phase ϕ_L defined at some arbitrary point in time. Hence as depicted in Figure 12.3 the two fields may be written as [Ref. 19]:

$$e_S = E_S \cos(\omega_S t + \phi) \tag{12.1}$$

and

$$e_L = E_L \cos(\omega_L t) \tag{12.2}$$

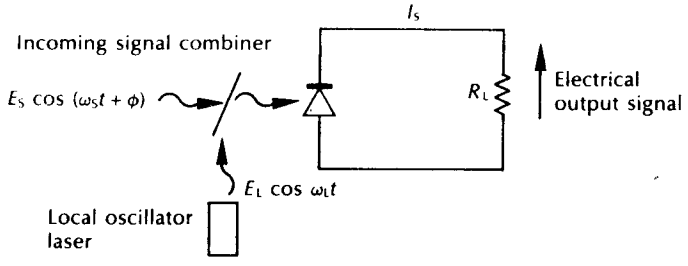

Figure 12.3 Basic coherent receiver model.

* It is a little confusing but reference is made in the literature to (a) heterodyne, coherent detection and (b) to heterodyne, noncoherent or incoherent detection, both of which are coherent optical detection schemes. The former terminology means an optical heterodyne receiver using a synchronous electrical demodulation technique, whereas the latter corresponds to a heterodyne receiver with a nonsynchronous demodulation scheme.

where E_S is the peak incoming signal field and ω_S is its angular frequency, and E_L is the peak local oscillator field and ω_L is its angular frequency. The angle $\phi(t)$ representing the phase relationship between the two fields contains the transmitted information in the case of FSK or PSK. However, with ASK $\phi(t)$ is constant and hence it is simply written as ϕ in Eq. (12.1), the information being contained in the variation of E_S for ASK as may be observed in Figure 12.2(a)

For heterodyne detection, the local oscillator frequency ω_L is offset from the incoming signal frequency ω_S by an intermediate frequency (IF) such that:

$$\omega_S = \omega_L + \omega_{IF} \tag{12.3}$$

where ω_{IF} is the angular frequency of the IF. As mentioned in Section 12.1 the IF is usually in the radiofrequency region and may be a few tens or hundreds of megahertz. By contrast, within homodyne detection there is no offset between ω_S and ω_L and hence $\omega_{IF} = 0$. In this case the combined signal is therefore recovered in the baseband.

The two wavefronts from the incoming signal and the local oscillator laser must be perfectly matched at the surface of the photodetector for ideal coherent detection. This factor creates the normal requirement for polarization control of the incoming optical signal which is discussed further in Section 12.4.

In the case of both heterodyne and homodyne detection the optical detector produces a signal photocurrent I_p which is proportional to the optical intensity (i.e. the square of the total field for the square law photodetection process) so that:

$$I_p \propto (e_S + e_L)^2 \tag{12.4}$$

Substitution in the expression Eq. (12.4) from Eqs. (12.1) and (12.2) gives:

$$I_p \propto [E_S(\cos \omega_S t + \phi) + E_L \cos \omega_L t]^2 \tag{12.5}$$

Assuming perfect optical mixing expansion of the right hand side of the expression shown in Eq. (12.5) gives:

$$\begin{aligned}[E_S^2 \cos^2(\omega_S t + \phi) + E_L^2 \cos^2 \omega_L t + 2E_S E_L \cos(\omega_S t + \phi)\cos \omega_L t] \\ = [\tfrac{1}{2}E_S^2 + \tfrac{1}{2}E_S \cos(2\omega_S t + \phi) + \tfrac{1}{2}E_L^2 + \tfrac{1}{2}\cos 2\omega_L t \\ + E_S E_L(\cos \omega_S t + \phi - \omega_L t) + E_S E_L \cos(\omega_S t + \phi + \omega_L t)]\end{aligned}$$

Removing the higher frequency terms oscillating near the frequencies of $2\omega_S$ and $2\omega_L$ which are beyond the response of the detector and therefore do not appear in its output, we have:

$$I_p \propto \tfrac{1}{2}E_S^2 + \tfrac{1}{2}E_L^2 + 2E_S E_L \cos(\omega_S t - \omega_L t + \phi) \tag{12.6}$$

Then recalling that the optical power contained within a signal is proportional to the square of its electrical field strength, Eq.(12.6) may be written as:

$$I_p \propto P_S + P_L + 2\sqrt{P_S P_L} \cos(\omega_S t - \omega_L t + \phi) \tag{12.7}$$

where P_S and P_L are the optical powers in the incoming signal and local oscillator signal respectively.

Furthermore, a relationship was obtained between the output photocurrent from an optical detector and the incident optical power P_o in Eq. (8.8) of the form $I_p = \eta e P_o / hf$. Hence the expression in Eq. (12.7) becomes:

$$I_p = \frac{\eta e}{hf} [P_S + P_L + 2\sqrt{P_S P_L} \cos (\omega_S t - \omega_L t + \phi)] \tag{12.8}$$

where η is the quantum efficiency of the photodetector, e is the charge on an electron, h is Planck's constant and f is optical frequency. When the local oscillator signal is much larger than the incoming signal, then the third a.c. term in Eq. (12.8) may be distinguished from the first two d.c. terms and I_p can be replaced by the approximation I_S where [Ref. 5]:

$$I_S = \frac{\eta e}{hf} [2\sqrt{P_S P_L} \cos (\omega_S t - \omega_L t + \phi)] \tag{12.9}$$

Equation (12.9) allows the two coherent detection strategies to be considered. For heterodyne detection $\omega_S \neq \omega_L$ and substituting from Eq. (12.3) gives:

$$I_S = \frac{2\eta e}{hf} \sqrt{P_S P_L} \cos (\omega_{IF} t + \phi) \tag{12.10}$$

indicating that the output from the photodetector is centred on an intermediate frequency. This IF is stabilized by incorporating the local oscillator laser in a frequency control loop. Temperature stability for the signal and local oscillator lasers is also a factor which must be considered (see Example 12.1). The stabilized IF current is usually separated from the d.c. current by filtering prior to electrical amplification and demodulation.

For the special case of homodyne detection, however, $\omega_S = \omega_L$ and therefore Eq. (12.9) reduces to:

$$I_S = \frac{2\eta e}{hf} \sqrt{P_S P_L} \cos \phi \tag{12.11}$$

or

$$I_S = 2R\sqrt{P_S P_L} \cos \phi \tag{12.12}$$

where R is the responsivity of the optical detector. In this case the output from the photodiode is in the baseband and the local oscillator laser needs to be phase locked to the incoming optical signal.

Example 12.1

A semiconductor laser used to provide the local oscillator signal in an ASK optical heterodyne receiver exhibits an output frequency change of 19 GHz $^{\circ}C^{-1}$. If the receiver has a nominal IF of 1.5 GHz and assuming that there is no other form of laser frequency control, estimate the maximum temperature change that could be

allowed for the local oscillator laser in order that satisfactory detection could take place.

Solution: Initially it is necessary to estimate the maximum frequency excursion allowed for the IF signal such that detection can still be facilitated. This must be no greater than 10% of the frequency of the IF. Hence the maximum allowed frequency change to the local oscillator laser output is around 150 MHz.

The maximum temperature change allowed for the local oscillator laser is therefore:

$$\textit{Max. temp. change} = \frac{150 \times 10^6}{19 \times 10^9}$$

$$\simeq 8 \times 10^{-3}\ ^\circ\text{C}\ (0.008\ ^\circ\text{C})$$

Very small temperature changes can therefore adversely affect the detection process if the IF is not otherwise stabilized.

It may be observed from the expressions given in Eqs. (12.10) and (12.11) that the signal photocurrent is proportional to $\sqrt{P_S}$, rather than P_S as in the case of direct detection (Eq. (8.8)). Moreover, the signal photocurrent is effectively amplified by a factor $\sqrt{P_L}$ proportional to the local oscillator field. This local oscillator gain factor has the effect of increasing the optical signal level without affecting the receiver preamplifier thermal noise or the photodetector dark current noise (see Sections 9.2 and 9.3); hence the reason why coherent detection provides improved receiver sensitivities over direct detection.

The requirement for coherence between the incoming and local oscillator signals in order to obtain coherent detection was mentioned in Section 12.2 and is discussed further in Section 12.4.2. Hence for successful mixing to occur, then some correlation must exist between the two signals shown in Figure 12.3. Care must therefore be taken to ensure that this is the case when two separate laser sources are employed to provide the signal and local oscillator beams. It may be noted that this problem is reduced when a single laser source is used with an appropriate path length difference as, for example, when taking measurements by interferometric techniques (see Section 14.5.1).

When the local oscillator signal power is much greater than the incoming signal power then the dominant noise source in coherent detection schemes becomes the local oscillator quantum noise. In this limit the quantum noise may be expressed as shot noise following Eq. (9.8) where the mean square shot noise current from the local oscillator is given by:

$$\overline{i_{SL}^2} = 2eBI_{pL} \tag{12.13}$$

Substituting for I_{pL} from Eq. (8.8), where the photocurrent generated by the local oscillator signal is assumed to be by far the major contribution to the photocurrent,

gives:

$$\overline{i_{SL}^2} = \frac{2e^2\eta P_L B}{hf} \tag{12.14}$$

The detected signal power S being the square of the average signal photocurrent* is given by Eq. (12.9) as:

$$S = \left(\frac{\eta e}{hf}\right)^2 P_S P_L \tag{12.15}$$

Hence the SNR for the ideal heterodyne detection receiver when the local oscillator power is large (ignoring the electronic preamplifier thermal noise and photodetector dark current noise terms) may be obtained from Eqs. (12.14) and (12.15) as:

$$\left(\frac{S}{N}\right)_{\text{het-lim}} = \left(\frac{\eta e}{hf}\right)^2 P_S P_L \Big/ \frac{2e^2\eta P_L B}{hf}$$

$$= \frac{\eta P_S}{hf\,2B} = \frac{\eta P_S}{hf\,B_{IF}} \tag{12.16}$$

Equation (12.16) provides the so-called shot noise limit for optical heterodyne detection in which the IF amplifier bandwidth B_{IF} is assumed to be equal to $2B$† (i.e. $B_{IF} = 2B$) [Ref. 20]. It is also interesting to note that this heterodyne shot noise limit corresponds to the quantum noise limit for analog direct detection derived in Eq. (9.11). However, it is clear that optical heterodyne detection allows a much closer approach to this limit than does direct detection.

The shot noise SNR limit for optical homodyne detection can be deduced from Eq. (12.16) by reducing the receiver bandwidth requirement from B_{IF} to B as the output signal from the photodetector appears in the baseband when using the homodyne scheme. Hence the SNR limit for optical homodyne detection is:

$$\left(\frac{S}{N}\right)_{\text{hom-lim}} = \frac{\eta P_S}{hf\,B} \tag{12.17}$$

It should be remembered that the expressions given in Eqs. (12.16) and (12.17) are based on simple on-off keying (i.e. OOK) and have effectively been derived in terms of carrier to noise ratio. Nevertheless, they display the potential 3 dB improvement in SNR when using optical homodyne detection over heterodyne detection. The improvement occurs as a direct result of the reduction in the receiver bandwidth provided by the former technique. Therefore, homodyne detection displays the twin advantages over heterodyne detection of increased sensitivity coupled with a reduced receiver bandwidth requirement. The latter factor implies that a higher

* is implicit from Eq. (12.9) that the photodetector is a unity gain device (e.g. p–i–n photodiode) and not an APD. In the latter case the effect of the multiplication factor M on both the signal and noise powers must be taken into account (see Sections 9.3.3 and 9.3.4).

† This constitutes the minimum bandwidth requirement for optical heterodyne detection.

maximum transmission rate should be facilitated by coherent optical fiber systems employing homodyne detection as they will be less restricted by the speed of response of the photodetector.

Example 12.2

The incoming signal power to an optical homodyne receiver operating at a wavelength of 1.54 μm, and at its shot noise limit, is -55.45 dBm. When the photodetector in the receiver has a quantum efficiency of 86% at this wavelength and the received SNR is 12 dB, determine the operating bandwidth of the receiver.

Solution: The incoming signal power P_S is given by:

$$-85.45 = 10 \log_{10} P_S$$

Hence

$$P_S = 10^{0.455} \times 10^{-9} = 2.851 \text{ nW}$$

The operating bandwidth B of the homodyne receiver may be obtained from Eq. (12.17) as:

$$B = \frac{\eta P_S}{hf} \left(\frac{S}{N}\right)^{-1}_{\text{hom-lim}} = \frac{\eta P_S \lambda}{hc} \left(\frac{S}{N}\right)^{-1}_{\text{hom-lim}}$$

$$= \frac{0.86 \times 2.851 \times 10^{-9} \times 1.54 \times 10^{-6} \times 10^{-1.2}}{6.626 \times 10^{-34} \times 2.998 \times 10^{8}}$$

$$= 1.2 \text{ GHz}$$

The above analysis of SNR for optical heterodyne and homodyne detection applies only to ASK and is not appropriate for FSK and PSK. The final SNR at the signal decision point is therefore dependent on the modulation scheme utilized, and in the case of heterodyne detection on the type of IF demodulator and baseband filter employed. More detailed considerations of the SNR for different modulation schemes are dealt with in Section 12.7.

12.4 Practical constraints

It was indicated in Section 12.1 that until quite recently various practical constraints had inhibited the development of coherent optical fiber communications. These constraints are largely derived from factors associated with the elements of the coherent optical fiber communication system shown in Figure 12.1, and they are exacerbated by the stringent demands of coherent transmission. Substantial

developments, however, in the component technology associated with optical fiber communications particularly over the last few years, have allowed the earlier difficulties experienced with coherent optical fiber transmission to be largely overcome. Nevertheless, the practical constraints still exist and they still dictate the performance characteristics required from components and devices which are to be utilized in coherent optical fiber systems. It is therefore important to consider the major constraints and their effect on the choice of system elements. We start by discussing the aspects which determine specific requirements for the achievement of coherent optical transmission at both the transmit and receive terminals prior to outlining certain limitations of the fiber transmission medium which may affect the performance of future coherent optical communication systems.

12.4.1 Injection laser linewidth

For coherent transmission the several hundred gigahertz wide linewidths of earlier multimode semiconductor injection lasers required a substantial reduction to very narrow linewidth (ideally, less than a megahertz) single-mode spectra. The major reasons for the use of a narrow linewidth injection laser within the coherent detection process are the phase locking requirement (for synchronous detection) as well as the minimum frequency locking requirement for nonsynchronous detection. In addition, both the amplitude and phase of semiconductor laser emissions are noisy, causing a reduction in the SNR performance of the coherent system. Laser linewidth reduction therefore improves the spectral purity of the device output and thus reduces its noise content. However, it was not until the latter half of the 1970s that semiconductor device technology evolved to a point where injection lasers, with good reproducibility which could operate in a single longitudinal mode, could be fabricated. However, the spectral linewidths associated with the most sophisticated of these devices such as the distributed feedback laser (see Section 6.6.2) were of the order of 5 to 50 MHz which was too broad for most of the coherent techniques [Ref. 18].

Several approaches to the solution of this laser linewidth problem have recently evolved. They include the narrowing of injection laser linewidths through the use of an external resonator cavity in the long external cavity (LEC) laser (see Section 6.10.1), the use of integrated external cavity lasers in the form of advanced DFB and DBR structures (see Section 6.10.2) and the potential provided by injection locked semiconductor lasers [Refs. 21, 22]. This latter technique is dependent upon the injection of a sufficiently strong optical signal from an external source such that the frequency and phase of the output from the primary semiconductor laser will follow those of the injected signal. Hence in a coherent optical system this technique potentially allows for direct control of the local oscillator laser by the incoming signal. Unfortunately, injection locking in this way requires excessive power at the receiver input which far exceeds the target sensitivity for most homodyne* detection systems [Ref. 23].

* The injection locking technique described can only be employed with homodyne detection as the incoming signal and local oscillator will have the same frequency.

In particular, injection laser phase or frequency noise (see Section 6.7.4) can affect the coherent system performance as it is the principal cause of linewidth broadening in such devices [Ref. 24]. Randomly occurring spontaneous emission events, which are an inevitable aspect of injection laser operation, lead to sudden shifts (of random magnitude and sign) in the phase of the electromagnetic field generated by the laser causing the broadening effect. Hence, phase noise together with other linewidth broadening factors [Ref. 25] must be minimized in devices which are to be employed for coherent optical transmission. Nevertheless, phase locking techniques are often employed within the coherent receiver (see Section 12.6.1).

Overall, the injection laser linewidth requirements are critically dependent on the modulation format employed (i.e. ASK, FSK or PSK), the coherent detection mechanism (i.e. heterodyne or homodyne) and the electrical demodulation technique (i.e. synchronous, nonsynchronous or other). Although these issues are discussed in greater detail in Section 12.6, it is useful to comment on the narrowed linewidths achieved by the extended cavity lasers currently favoured for coherent optical fiber communications. At present the most exacting coherent optical transmission techniques necessitate the use of long external cavity (LEC) lasers which can provide linewidths of around 10 kHz or less [Ref. 17]. Whereas typical lengths for these devices are between 10 and 20 cm, developments in more rugged prototype units with cavity lengths in the range 2 to 3 cm have already taken place [Ref. 26]. This commercially available device provides linewidths of less than 100 kHz. Although submegahertz linewidths have been achieved with integrated external cavity lasers (see Section 6.10.2), these devices at present generally display significantly larger linewidths than LEC lasers. Hence, their use can only be contemplated with the less demanding coherent optical fiber transmission schemes.

Another important factor concerning the favoured narrow linewidth injection lasers for coherent optical transmission is their inherent tunability. This aspect, which is discussed in more detail in Sections 6.10.1 and 6.10.2, provides the ability to tune the frequency of the local oscillator laser to that of the incoming optical signal for homodyne detection, or alternatively to tune the appropriate frequency difference to maintain the correct IF signal for heterodyne detection.

12.4.2 State of polarization

To enable either heterodyne or homodyne detection the polarization states of the incoming optical signal and the local oscillator laser output must be well matched in order to provide efficient mixing of the two signals within the coupling element shown in Figure 12.3. Conventional circularly symmetric single-mode fiber allows two orthogonally polarized fundamental modes to propagate. Within a perfectly formed fiber both modes would travel together but in practice the fiber contains random manufacturing irregularities which produce geometric and strain related anisotropic effects. This results in a progressive spatial separation between the two polarization modes as they propagate along the fiber, an effect which is usually

$$P(\mathrm{e}) \simeq \tfrac{1}{2} \exp - \qquad (12.35)$$

referred to as modal birefringence (see Section 3.13.1). Hence at any particular point along the fiber the state of polarization (SOP) can be linear, elliptical or circular. To date, several counter-measures have been investigated to overcome this fluctuation in the SOP with coherent transmission. They are:

(a) the use of polarization maintaining (PM) single-mode fiber;
(b) the use of an SOP control device at the coherent optical receiver;
(c) the use of a polarization diversity receiver, or a polarization scrambling transmitter.

As mentioned in Section 12.2 early studies focused on the polarization stability of the transmission medium which was considered sufficiently important to necessitate the use of specially fabricated PM fiber (see Section 3.13.2). Such fibers, however, generally exhibit higher losses and are more expensive to fabricate than conventional single-mode fiber. Furthermore, much circularly symmetric single-mode fiber has already been installed and therefore coherent transmission techniques which utilize this medium are desirable.

Measurements of polarization stability for light propagating in conventional single-mode fiber over a ninety-six hour period are shown in Figure 12.4 [Ref. 16]. A single frequency linearly polarized 1523 nm emitting helium–neon gas laser together with a receiver which contained a polarization dependent beam splitter to

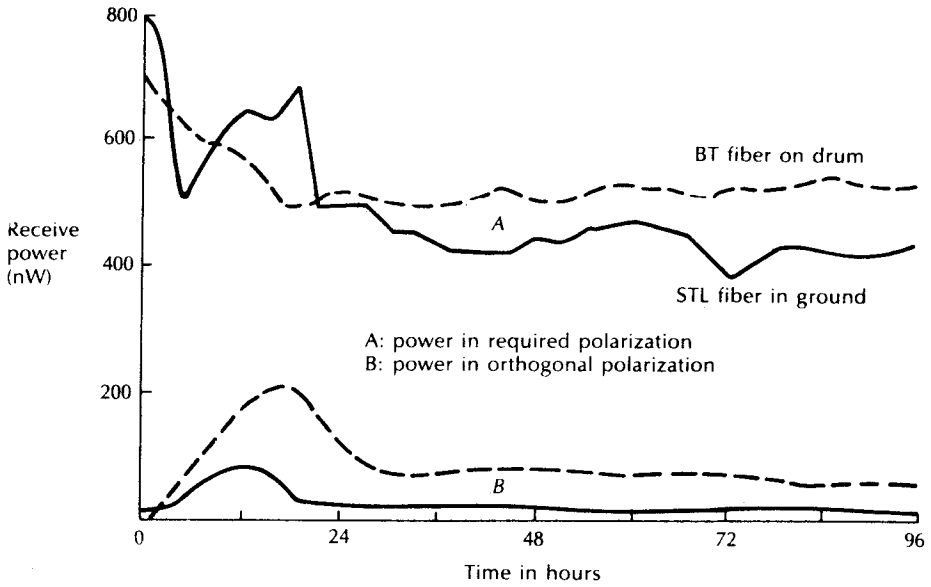

Figure 12.4 Characteristics displaying polarization stability in single-mode optical fiber. Reproduced with permission from D. W. Smith, R. A. Harmon and T. G. Hodgkinson, *Br. Telecom Technol. J.*, **1** (2), p. 12, 1983.

isolate the components were used in these measurements. It may be observed from Figure 12.4 that, as expected, the polarization state of the optical signal was not temporarily constant. Nevertheless, although polarization changes did occur, it was over periods of minutes or hours. These observations of the relatively slow changes in the polarization state of the transmitted signal, which were also verified on long cable links [Ref. 27], provided the potential for polarization matching at the coherent optical receiver. Polarization control devices with achievable response times could therefore be located at the receiver to provide polarization correction and hence matching of the SOP of the incoming signal and the local oscillator signal.

12.4.2.1 Polarization-state control

Active polarization-state control can be accomplished using mechanical, electro-optical or magneto-optical techniques. A polarization error signal may be generated and fed back to the polarization control device in all cases. In general, the SOP is described by the amplitude ratio of the x and y components of the electric field vector and their relative phase difference (see Section 3.13.1). As the two parameters which vary randomly at the coherent receiver are the ellipticity of the SOP and its orientation, the error signal must correct for both of these factors such that the incoming signal and the local oscillator output have identical states of polarization.

A number of mechanisms have been developed for polarization-state control within coherent optical fiber communications. Initial implementations of such devices which were based on birefringent elements (i.e. elements which induce modal birefringence in order to correct the SOP) included fiber squeezers [Ref. 28], electro-optic crystals [Ref. 29], rotatable fiber coils [Ref. 30], rotatable phase plates [Ref. 31] and rotatable fiber cranks [Ref. 32]. In addition, the possibility of using the Faraday effect to rotate the SOP of the incoming optical signal has also been demonstrated [Ref. 33]. Developments have also encompassed integrated optical electro-optic polarization control devices. Such controllers have been incorporated into integrated optical coherent receiver devices (see Section 10.6.4). At least two compensator devices are required to provide full polarization-state control. They can be placed in either the incoming signal path or the local oscillator output path; however the latter position is preferable if the device introduces significant signal attenuation.

Until recently a major concern was the insufficient range exhibited by these polarization control schemes in tracking the continuously varying SOP which can change unpredictably over virtually unlimited range. Polarization-state control schemes with infinite ranges of adjustments have, however, now been demonstrated [Refs. 34 to 37]. In particular, a control technique using four fiber squeezers, which is illustrated in Figure 12.5(a), was found to provide an infinite range of adjustment or so-called endless polarization control [Ref. 35]. Stress was applied to the fiber in the local oscillator path using the squeezers which were angled at 45° to each other. The SOP could therefore be manipulated to the appropriate matching point

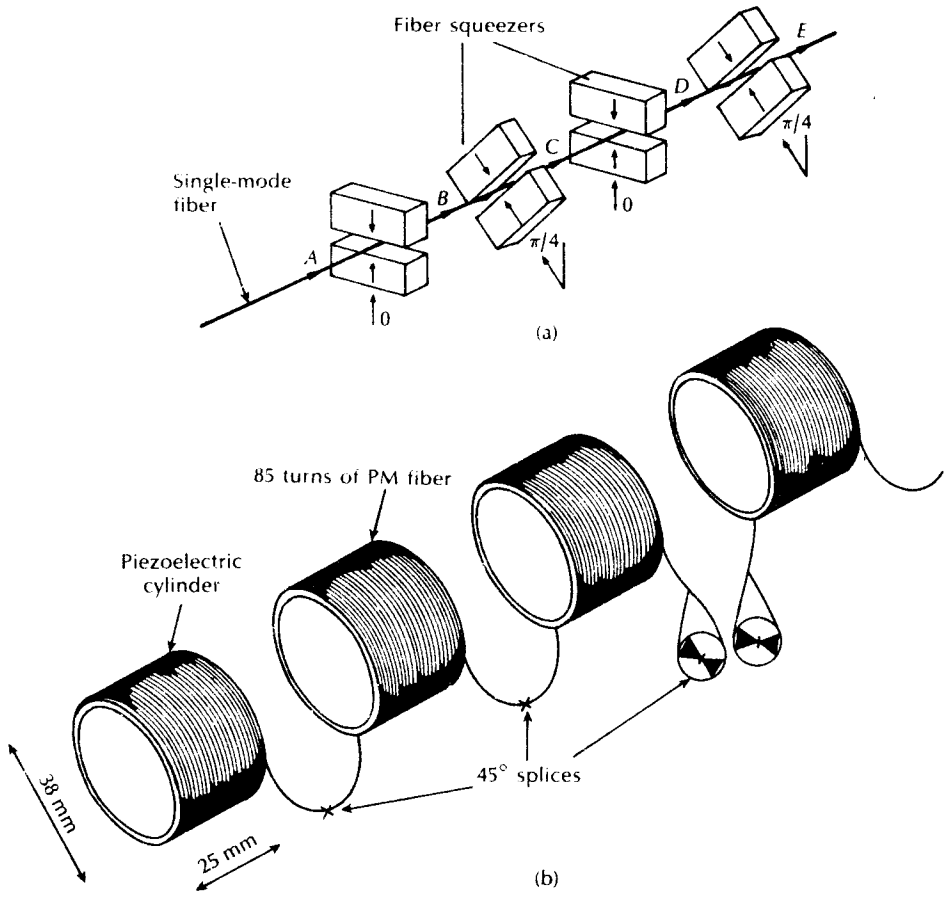

Figure 12.5 Techniques for endless polarization control: (a) four fiber squeezers; (b) polarization maintaining (PM) fiber controller.

Moreover, the polarization control system was automated using a control algorithm whereby a dither signal was applied to the bias on each squeezer in a defined order, and the variation of the received demodulated signal was used to identify the optimum operating point. This strategy removed the need to optically sense the SOP.

Although the squeezers are simple to configure, a drawback with the technique is that they tend to damage the fiber. Moreover, it is questionable as to whether they could be engineered into reliable transducers for practical systems. A more rugged and reliable controller is shown in Figure 12.5(b) [Ref. 36]. It comprised four piezoelectric cylinders each wound around with 85 turns of polarization maintaining (PM) fiber. The PM fibers on each cylinder were spliced together with

the principal axis of the fibers mutually aligned at 45°, as illustrated in Figure 12.5(b). As the PM fiber used was highly birefringent with a beat length of only a few millimetres, then the SOP changed many times along each element. The application of a voltage caused the piezoelectric cylinders to expand slightly and stretch the fiber, thus modifying the fiber birefringence. Hence, the overall effect was a variable retardation which gave polarization control. Again a control algorithm was devised to provide automatic operation.

An analogous control technique has also been demonstrated with an integrated optical, electro-optic polarization control device [Refs. 36, 37]. This lithium niobate waveguide structure which comprised two elements is shown in Figure 12.6. Each element consisted of three longitudinal electrodes placed symmetrically over the Z-propagating waveguide diffused into an X-cut substrate. Voltages applied to the electrodes produced an electric field that could be orientated in any direction transverse to the waveguide to provide a virtually infinite range of polarization-state control. This technique appears to offer a robust mechanically stable method of polarization control which has been demonstrated in both a laboratory-based and a field-installed coherent optical fiber systems, with no measurable sensitivity penalties [Refs. 36, 37].

Although the above are encouraging developments in polarization-state control techniques, problems with such methods may exist in advanced network applications using optical FDM and passive routeing (see Section 12.8.2). For example, a significant spectral variation in the SOP has been observed over relatively large spectral bandwidths (100 nm) for short interaction lengths in polarization couplers [Ref. 23]. Such spectral variation could cause difficulties for coherent optical FDM systems with active polarization correction. Furthermore, within advanced networking applications the time to acquire polarization matching may be an unacceptable overhead.

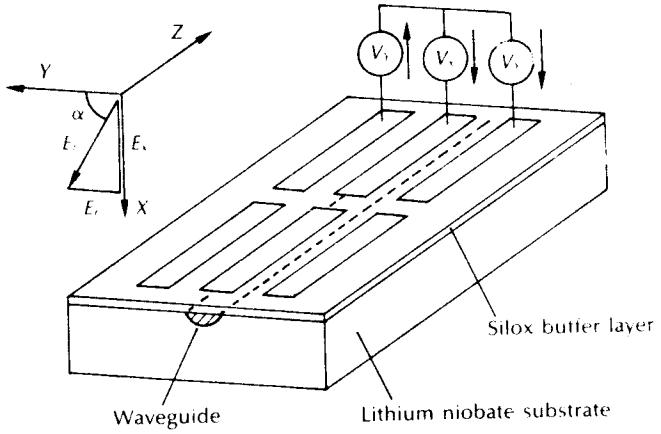

Figure 12.6 Lithium niobate waveguide polarization controller.

12.4.2.2 Polarization diversity reception and polarization scrambling transmission

Alternative approaches which avoid the requirement for polarization-state control devices, but which also allow the use of conventional circularly symmetric single-mode fiber, include polarization diversity reception [Refs. 38 to 42] and polarization scrambling transmission [Refs. 43, 44] techniques. A block schematic of a polarization diversity receiver is shown in Figure 12.7. This scheme, which is essentially polarization insensitive, employs separate heterodyne or homodyne detection for the two orthogonal polarization states of the incoming optical signal.

The incoming signal is therefore combined with a circularly polarized local oscillator signal and the composite signal is passed through a polarizing beam splitter. The two orthogonally polarized outputs from the beam splitter are then detected on separate photodiodes and, in the heterodyne case, demodulated down to baseband prior to recombination. Such electrical recombination provides a polarization independent signal as the IF is produced in one or other of the receivers regardless of the SOP of the incoming signal. The basic configuration illustrated in Figure 12.7 can incur a SNR performance degradation of 3 dB [Ref. 41] for particular input polarization states in which phase matching is difficult to maintain through both receivers. However, this penalty can be reduced to less than 1 dB with appropriate post demodulation processing.

Polarization insensitive heterodyne detection has also been demonstrated using polarization scrambling transmission. In this technique the polarization state of the

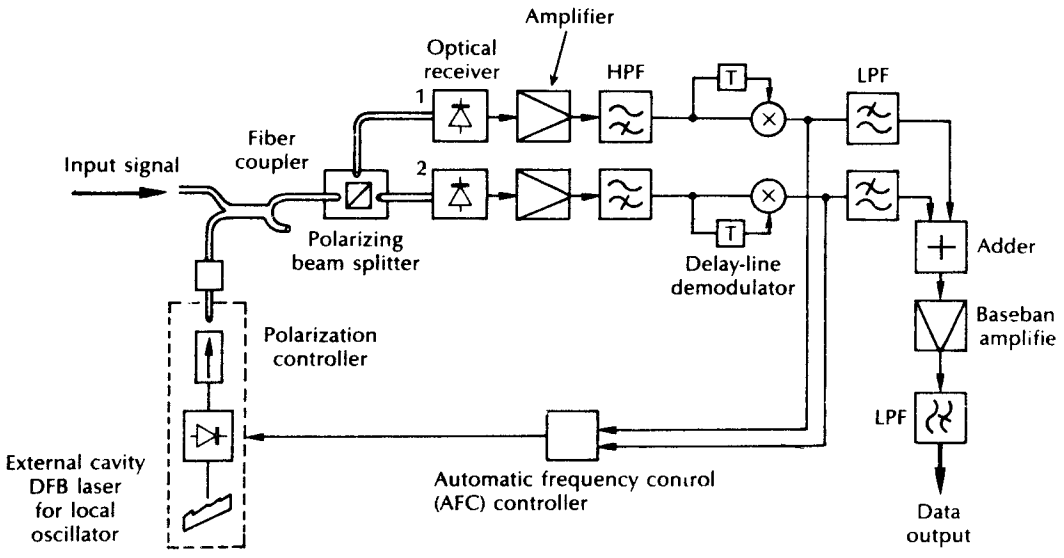

Figure 12.7 Polarization diversity FSK heterodyne receiver using one bit delayed demodulation [Ref. 39].

optical signal is deliberately changed at the coherent transmitter so that all possible polarization states are propagated during a single bit period. Although this method significantly reduces the receiver complexity in comparison with polarization diversity reception, it incurs a reduction in sensitivity at the coherent optical receiver. Moreover, the polarization scrambler is a relatively sophisticated arrangement which incorporates a polarization beam splitter. Hence, an earlier difficulty with this technique, in common with polarization diversity reception, concerned the realization of the optical devices in a rugged form. More recently, however, polarization maintaining fiber directional couplers have become commercially available.

12.4.3 Local oscillator power

In a practical coherent receiver the theoretical performance may not be attained for the reason already outlined in Sections 12.4.1 and 12.4.2. In addition, there may be insufficient local oscillator power to achieve the shot noise detection limits discussed in Section 12.3. This factor, which highlights the need to ensure a low loss signal path, can be facilitated by an appropriate choice of an incoming signal/local oscillator combiner which has high coupling efficiency. In particular, it is clear that when the basic coherent detector shown in Figure 12.3 is considered, the optical combiner or coupler has only one output port utilized, whereas in reality such devices have two output ports (see Section 5.6.1). There is, therefore, an optical loss associated with the power which is coupled to the other output port. Although the combiner or coupler can be designed so that the majority of the incoming signal power is coupled into the optical detector, a consequence of this process is that there will be reduction in the power from the local oscillator laser coupled into the detector. It therefore becomes more difficult to maintain a high local oscillator signal power and thus to obtain shot noise limited receiver performance.

The dramatic effect of the local oscillator power on an optical homodyne receiver sensitivity is illustrated by the theoretical characteristic shown in Figure 12.8 which corresponds to a PIN–FET receiver operating at 140 Mbit s^{-1} [Ref. 45]. One method to overcome limited local oscillator power is by the use of a low noise photodiode/preamplifier combination such as the PIN–FET hybrid configuration (see Section 9.5.2) at the front end of the coherent receiver. Near shot noise limited detection has been obtained with just 1 μW of local oscillator power at a transmission rate of 140 Mbit s^{-1} when employing this strategy [Ref. 46]. In addition a heterodyne PIN–FET receiver with 8 GHz bandwidth and 10 pA $Hz^{-\frac{1}{2}}$ equivalent circuit noise current at an IF of 4.6 GHz has been demonstrated [Ref. 47].

An alternative approach which compensates for the losses due to coupling optics and also suppresses excess noise in the local oscillator signal is the use of a balanced receiver.* This scheme, which has often been employed for heterodyne detection in

* It is also referred to as the balanced-mixer receiver [Refs. 23, 48].

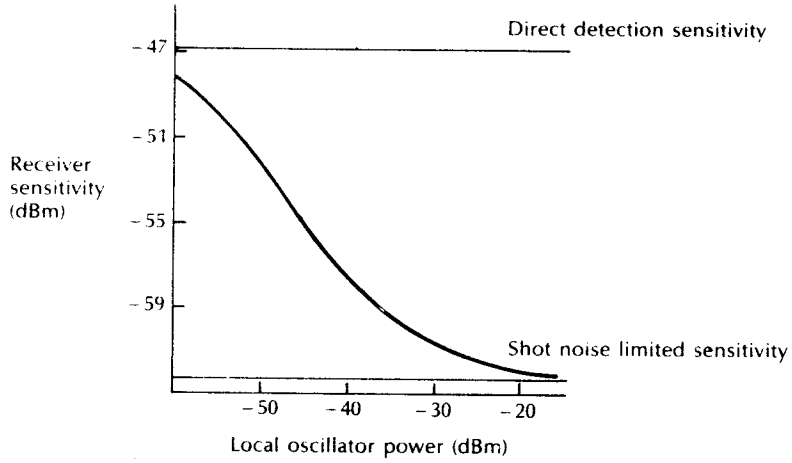

Figure 12.8 Theoretical characteristic showing the effect of local oscillator power on homodyne receiver sensitivity for a PIN–FET receiver operating at 140 Mbit s^{-1}. Reproduced with permission from D. W. Smith, 'Techniques for multigigabit coherent optical transmission', *J. Lightwave Technol.*, **LT-5**, p. 1466, 1987. Copyright © 1987 IEEE.

microwave communications to suppress local oscillator fluctuations [Refs. 49, 50], is shown in Figure 12.9. In this technique the local oscillator output and the incoming optical signal are usually combined using a four port (i.e. 3 dB) single-mode fiber directional coupler.* The signal in one fiber in this device suffers a $\pi/2$ phase shift upon transfer to the other fiber. In effect complete coupling is only possible because this phase shift in the coupled signal is $\pi/2$ out of phase with the throughput signal.† Hence the throughput and coupled signals can be represented

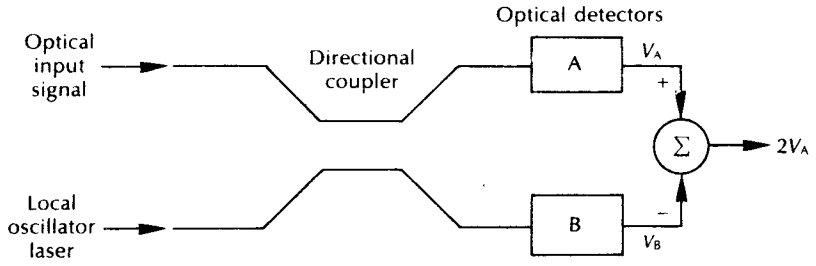

Figure 12.9 Schematic of a balanced optical receiver using two matched optical detectors.

* Other devices which may be utilized are bulk optic or waveguide beam splitters [Ref. 22].
† This signal becomes out of phase if it is coupled back to the throughput fiber where it would interfere destructively with the throughput signal.

as a sine wave and cosine wave respectively. Considering Figure 12.9 the inputs to the optical detectors A and B can therefore be written as $E_S \sin \omega_S t + E_L \cos \omega_L t$ and $E_S \cos \omega_S t + E_L \sin \omega_L t$ respectively.

The two detector output voltages are thus given by:

$$V_A = E_S E_L \sin (\omega_S - \omega_L)t \tag{12.18}$$

$$V_B = E_S E_L \sin (\omega_L - \omega_S)t \tag{12.19}$$

It may be observed that these output voltages are similar but of opposite sign in that $V_A = -V_B$.

The two output voltages are operated upon by the combiner function (Σ) depicted in Figure 12.9 and as one is a positive input and the other is a negative input, then the output from the combiner function V_o will form the difference between the two inputs such that:

$$V_o = V_A - V_B = 2V_A \tag{12.20}$$

Equation (12.20) indicates that twice the voltage, or four times the power, is provided in comparison with the single optical detector scheme (Figure 12.3). This technique therefore gives a 6 dB improvement over the single optical detector. Furthermore, as the two photocurrents are effectively subtracted, the process results in both a cancelling out of the large d.c. term produced by the local oscillator signal, together with any local oscillator excess noise. It is particularly useful in reducing the excess AM noise generated by the local oscillator [Ref. 18]. Moreover, as a result of the efficient use of the local oscillator and incoming signal powers, the constraints imposed by the earlier requirement for a widespread ultra-low noise preamplifier are relaxed. Close matching of the two arms of the balanced receiver is essential, however, if good excess noise cancellation is to be obtained. For example, a balanced receiver with an estimated equivalent circuit noise of 5.4 pA $Hz^{-\frac{1}{2}}$ at 1 GHz and 10.7 pA $Hz^{-\frac{1}{2}}$ at 2 GHz has been reported [Ref. 51]. Furthermore, the similar receiver design was operated with an IF of 3 GHz within a 2 Gbit s^{-1} system experiment [Ref. 52].

12.4.4 Transmission medium limitations

Although, in common with IM/DD systems, the fiber loss is the major limitation on the performance of single carrier coherent optical systems that can be ascribed to the transmission medium, there are nevertheless other factors that may well affect the operation of future coherent systems. These include intramodal or chromatic dispersion, polarization dispersion and the nonlinear scattering effects [Ref. 44].

The intramodal dispersion in conventional single-mode fiber which has a dispersion zero at a wavelength of 1.3 μm is around 15 ps km^{-1} nm^{-1} when the fiber is operated at a wavelength of 1.55 μm. This factor can lead to significant dispersion penalties (i.e. receiver sensitivity degradations) for IM/DD systems even at modest

transmission rates and distances. It results from the transmitted spectrum usually being far wider than the information spectrum due to laser frequency chirp (see Section 6.7.3) caused by the direct amplitude modulation of the semiconductor laser. By contrast coherent optical transmission systems have the advantage of a compact spectrum even if the injection laser is directly modulated but particularly when an external modulator is employed. Receiver sensitivity degradation due to intramodal dispersion has, however, been observed in FSK transmission experiments at transmission rates greater than 4 Gbit s^{-1} [Ref. 44]. Furthermore, as both the transmission rates and distances for coherent transmission are increased, then greater chromatic dispersion penalties will be incurred. For example, calculations have indicated the maximum transmission rates to incur a 2 dB penalty after a 100 km distance on a conventional 1.3 μm single-mode fiber when operating at a wavelength of 1.55 μm to be in the range 5 to 9 Gbit s^{-1} depending on the modulation format used [Ref. 53].

As in the case of IM/DD the intermodal dispersion problem can be reduced through the use of dispersion shifted fiber which exhibits a dispersion zero in the 1.55 μm wavelength window (see Section 3.12.1). However, this solution is only partially satisfactory as there is a massive base of installed conventional single-mode fiber. An alternative strategy is to compensate for the chromatic dispersion in either the optical domain [Ref. 44] or the electrical domain [Ref. 54]. The latter method in particular has shown some limited success using stripline delay equalizers which have demonstrated the potential to compensate for dispersion-induced distortion up to transmission rates of 10 Gbit s^{-1}.

Polarization mode dispersion results from birefringence in the single-mode fiber and it corresponds to the difference in the propagation time associated with the two principal orthogonal polarization states (see Section 3.13.1). Whereas in IM/DD systems polarization mode dispersion simply results in pulse broadening due to the different spectral components arriving at different times, in coherent systems these components can also arrive with different polarizations. Moreover, both of these effects may be detrimental to coherent system performance. However, the differential propagation time is dependent upon the amount of mode mixing which takes place in the fiber, an effect which results from internal and external fiber perturbations. Assuming some mode mixing, the effects of polarization mode dispersion are therefore not expected to become important in a single carrier system with a fiber distance of 100 km until transmission rates exceed 10 Gbit s^{-1} [Ref. 44]. Although in multicarrier systems (see Section 12.8.2) the problem associated with receiving optical carriers at different wavelengths in different polarization states will generally be at lower transmission rates, it may be avoided by using either PM fiber, polarization diversity reception or polarization scrambling transmission (see Section 12.4.2.2).

The nonlinear phenomena which may be of importance within coherent optical transmission include stimulated Raman scattering (SRS), stimulated Brillouin scattering (SBS), cross-phase modulation and four wave mixing [Ref. 44]. ASK systems prove particularly susceptible to such nonlinear effects which result from

optical power level changes. Moreover, a potential advantage of the FSK and PSK modulation formats over ASK is that they produce a constant amplitude signal which provides some immunity to certain nonlinear effects. Although SRS should not be a consideration in single carrier coherent optical systems operating at power levels below 1 W, Raman induced crosstalk may be a concern in multicarrier systems [Ref. 55].

Stimulated Brillouin scattering may be a problem at lower light levels than SRS as its threshold power level is significantly smaller (see Section 3.5). However, unlike SRS, SBS is a narrowband process with a bandwidth of only around 20 MHz at a wavelength of 1.55 μm (see Section 3.14). The maximum SBS gain which also is maximized in the reverse direction will therefore occur for lasers with linewidths less than 20 MHz. Moreover, as a result of information broadening of the linewidth, SBS will be greatly reduced when using modulation formats which do not contain a residual carrier component (i.e. PSK and narrow deviation FSK, see Section 12.5).

Self-phase modulation is a phenomenon which occurs in single carrier systems due to small refractive index changes induced by optical power fluctuations which affect the phase of the transmitted signal (see Section 3.14). For digitally modulated coherent optical systems this effect is perceived to be negligibly small at launched power levels up to a few hundred milliwatts [Ref. 44]. With multicarrier systems, however, a cross-phase modulation phenomenon occurs which can cause high levels of phase noise in long fiber lengths. In this case it has been shown that the power of each carrier should be restricted in order to limit the degradation caused by this phase crosstalk [Ref. 55]. Nevertheless, this limitation on transmitter power in a multicarrier system may not be as severe as the one imposed by the four wave mixing nonlinear phenomenon. It is suggested that this latter process will be present in all frequency division multiplexed systems with channel separations less than 10 GHz and that the crosstalk will restrict the maximum power per carrier to around 0.1 mW when the fiber lengths exceed 10 km [Refs. 44, 55].

12.5 Modulation formats

12.5.1 Amplitude shift keying

Several techniques may be employed to amplitude modulate an optical signal. Digital intensity modulation used in direct detection systems is essentially a crude form of amplitude shift keying* (ASK) in which the received signal is simply detected using the photodetector as a square law device (see Figure 12.2(a)). It is apparent, therefore, that the simplest approach to ASK is by direct modulation of the laser drive current. A problem exists, however, with this approach because of the inability of semiconductor lasers to maintain a stable output frequency with

* It should be noted that ASK is also referred to as on–off keying (OOK).

transmission rates and distances. It results from the transm-
being far wider than the information spect-
Section 6.7.3) caused by th-
laser. By con-

changing drive current. The resulting frequency deviation, which can be of the order of 200 MHz mA^{-1} [Ref. 23], broadens the linewidth of the modulated laser which creates difficulties for coherent optical detection (see Section 12.4.1).

Although direct modulation of the semiconductor laser in ASK coherent optical fiber systems has been demonstrated [Ref. 4], external modulation using active integrated optical devices, such as the directional coupler or the Mach–Zehnder interferometer (see Section 10.6.2), present attractive alternatives [Refs. 23, 45]. It should be noted, however, that all external ASK modulators suffer the drawback that around half of the transmitter power is wasted. Nonsynchronous detection can also be employed with the ASK format which puts the least demands on the injection laser phase stability. In principle this modulation scheme can be used with laser sources exhibiting linewidths comparable with the bit transmission rate. In practice the linewidth in the range 10 to 50% of bit rate is normally specified for ASK heterodyne detection [Refs. 45, 56], although some authors indicate 10 to 20% [Refs. 5, 44]. Nevertheless, nonsynchronous heterodyne and phase diversity (see Section 12.6) detection receivers which use ASK can tolerate the linewidths of currently available DFB lasers.

12.5.2 Frequency shift keying

The frequency deviation property of a directly modulated semiconductor laser can be usefully employed with wideband frequency shift keying (FSK) coherent optical fiber systems. Hence optical FSK (see Figure 12.2(b)) in common with ASK has the advantage that it does not necessarily require an external modulator, thus allowing higher launch powers and a more compact transmitter configuration, as illustrated in Figure 12.10(a). The direct frequency modulation characteristics of the laser are determined by changes in the device carrier density in the high modulation frequency region, and by the temperature modulation effect in the low frequency region. Thus at frequencies above 1 MHz where the carrier modulation effect occurs, the frequency deviation is typically 100 to 500 MHz mA^{-1}, whereas below 1 MHz it is around 1 GHz mA^{-1} due to the predominant temperature effect [Ref. 45]. Although the response under frequency modulation of the semiconductor laser is therefore not uniform, a frequency shift of between 100 MHz to 1 GHz is readily obtained from the device without serious intensity modulation effects [Ref. 18].

The laser linewidth requirements for wide frequency deviation FSK heterodyne nonsynchronous detection are similar to those of ASK with nonsynchronous heterodyne detection and are in the range 10 to 50% of the transmission bit rate [Refs. 45, 55]. Therefore, the use of FSK with broad linewidth injection lasers has been relatively successful, particularly at low bit rates. For example, the direct modulation of the laser drive current causing variations in the lasing wavelength has provided FSK transmission over 300 km at a rate of 34 Mbit s^{-1} with a receiver sensitivity of 165 photons per bit [Ref. 57]. However, due to the presence of large thermal effects at linewidths less than 10 MHz the FM response of semiconductor lasers is typically nonuniform and hence electronic equalization may be required